

## Section A

### **Use DNA as a polymeric vector to assemble a viral and non-viral hybrid multi-drug delivery system**

Yougen Li, Soongho Um, Yen Cu and Dan Luo  
Department of Biological and Environmental Engineering  
Cornell University, Ithaca, New York 14853, USA

For gene therapies, viral vectors (infection) are by far the most specific, efficient and effective means of DNA delivery, due to highly evolved, and specialized, viral proteins and peptides. However, enthusiasm for viral-vector mediated DNA delivery, unfortunately, has been tempered by growing concerns over the drug carriers -- viral vectors. Non-viral vectors, on the other hand, have much better safety profiles although they are still generally inferior to most viral vectors. A hybrid system that combines both viral and non-viral advantages may overcome the major barriers to DNA delivery safely and efficiently.

To design such a hybrid system, only those viral components that are responsible for efficient delivery were selected. Non-viral chemicals such as polymers were also needed in this hybrid system to serve as scaffolding to harness the power of many viral components without the entire virion. We believe that DNA themselves are ideal polymers to serve as drug delivery vectors. Besides their biological functions as genetic molecules, DNA molecules are bona fide polymeric materials that possess many desirable chemical and physical properties. Through nucleic acid engineering, nanoscale, synthetic DNA molecules were self-assembled into a dendrimer that was multivalent and anisotropic, making conjugation of different entities precisely controlled. These nucleic acid engineered materials (NAEM) are able to serve as the backbone for a viral non-viral hybrid system.

We have successfully synthesized both in a solution and on a solid-phase a DNA-based, viral-peptide conjugated, anisotropic dendrimer that served as a carrying vector for multiple drug delivery including gene and anti-gene delivery. This viral and non-viral hybrid system successfully condensed plasmid DNA and crossed cell plasma membrane by viral peptides. In addition, the gene expression was much higher than controls. We believe that this is the first time to realize a modular, viral/non-viral hybrid drug-delivery system that is using DNA molecules themselves as a polymeric carrier to delivery other DNA drugs. These preliminary data promises a unique, efficient and specific viral and non-viral hybrid system for both gene and anti-gene delivery.

## Charge-Reversal Amphiphiles for Gene Delivery

Carla A. H. Prata, Yuxing Zhao, Philippe Barthelemy,<sup>†</sup> Yougen Li,<sup>‡</sup> Dan Luo,<sup>‡</sup> Thomas J. McIntosh,<sup>¶</sup> Stephen J. Lee,<sup>Ⓞ</sup> and Mark W. Grinstaff\*

Departments of Biomedical Engineering and Chemistry, Boston University, Boston MA 02215. <sup>†</sup> Departement de Chimie, Université D'Avignon, 33 rue Louis Pasteur, F-84000 Avignon, France. <sup>¶</sup>Department of Cell Biology, Duke University Medical Center, Durham, North Carolina, 27710. <sup>‡</sup>Department of Biological and Environmental Engineering, Cornell University, Ithaca, New York, 14853. <sup>Ⓞ</sup>Army Research Office Research Triangle Park, North Carolina, 27709.

The two most common methods of gene delivery use either viral or synthetic vectors. Viruses are efficient carriers of genes, but there are risks associated with their clinic application. Consequently, there is intense activity in developing and evaluating synthetic non-viral vectors including cationic amphiphiles, linear polymers dendrimers, and micro/nanospheres. Since the pioneering research by Felgner, MacDonald, and Magee, cationic amphiphiles have been investigated due to their low toxicity, nonimmunogenicity, and ease of synthesis; today, these amphiphile-DNA vectors are in clinical trials. Yet with these amphiphiles, the gene transfection activity is low, reflecting inefficiencies in the overall transfection pathway. Our immediate research effort is focused at improving the release of DNA from the DNA-cationic amphiphile supramolecular complex. We designed and characterized a functional amphiphile for gene delivery that undergoes an electrostatic transition from cationic to anionic to release DNA. These charge-reversal or charge-switchable amphiphiles bind or release DNA based on favorable or unfavorable electrostatic interactions and were designed based on the mechanism of the DNA-synthetic vector transfection pathway. The transfection activity observed with the charge-reversal amphiphile is significant and greater than the enzymatically non-active analogs. These amphiphiles represent a conceptual departure from the current cationic molecules under investigation, and these results are likely to facilitate the design, development, and evaluation of new synthetic non-viral vectors for the delivery of therapeutic DNA.

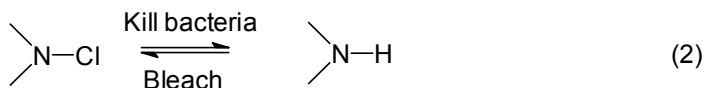
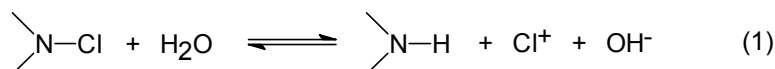
# Halamine Chemistry and its Applications in Biocidal Textiles and Polymers

Gang Sun

Division of Textiles and Clothing, University of California, Davis, CA 95616

## Introduction

N-halamine chemistry can be expressed in equations 1 and 2. When N-halamine structures are exposed to water, the reaction shown in equation 1 may occur. The equilibrium in equation 1 may shift toward either reactants or products depending on the N-halamine structures.



N-halamine structures can kill microorganisms directly also without the release of free chlorine, as in equation 2. In fact, N-halamine structures may only release very limited amounts of free chlorine because the dissociation constants of equation 1 are in the scale of  $10^{-4-12}$  for imide, amide and amine halamines. Since N-halamine structures are biocidal, and more importantly quite stable in ambient environments, incorporation of the N-halamine into polymeric and textile materials will bring biocidal functions to them. Moreover, since equation 2 is a reversible reaction, the biocidal functions on the materials are rechargeable with a chlorinating agent, such as chlorine bleach. This rechargeable function is most suitable for reusable medical textiles and clothing. In this paper we will review the latest progresses in the application of N-halamine chemistry to textiles and polymers.

## Incorporation of N-halamine to textiles

Both amide and imide N-halamines have been incorporated into cellulose-containing fabrics by a conventional finishing method with 1,3-dimethylol-5,5-dimethylhydantoin (DMDMH). The DMDMH-treated fabrics exhibited rapid biocidal functions, but the washing durability of the functions requires improvement, due to the dominating imide N-halamine functionality, which is the most reactive, but least stable on the fabrics. However, DMDMH fabrics can be employed in personal protection against various biological agents such as bacteria, viruses, fungi, yeasts, and spores. Examples of the treated fabrics demonstrated a complete elimination of pathogens in a contact time as short as two minutes. The biocidal functions could be recharged repeatedly for at least 50 machine washes.

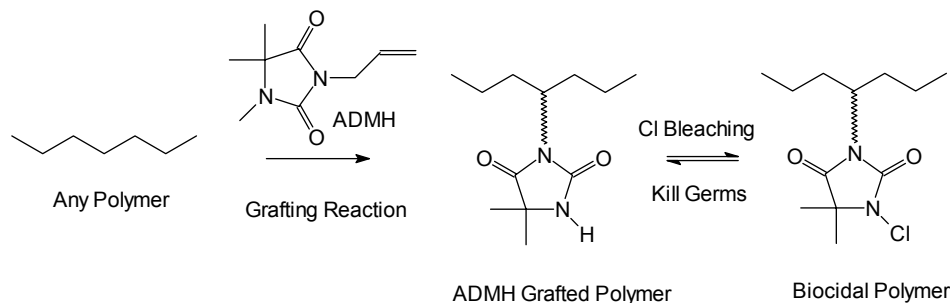
## MTMIO-TREATED CELLULOSE

In order to increase washing durability of the N-halamine-treated textiles, the more stable amine N-halamine has been grafted to cellulose in a similar approach by using 3-methylol-2,2,5,5-tetramethylimidazolidin-4-one (MTMIO). The resulting fabrics contained the more stable, and less reactive, amine N-halamine structure, thus providing slow, but durable, biocidal functions.

## ADMH-TREATED FIBERS

Recently, a hydantoin-containing monomer, 3-allyl-5,5-dimethylhydantoin (ADMH, as shown in Scheme 1) was prepared to incorporate only amide N-halamine structures into synthetic fibers. Due to the amide structure, the thus-produced fabrics could demonstrate both powerful and durable biocidal functions. Synthetic fabrics such nylon-66, polyester (PET), polypropylene (PP), acrylics, Nomex IIIa, PBI/Kevlar, and Kermel, as well as pure cotton fabrics, were used in the chemical modification. The ADMH can be incorporated in surfaces of fibers by a controlled radical grafting reaction which can ensure short chain grafts instead of long chain self-polymerization of the monomers(Scheme 1).

Scheme 1. Structure of ADMH and its grafting reactions on synthetic polymers.



Biocidal properties of the modified fibers could be demonstrated after a chlorination reaction by exposing the grafted fibers to a diluted chlorine solution, with which the grafted hydantoin rings were converted to N-halamine structures. The polymeric N-halamines could provide powerful and rapid antibacterial activities against *E. coli* and *S. aureus*. Most of the fibers could completely inactivate a large number of bacteria ( $1 \times 10^6$  CFU) in a 10-30 minute contact time. In addition, the antibacterial activities of these polymeric N-halamines could be easily recovered after usage by simply exposing to chlorine solution again.

## ACKNOWLEDGEMENTS

The research was support by a CAREER award from The National Science Foundation (DMI 9733981), the National Textile Center (C02-CD06) and Vanson-HaloSource Inc. Drs. Xiangjing Xu, Lei Qian, and Yuyu Sun contributed to the research.



# Durable and Rechargeable Antimicrobial Cellulose with Peroxy Moieties

Louise Ko Huang, Gang Sun

*Division of Textiles & Clothing, University of California, Davis, CA 95616*

## Introduction

Recently, our research group has reported the design and development of durable and regenerable antimicrobial textile and polymeric materials based on halamine chemistry<sup>1-3</sup>. However, there is a potential concern arising from such development, that is, the use of non-environmental friendly chlorine bleach as both the activating and regenerating agent. Consequently, we were prompted to examine alternatives to the existing antimicrobial technology. One strategy is the employment of peroxy moieties. Peroxy moieties such as peroxide and peroxyacids have been widely used as disinfectants in the food and beverage industries as well as bleaching agents for textile and paper<sup>4-6</sup>.

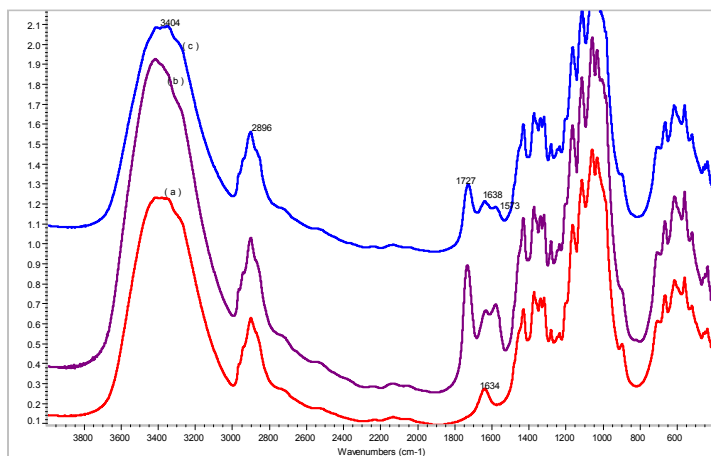
The formation of peroxyacids on cellulose can be carried out in two steps: (1) grafting/crosslinking polycarboxylic acids (PCA) onto cellulose, (2) oxidation of unreacted free acids of PCA-incorporated cellulose to the desired peroxyacid moieties.

As an exploratory study, PCA such as 1,2,3,4- butanetetracarboxylic acid (BTCA) and citric acid were grafted/crosslinked onto cellulose. Both of these PCA provided sources of unreacted free acid groups that can be further oxidized. Commercially available oxygen bleaches converted the free carboxylic acid groups into peroxyacid moieties on cellulose. In this paper, the formation of the peroxyacids and their antimicrobial properties on the treated fabrics as well as the regenerable conditions will be discussed.

## Experimental

Cotton and polyester/cotton blend fabrics were treated with 6% PCA. These finished fabrics were then treated with 0.1% and 0.01% dilute oxygen bleach at various temperatures and duration. All treated fabrics were rinsed several times in distilled water, air-dried and stored under standard condition prior to further testing, analysis and characterization.

FT-IR spectroscopy was used to analyze the structures of these fabrics. BTCA compounds bear carbonyl groups that do not exist in cellulose. The prominent band at 1726 cm<sup>-1</sup> (Figure 1) from the treated fabric indicates the presence of the carbonyl group on the treated cellulose and thus, confirms the successful impregnation of BTCA onto cellulose. This proves that crosslinking agent BTCA formed ester linkages with cellulose during the wet finishing treatments. Moreover, the FTIR spectrum of the bleached, modified cellulose shows almost the same band intensity for the ester bond at 1726 cm<sup>-1</sup>, indicating that the oxygen bleach treatment did not significantly damage the crosslinking between cellulose and BTCA. Thus, such ester bond formation has proven to be stable and unaffected even by further bleaching of the treated fabrics<sup>7</sup>.

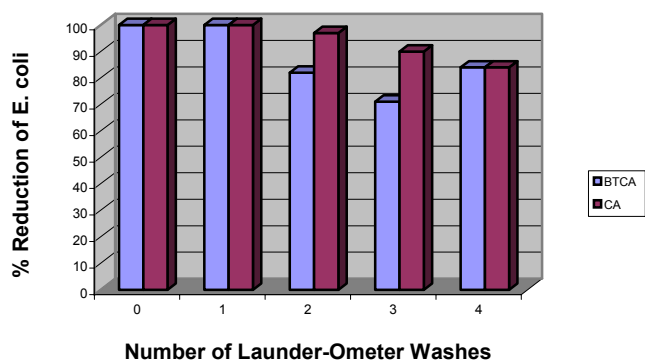


**Figure 1. FT-IR spectra of (a) untreated, (b) BTCA-treated and (c) BTCA-treated and bleached cotton fabrics.**

Biocidal properties of the modified fabrics were quantitatively evaluated against bacterium, *Escherichia coli* according to the American Association of Textile Chemists and Colorists (AATCC) standard test method 100<sup>8</sup>. Repeated laundering tests were also carried out in a Launder-Ometer at room temperature, following AATCC standard test method 161-2A<sup>7</sup>. We found that the efficacy of *Escherichia coli* decreased as the bleaching temperature was raised (Table 1). The reduction of *Escherichia coli* by fabrics treated at elevated temperatures (45°C, 60°C) indicates higher levels of peroxyacid formation on these fabrics than those treated at room temperature. This suggests that the formation of peroxyacids might be an endothermic reaction as it is favored at higher temperatures<sup>7</sup>. Repeated laundering tests showed that the peroxyacid containing cellulose was indeed regenerable and durable (Figure 2).

**Table 1. Efficacy of PCA-treated cotton with oxygen bleach against *Escherichia coli*.**

Treatment	%Oxygen Bleach	Bleaching Temp. (°C)	% Reduction of <i>E. coli</i>
100% cotton (control)	0	N/A	0
6% BTCA	0.1	60	100
6% BTCA	0.1	45	100
6% BTCA	0.1	room temp.	61
6% CA	0.1	60	100
6% CA	0.1	45	100
6% CA	0.1	room temp.	83



**Figure 2. Antimicrobial efficacy on laundered PCA-treated fabrics with 0.1% oxygen bleach.**

#### References

1. Sun, G. and Xu, X. *Textile Chemist and Colorist*. **1999**, 31(1), 21-24.
2. Sun, G. and Sun, Y. *J. Polym. Sci.: Part A: Polymer Chemistry*. **2001**, 39, 3348-3355.
3. Kim, Y. H. and Sun, G. *Tex. Res. J.* **2001**, 71(4), 318-323.
4. Pinkernell, U., Effkemann, S., Nitzsche, F., and Karst, U. *J. Chromatography. A*. **1996**, 730, 203-208.
5. Winkler, J., Smith, E. R., and Compton, R. G. *J. Coll. Interface Sci.* **1997**, 195, 229-240.
6. Cai, J. Y., Evan, D. J., and Smith, S. M. *Amer. Assoc. Tex. Chem. Color. Review*. **2001**, 1(12), 31-34.
7. Huang, L. K. and Sun, G. *Amer. Assoc. Tex. Chem. Color. Review*. **2003**, 3(10), 17-21.
8. American Association of Textile Chemists and Colorists. *AATCC Technical Manual*. AATCC Press, Research Triangle Park, **1996**, p.92-95, 146-147.

## Radiochemical Sterilization of New Absorbable Sutures

S. W. Shalaby, Ph.D., Poly-Med, Inc., 6309 Highway 187, Anderson, SC 20625

Radiochemical sterilization (RC-S) is a novel process developed for the effective sterilization of radiosensitive polymers, such as polypropylene and all absorbable polyester-based surgical devices. The RC-S process is based on using a low dose of high-energy radiation of about 5 kGy in conjunction with a predetermined amount of radiolytically generated formaldehyde in a dry, oxygen-free, hermetically sealed package. The successful application of the RC-S process to polyglycolide braided sutures without compromising their clinically important properties, led to the pursuit of the present study. This entailed a number of new sutures with a broad range of *in vitro* and *in vivo* properties. More specifically, the study was designed to explore the use of RC-S as a viable process for the effective sterilization of new, molecularly tailored absorbable sutures. Among the examined sutures are (1) linear segmented, high glycolide-based copolyesters in the form of monofilaments; (2) linear segmented, high lactide-based copolyesters in the form of monofilaments and braided multifilaments; and (3) polyaxial segmented, high glycolide-based copolyesters in the form of monofilaments and braided multifilaments. Results of the *in vitro* and *in vivo* evaluation of key suture properties indicate that RC-S is indeed a viable process for the effective sterilization of most of the examined sutures, without causing significant change in their clinically relevant properties.

## **The Benefits of Nanofibers in Biomedical Applications**

M. Jaffe, S. Shanmukasundaram, A. Patlolla, K. Griswold, S. Wang, J. Mantilla,  
R. Walsh, T. Arinzeh, C.J. Prestigiacomo, L.H. Catalani  
Department of Biomedical Engineering, New Jersey Institute of Technology, Newark, NJ  
Medical Device Concept Laboratory

Electrospinning is a technique that has been known for more than 70 years. Although the number of papers in the literature exceeds 1000, most of the information is observational or empirical with little emphasis on process engineering; hence, minimal control is exerted over important parameters such as fiber diameter, diameter uniformity, take-up formatting (non-woven, bobbin, specific pattern, etc), etc. As a result, successful applications of the resultant fibers are random and commercialization of electrospun products is in its infancy.

The potential impact of nanofibers in biomedical applications is high owing to (i) fiber diameter similar to those found in the extracellular matrix, allowing the design of more effective scaffolds (ii) very high surface area in contact with bio-environment, a key pre-requisite in many applications such as drug delivery, bio-erodable implants, protein filtering, and others applications that require a high concentration of active surface groups; (iii) high morphological stability, lacking mechanisms to thicken or agglomerate as is common with nanoparticles, and (iv) with possible improved safety in use.

The electrospinning theory is based on the premise that excess charge dissipation – opposed by surface tension – is the driving force for Taylor cone formation and the subsequent extrusion of submicrometer diameter filaments. Recent attempts to model the process are complex, describing a unique extrusion process that is inherently difficult to control in the way it is currently practiced.

Our group efforts have been directed to develop a true controllable process through: (i) imposing unit operations analysis (metering, filtration, quench, mass transfer, take-up, post-treatment, etc); (ii) application of relevant polymer fiber theory and practice to some key issues: dry spinning variables, jet design, the impact of chain entanglement, control of molecular orientation, morphology control; (iii) innovative approaches to process design in order to achieve steady state electrospinning conditions.

A major focus of the work has been the use of polyesters (erodable and non-erodable) in the development of biomedical devices. Electrospinning was utilized to fabricate poly-L-lactide (PLLA) non-woven mats of two distinctly different fiber diameters (13 micron and about 130 nanometers). The potential of these non-woven mats as tissue engineering scaffolds was assessed by cell proliferation studies of Human Mesenchymal Stem Cells (hMSCs). Cell proliferation studies were performed, with the results showing that hMSCs tend to proliferate more on nanofiber scaffolds than on the conventional diameter microfiber scaffolds.

For the development of a drug delivery system, targeted for catheter delivery through small diameter blood vessels, poly (D,L-lactide-co-glycolide) (DLPLGA) nanofibers were electro-spun from a tetrahydrofuran (THF) solvent. Three different concentration ratios of DLPLGA, 85/15, 80/20, and 75/25 were analyzed as the base polymer for drug release studies. A highly researched chemotherapy compound was chosen as a model compound for release studies. A homogeneous solution of polymer and drug was

electrospun and the resulting nanofibers were analyzed for drug incorporation and retention of drug chemistry.

The effect of aging solution of polycaprolactone nanofiber mats showed a extensive change in its tensile properties going from a brittle mat, when spun from recent made solutions, to ductile mats when 48 hs old solutions were spun. Explanations for this effect range from completion of dissolution, kinetic of a potential gel-to-sol transition, to a possible late crystallization regime.

Work is also proceeding on the fabrication of 3D structures of polyethylene terephthalate/polyethylene terephthalate-collagen hybrids composed of submicro- and nanofibers, anticipating advantageous properties including high surface area and high mesh size. The functionalization of the fibers surface by creating activated binding sites, a known methodology for PET surface modification, will allow the anchorage of biomolecules for surface biocompatibilization.

The “whipping” movement of the fiber during extrusion leads to lack of control over the final fiber mat architecture. To overcome these challenges we are exploring secondary electrostatic fields to dampen the fluid jet instability, and the use of shaped, controlled charge density collecting elements. Two experimental systems have been created to test these concepts. The first consists of copper rings charged with a greater voltage than the voltage on the syringe tip with a ground plated behind the rings. The second uses a uniform metal cylinder charged with the same voltage as the syringe tip, and a grounding plate placed behind. With these two systems we are able to dampen the fluid jet instability, target the fluid jet enabling us to create patterned fiber deposition, and be able to produce nano-fiber mats efficiently, and from a wide variety of polymer solutions.

As a general conclusion we are able to demonstrate that electrospinning is a dry spinning process, where all rules apply, and utilize secondary electrostatic fields to control the extruded fiber.

# **Thermomechanical and Dynamical Mechanical Analysis of Sutures**

Meng Deng and Jack Zhou

R&D Division, Ethicon, a Johnson & Johnson Company, P.O.Box 151, Somerville, NJ 08876-0151, USA.

Sutures are the oldest implants and the most important wound closure medical devices at the present time. Although small, they have wide, irreplaceable applications in surgery. For many years, researches on sutures have focused on static tensile mechanical and chemical properties, and *in vitro* and *in vivo* studies. However, one under-explored area is the viscoelastic behaviors of these materials, particularly in the form of medical devices. It is understandable that response of sutures to dynamic loading and temperature change will be different from that under static loading and constant temperature.

Performing thermomechanical analysis (TMA) and dynamical mechanical analysis (DMA) of a material not only requires specialized equipment and skilled personnel, but also knowledge of advanced polymer science. As application of sutures becomes more and more sophisticated, needs arise for the understanding of viscoelastic behaviors of these medical devices. Therefore, to try to close the gap, our lab has performed some exploratory work on test method development for TMA and DMA for sutures. This presentation illustrates the thermomechanical and dynamical mechanical properties of several sutures. Dependence of properties on frequency, temperature, and type of the sutures is investigated.

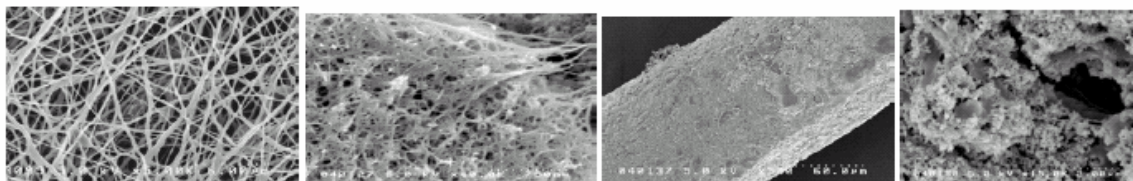
## Carbon Nanotube Substrates for Biomedical Sensors

Konstantin G. Kornev<sup>1</sup>, Gerardo Callegari<sup>1</sup>, Peter I. Ravikovitch<sup>1</sup>, Sigrid Ruetchi<sup>1</sup>, Vijaykumar Rajendran<sup>2</sup>, Plamen Atanassov<sup>2</sup>, Alexander V. Neimark<sup>1</sup>

<sup>1</sup>Center for Modeling and Characterization of Nanoporous Materials  
TRI/Princeton, P.O. Box 625, Princeton, New Jersey 08542, U.S.A.

<sup>2</sup>Chemical and Nuclear Engineering Department MSC01 1120, 1 University of  
New Mexico, Albuquerque, NM 87131-0001

Recent discovery of the particle coagulation process (PCP) to spin fibers from single wall carbon nanotubes [1,2] and electrospinning method to produce nanowebs [3] open new horizons in manipulation of membrane/fiber functionality by using some dopes and fillers. We report on a new application of the single wall carbon nanotube (SWNT) composite substrates as supports for electrochemical biosensors. Nanotube fibers with diameters ranging from 10 to 50  $\mu\text{m}$  were produced by the PCP from purified single wall carbon nanotubes. The characterization of the porous structure and wetting properties of these fibers was done by various techniques including SEM, gas adsorption, droplet absorption and electrochemical methods. Functional membranes were prepared by the PCP and by coating of electrospun nanowebs with SWNT ink. We show that obtained nanofibrous materials are highly porous, capable of absorbing liquids and vapors in significant amounts. Nanotube fibers possess a hierarchical structure with different levels of pore organization. Unlike classical carbon fibers



**Fig.1** Electrospun PVA-based nanoweb before and after application of aqueous solution of PVA/SWNT. In the third and fourth pictures is the fiber made of SWCN by the particle coagulation spinning.

and bucky papers, our nanofibrous materials can be strongly bent without breaking. We analyzed the mechanical properties of fibers at different environmental conditions by using the image analysis system and employing the Euler's elastica equations.

The produced materials have high surface area and open porosity thus providing a significant absorption capacity and selective permeability. Employing horseradish peroxidase (HRP), we examined Direct Electron Transfer (DET) on SWCN nanoporous substrates as a signal generation mode in electrochemical biosensing. The high surface area allows for HRP immobilization by adsorption and the resulting surface complex exhibits DET behavior. The dependence of the

current on the HRP concentration is non-linear suggesting a kinetic controlled response. We discuss different designs of biosensors to exploit specific hydrodynamic and adsorption properties of SWNT nanoporous substrates. We will also discuss some other means to functionalize the nanofibrous materials produced by the PCP and electrospinning.

Acknowledgement. The work is supported by the NIH grant R21EB002889-01

#### References.

1. Vigolo B, Penicaud A, Coulon C, et al. Macroscopic fibers and ribbons of oriented carbon nanotubes. *SCIENCE* **290** (5495): 1331-1334 (2000)
2. Neimark A.V., Ruetsch S., Kornev K.G., Ravikovitch P.I., Poulin P., Badaire S., Maugey M., Hierarchical pore structure and wetting properties of single wall carbon nanotube fibers, *Nano Letters*, **3**, 419-423(2003).
3. Reneker D.H., Chun I., Nanometre diameter fibres of polymer, produced by electrospinning *Nanotechnology*, **7**, 216(1996).



# **The application of acoustic emission to characterize the lubrication of a fibrous collagen material: leather**

CHENG-KUNG LIU

United States Department of Agriculture, Agricultural Research Service,  
Eastern Regional Research Center, 600 East Mermaid Lane, Wyndmoor, PA 19038-8598

For thousands of years, collagen materials, such as leather, have been among the most dominant natural fibrous materials used by humans, especially for clothing, upholstery, and shoes. Leather is economically significant because it is the major by-product derived from the meat industry. Fatliquoring is an oil-addition process by which the leather fibers are lubricated so that after drying they will be capable of slipping over one another. The fatliquored leather therefore attains a greater softness and flexibility than is imparted by the tannages. The fatliquoring process must be done properly to ensure that the leather's fibrous structure is adequately lubricated in order to prevent its fibers from sticking together during the leather drying process. Currently the method described in this report is the only method to measure the degree of lubrication. Lubrication affects the resistance of fiber movements and deformations, and from previous studies we learned that acoustic emission measurements are very sensitive to these changes in resistance. Therefore, we recently investigated the feasibility of using acoustic emission technology to measure the degree of lubrication associated with the fatliquoring process. As a natural fibrous material, leather emits sound waves engendered by a sudden stress accompanied with any significant fiber movement or fiber deformation including breakage. From analysis of the hits, frequency and energy associated with emitted sound waves during the tensile tests of leather treated with various amounts of fatliquor, one may gain a correlation between acoustic emission quantities and the degree of lubrication. The proper lubrication of a fibrous structure such as leather is essential to its mechanical performance, and consequently to its quality. We have examined the feasibility of using the acoustic emission (AE) technique to characterize the degree of lubrication of leather produced with various fatliquor concentrations. In a tensile test, an acoustic transducer was contacted with the leather samples to collect their AE quantities and properties. The samples lubricated with a fatliquor concentration less than 10 % showed twin peaks on the plot of hits rate versus time. This implied that a non-uniform fracture occurred in a leather structure that was not sufficiently lubricated. In contrast, a sufficiently lubricated leather structure showed a steady increase in hits rate with time until it fractured. This provides an insight into the reason for the increased strength of fatliquored leather. Traditional stress-strain tests did not reflect these behaviors. Observations also showed a direct correlation between the cumulative hits and fatliquor concentration. The results of this work may provide a route to identify an adequate degree of lubrication in the leather, which was previously difficult to determine. Besides using AE to measure the degree of lubrication as reported in this presentation, we also have developed AE techniques to predict tensile strength without breaking the leather, to gain insights into the reasons for tear failure and provide a new route to characterize the tear resistance of leather, to measure the degree of opening-up of the

leather fibrous structure, and to quantify the bonding strength of coatings on finished leather. This research program at USDA, Agricultural Research Service (ARS), Eastern Regional Research Center (ERRC) has provided the leather industry with insights into the structure/property relationship. These techniques drastically improve leather quality control.

# Novel Fibrous Scaffold for Wound Management

Patti Lewis

Department of Textiles and Apparel, Cornell University

Nonwoven fibrous matrices have been widely used as scaffolds for tissue engineering. Modifying the microstructure of these matrices aids in the cell organization process in a three-dimensional space. In addition, the three-dimensional matrix must allow the required surface area to create a balanced proliferation and differentiation cell process for functional tissue development. The objective of this study was to evaluate the potential of a new class of biodegradable poly(ester amide)s (PEAs) as fibrous substrates for tissue engineering in human body repair.

Electrospinning technique was used and optimized for fabricating several selected PEAs into 3 D porous fibrous matrices shown in Figure 1. The fibrous matrices were characterized for their tensile properties, fiber diameter, air permeability, surface area and water vapor transmission. In addition, PEA films were characterized for surface tension and wettability. PEA fibrous matrices of density of  $40 \text{ g/m}^2$  had an average fiber diameter of 2-4  $\mu\text{m}$ , median pore size of 50  $\mu\text{m}$ , surface area of  $220 \text{ m}^2/\text{g}$ , average air permeability of  $50 \text{ ft}^3/\text{min}/\text{ft}^2$ , and average water vapor transmission of  $0.7 \text{ g/m}^2\text{h}$ . The mechanical properties of the electrospun PEA matrices were determined with an Instron 1122 under a crosshead speed of 50 mm/min at room temperature. The selected electrospun PEA matrices behaved similar to rubber, shown in Figure 2, such as a low modulus of 2-14 MPa, average tensile of  $0.05 \text{ kgf/mm}^2$ , and high elongation of 144-769%.

The biodegradable poly(ester amide) scaffolds were further examined for cell attachment, proliferation, and morphology to determine the cell-matrix interaction. Normal human keratinocyte cells were seeded on the PEA fibrous matrices and evaluated on 1, 3, and 7 days by Calcein-AM and Alamar Blue assays. From these results, the 8-L-Phe-4 (ACP) fibrous matrix was the most favorable for supporting cell attachment and proliferation. Furthermore, the cells on the 8-L-Phe-4 matrix tend to maintain a phenotypic shape through observations by the Calcein-AM assay and scanning electron microscopy (SEM). This novel biodegradable scaffold verified to be an applicable substrate for tissue engineering based upon its unique architecture, in which acts to support cell growth.

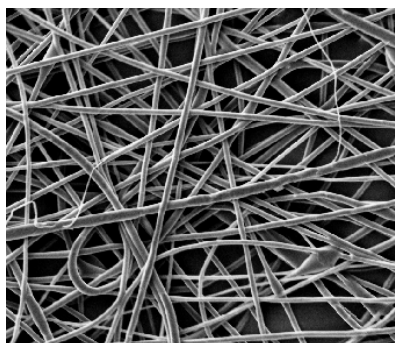


Figure 1. SEM of electrospun 8-L-Phe-4 (ACP)

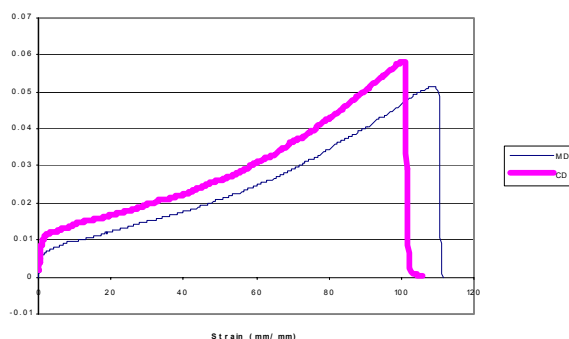


Figure 2. Stress/strain curve of 8-L-Phe-6 (ICP)

## Dynamic Mechanical Properties of Spider Silk

Gaurang Narasimhan\*, Malcolm Skove §, Jacqueline Palmer£ and Michael Ellison\*

\*School of Materials Science and Engineering, §Department of Physics and Astronomy,  
£ Department of Biological Sciences, Clemson University, Clemson, South Carolina,  
USA 29631-0971

### Abstract

The mechanical characteristics of *Nephila clavipes* dragline silks have been researched extensively due to their unusual mechanical properties including high values of toughness. However, there have not been extensive studies of the dynamic mechanical properties of single silk fibers. In this work, we describe the dynamic properties including time-dependent creep and frequency dependence of single fibers of *N. clavipes* dragline silks.

Spider silks are non-linear viscoelastic, history dependent materials with a semicrystalline microstructure. It is believed that these fine structural elements contribute to the time-dependent properties of the silks. The creep studies were conducted by the application of a step stress to a single fiber and then measuring the resultant strain over time. The time response of the strain for selected constant stress levels is well fit by a standard 4-parameter viscoelastic model. The frequency dependence of the complex elastic modulus was measured for oscillating stresses of constant maximum amplitude at selected frequencies from 0.15 Hz to 15 Hz.

## **Section B**

### **DuPont Sorona® Polymer and Fibers: A New Bio-Based Platform for the 21<sup>st</sup> Century**

Joseph V. Kurian Ph.D., Bio-Based Materials,  
E.I. duPont de Nemours and Company, Inc  
Wilmington, Delaware 19880, USA

Responding to environmental, sustainability, business and market needs, DuPont has recently commercialized a new polymer platform, Sorona®, based on 1,3-propanediol. Sorona® polymer can be shaped into fibers and other articles to offer a unique combination of properties. Sorona® imparts distinctive characteristics to fabrics and a vast array of other applications such as upholstery and specialty resins. The technology behind Sorona® enables manufacturers of apparel, upholstery, specialty resins to use their existing assets to make new, higher-value products to meet customer needs.

DuPont is scaling-up a biological process for the large-scale production of 1,3-propanediol. Currently, DuPont is testing the jointly developed bio-process with Genencor at a pilot plant operated by Tate & Lyle. Because corn is a renewable resource, and can be produced anywhere in the world, PDO becomes less expensive to manufacture.

In addition to fibers, Sorona® is finding applications in engineering thermoplastics, films, non-wovens, mono and multicomponents, and several other markets. DuPont has licensed Sorona® fiber technology to a number of fiber manufacturers for applications development. From corn to polymer to future, Sorona® offers a multitude of advantages. Learn all about the advantages Sorona® offers by visiting <http://www.dupont.com/sorona>.

## **Biodegradable Composites From Ligno-Cellulosic Fibers and Thermoplastic Binders**

M.G. Kamath and Gajanan Bhat, Department of Materials Science and Engineering  
The University of Tennessee, Knoxville, TN 37996, email: [gghat@utk.edu](mailto:gghat@utk.edu)  
and  
D. Mueller, University of Bremen, Germany  
D. V. Parikh, USDA, New Orleans, LA, and  
Mac McLean, Cotton Incorporated, Cary, NC

The automotive industries throughout the world are continuously optimizing the cost effectiveness for greater value in automotive interiors in order to remain competitive in the market. Moreover, (a) increased importance of renewable resources for raw materials, and (b) recyclability and/or biodegradability of the product at the end of the useful life are demanding a shift from petroleum-based synthetics to agro-based natural fibers in automotive interiors<sup>1</sup>. Natural fiber composites can contribute greatly to the automotive manufacturers final goal of weight and cost reduction. The approach in this research has been to evaluate lingocellulose-based nonwoven composites for automotive, and other similar applications. Effect of different lingo-cellulose and binder fiber compositions on the structure and properties of the resulting composites will be discussed.

These lingo-cellulose fiber-based composites can be safely disposed off after their intended use without polluting the environment. It is shown that by suitably blending cotton and flax or kenaf, with an appropriate thermoplastic biodegradable fiber in the right proportion, a moldable automotive nonwoven-based composite can be produced. Cellulose acetate, biodegradable copolyesters, and other thermoplastic polymers/fibers will function as the binder fibers, eliminating the use of any non-biodegradable synthetic or a chemical binder. Recent studies are indicating that nonwoven composites with good tensile properties can be produced from such blends. Bonding between cellulosic fibers and binder polymer is very good when composites are made from webs of intimate fiber blends<sup>2</sup>.

These composites have shown good promise in tensile properties, and further experiments are being conducted with different combinations of cotton/flax or cotton/kenaf and different thermoplastic biodegradable binder fibers. Some of the biodegradable fibers are available through commercial providers, and some are produce exclusively for this research. The composite samples fabricated by thermoforming of nonwoven batts prepared from fiber blends are being evaluated for their physical and acoustical properties. Also, the effect of bleached vs. raw cotton on the performance of these composites are being investigated. Issues related to blending of different components, and adhesion between different matrix and fibers will be discussed in detail.

---

<sup>1</sup> R.Lan Mair, Tomorrow's Plastic Cars, ATSE Focus #113 Jul-Aug 2000.

<sup>2</sup> G. S. Bhat, M. G. Kamath, D. Mueller, D. V. Parikh and M. McLean, "Cotton-based Composites for Automotive Applications," GPEC Conference Proceedings, Feb 2004

## **Development of Thermoplastics Composites Containing High Fraction of Bamboo Fiber and Their Application**

Toru FUJII and Kazuya OKUBO  
Dept. of Mech. Engineering and Systems, Doshisha University  
Kyoto, 610-0394 Japan  
Tel. & Fax.: +81-774-65-6432  
e-mail: [tfujii@mail.doshisha.ac.jp](mailto:tfujii@mail.doshisha.ac.jp)

Tatsuya TANAKA  
Machinery division, KOBE STEEL CO. LTD.,  
Kobe, Japan

A new method has been established to fabricate pellets of green composites using thermoplastics such as Polypropylene (PP) for injection molding. Pellets are continuously fabricated by using a conventional two axis screw extruder contain a lot of bamboo short fibers higher than 80% in weight while no methods exist which can put a lot of bamboo fibers into thermoplastics matrix precisely and continuously. Firstly, non-woven strips of thermoplastics such as PP are prepared. Bamboo short fibers are dispersed onto the strips parallelly running. They are rounded and rolled like a spring roll (one of chines foods) containing bamboo fibers between non-woven strips. Then, they are supplied into the entrance of a two axis extruder. The weight fraction of bamboo fibers can be well controlled. It is easy to increase the weight fraction of bamboo fibers with respect to the based thermoplastic matrix. Other natural short (or recycled) fibers can be used instead of bamboo fiber. In order to increase the toughness of composites, some systhetic fibers such as PET fibers can be included into pellets in addition to bamboo fibers, whose melting temperature is higher than the melting temperature of the matrix resin. Mechanical properties of newly developed composites are as high as those of conventional FRTP containing 20% glass fibers.

# **Development of bamboo fiber-reinforced “green” composites**

Hitoshi Takagi

The University of Tokushima, Japan

## **INTRODUCTION**

Since newly developed biodegradable plastics have relatively lower strength than conventional plastics such as polypropylene and polyethylene, the application of biodegradable plastics has been restricted to low-strength products. Over the past few years a considerable number of studies have been made on “green” composites, however, in our understanding, many of them had a fiber volume fraction less than 40 pct, and thus there is a few “green” composites with tensile strength greater than 200 MPa.

The aim of this study is thus to develop high-strength “green” composites, which have excellent mechanical properties comparable to those of glass fiber reinforced plastic (GFRP). High strength bamboo fibers were used as reinforcement for starch-based “green” composites, and both unidirectional composites and random short fiber composites were fabricated under various process conditions.

## **EXPERIMENTAL PROCEDURES**

Specimens were fabricated as follows: Bamboo fibers were extracted by using a steam explosion method. A starch-based emulsion-type biodegradable resin was used as matrix, and put it on the surface of the bamboo fibers. The preliminary molded composite sheets were obtained after drying at 105°C for 7.2 ks in an oven.

Bamboo fiber-reinforced “green” composites were produced by the hot-pressing using a simple hand operated pressing machine. Sample was hot-pressed at 10 MPa and 140°C for 0.6 ks.

Three points flexural tests and tensile tests were carried out by using an Instron testing machine (Type 5567). Flexural tests were performed at a crosshead speed of 1 mm/min and a span length of 50 mm. Tensile tests were performed at a strain rate of  $6.67 \times 10^{-4} \text{ s}^{-1}$  and a gauge length of 30mm.

## **RESULTS AND DISCUSSIONS**

Both tensile strength and flexural strength for unidirectional composites increased linearly with increasing the fiber content. Their tensile properties, such as tensile strength and Young’s modulus, were described well with the rule of mixture, and their fracture behavior was governed by fiber fracture.

On the other hand, random short fiber composites have much lower strength than unidirectional composites. Both tensile strength and flexural strength of random short fiber composites were strongly affected by fiber aspect ratio and fiber content.

Experimental value of tensile strength of the random short fiber composites with 25 mm bamboo fibers is 45 MPa. This experimental value is almost half of the theoretical strength. Part of this discrepancy is attributed to the fiber/matrix interface adhesion strength. Tensile and flexural strengths of random “green” composites reinforced by short fiber with low aspect ratio were almost similar to those of the “green” composites made from bamboo powders and the same biodegradable resin. The Bamboo fibers with small aspect ratio do not act as reinforcement, but as filler.



## Study on Optically Transparent Composites reinforced with nanofibers

H. Yano, J. Sugiyama, A. N. Nakagaito (Research Institute for Sustainable Humanosphere, Kyoto University), M. Nogi (International Innovation Center, Kyoto University), T. Matsuura (Nippon Telegraph and Telephone Corp.), M. Hikita (NTT Advanced Technology Corp.), K. Handa (Mitsubishi Chemical Corp.)

Mechanical reinforcement of optically functional materials is of significant interest to various industries, due to the rapid expansion of related devices, e.g. displays. Nanocomposite materials with components less than one-tenth of the wavelength in size are free from scattering, making them acceptable for a variety of optical applications. Since fibers could provide the desired mechanical reinforcement of optically functional materials, reinforcement using nanofiber of electrospun nylon-4, 6 was studied. The optically transparent composite was obtained at a fiber ratio of 3.9%, which remains an inevitable difficulty in the way of obtaining high fiber volume composites. Here we report on the first example of a transparent composite reinforced with bacterial nanofibers. The composite is optically transparent at a fiber content as high as 70%, with low thermal expansion coefficient (similar to that of silicon crystal), and mechanical strength five times that of engineered plastics. These significant improvements in thermal and mechanical characteristics of the composite are due to the web-like network of semi-crystalline extended chains of nanofibers, produced by the bacterium *Acetobacter xylinum* (*Glucronobacter aceti*). The nanofiber-network reinforced polymer composite maintains its transparency, it is light, flexible, and easy to mould, thus making it an excellent candidate for a variety of applications, such as, substrate for flexible displays, components for precision optical devices, and windows for automobiles or trains, among others.

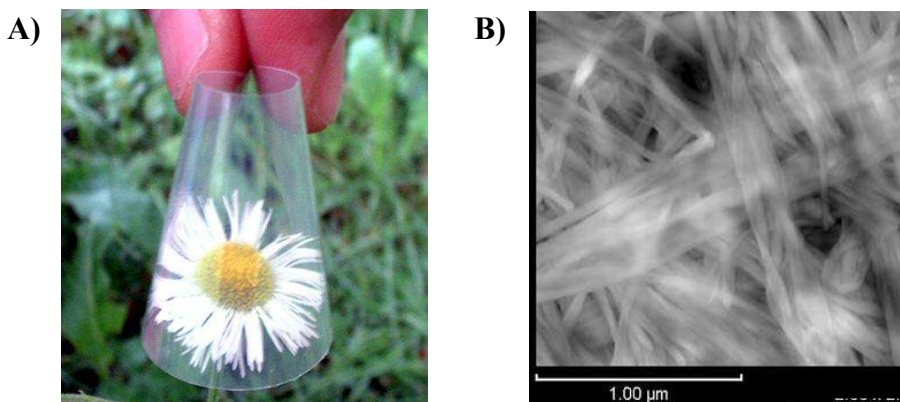


Fig. 1. A) Appearance of 65- $\mu\text{m}$ -thick bacterial cellulose sheet with acrylic resin, 62% fibre content, and B) AFM image, in the tapping mode, of BC/resin sheet (bar: 1  $\mu\text{m}$ ).

# Durable Transparent Materials: Electrospun Nanofibers Infused With Transparent Resin

Carl Krauthauser<sup>1</sup>, Joseph M. Deitzel<sup>1</sup>, John Hrychusko<sup>1</sup>, and Daniel O'Brien<sup>2</sup>

<sup>1</sup>Center for Composite Materials, University of Delaware, Newark, Delaware 19716

<sup>2</sup>U.S. Army Research Laboratory, Composites and Lightweight Structures Branch, Aberdeen Proving Ground, Maryland 21005

## **Introduction**

There is a need for light-weight, impact resistant transparent materials for use in a variety of applications, which could include vehicle windows and windsheilds, hand held protective shields, face shields, and protective eyewear. Solutions using glass and layered polymer/glass composites have the disadvantage of adding a significant weight penalty to a given application and are generally restricted to use in vehicle systems. Applications requiring light weight, such as face shields and protective eyewear, usually employ a transparent polymer resin like polycarbonate(PC) or poly(methyl methacrylate).(PMMA) However, the impact resistance of these materials is limited by their relatively low mechanical properties in comparison to high performance materials like Kevlar and carbon fiber. Reinforcement of these transparent resins with high performance materials is problematic due to the need to maintain optical clarity. Recent efforts by Hsieh [1] have looked at using nanoparticulate fillers and microlayering processing techniques to increase the impact performance of PC, and PC/PMMA blends.

We propose a novel approach to increasing the impact properties of transparent polymer resins like PC and PMMA by reinforcing these resins with high performance polymer nanofibers. The advantages of using nanofibers for reinforcement are two fold. First, the small diameter (~200nm; see Figure 1) of the fibers is below the diffraction limit of visible light ( $\lambda=400-700$  nm), therefore nanofibers dispersed in a transparent medium should not unduly scatter light in the visible range [2]. Second, nanofiber textiles have orders of magnitude greater specific surface area [3] than conventional fabrics, due to the small fiber diameter. The greater surface area will provide more interaction between the resin and reinforcing fiber, improving mechanical properties and potentially increasing the amount of energy dissipated during an impact event due to sliding friction associated with fiber pullout.

## **Experimental**

As a first step, we considered infusing an electrospun Nylon-6,6 non-woven mat with an Epon 828 resin mixed with *bis*-(P-amino)-cyclohexyl-methane (PACM) as a cross-linker in a 100 to 28 ratio. The Nylon-6,6 fibers were electrospun from a 20% w/w solution of Nylon in Formic Acid. The nylon fabric has a macroscopic texture that mirrors the aluminum screen upon which it was collected [3]. Preliminary AFM results suggest that the fiber sizes in the mat are approximately 200 nm or less. To ease the infusion, THF was added to the Epon-PACM resin mixture to reduce viscosity, and wet and dry Nylon samples were infused. After sample curing and post-curing, the samples were visually inspected for transparency. One initial concern was to determine if the amines in PACM provided a mechanism for the dispersion of the Nylon fibers in the Epon 828 resin. The Nylon was mixed with pure PACM and allowed to set for 72 hours with no discernible solvation.

Next generation samples have included infusing electrospun Nylon-6,6 with a Durakane epoxy vinyl-ester resin and with an Epo-Tek optical resin, as well as using electrospun Estane polyurethane with the same resins. The focus in these next generation studies has been three-fold, specifically, i) reducing the viscosity of the resin matrix, ii) determining what level of fiber

volume fraction is possible without significant loss of optical clarity, and iii) what level of enhanced mechanical performance as a function of fiber volume fraction.

### **Results and Discussion**

Results showed that, for the earlier studies, the non-woven mat infused with the Epon 828 resin is indistinguishable from the resin itself. Noticeable imperfections in the sample were due to bubbles that formed in the resin during mixing and curing, which can be eliminated with better processing controls. For some of the earlier samples, a faint outline of the macroscopic texture of the fiber mat can be seen when illuminated from behind with a strong light. The texture was primarily visible in samples that were infused with higher viscosity resins with relatively short gel times. For samples infused with epoxy diluted with THF, the texture is not visible. These preliminary results indicate that complete wet out of the nanofiber fabric is essential to maintaining optical clarity. Furthermore, nanofiber fabrics can be obtained by collecting the fibers on a target with a smooth surface.

Next generation composite samples showed marked improvement in the overall transparency and optical clarity. Earlier samples had fiber volume fractions on the order of 1-2%, while the newer samples had fiber volume fractions of ~10%. The next generation composite samples were also tested for mechanical properties, with preliminary results demonstrating a noticeable improvement in stiffness and durability over the resin matrix samples.

Future efforts will focus on making thin film composites from different combinations of resins (thermoplastic and thermoset) and fibers such as NOMEX and KEVLAR. The mechanical properties of these composite will be evaluated and the composites will be ranked in terms of strength, toughness, modulus and optical clarity. Here it is important to ensure that the non-woven mat is fully wetted, as trapped air tends to diminish the transparency.

### **Conclusions**

In this initial effort, we have infused electrospun Nylon-6,6 with a transparent Epon 828 resin, and demonstrated that nanofiber composite maintains a high degree of transparency. Imperfections in the transparent samples are due to processing and manufacturing issues; infused nano-fibers maintain the visual transparency of the resin used. Further work includes an analysis of the effects on transparency of infusing electrospun Nylon non-woven mats with vinyl-ester and PMMA, as well as using electrospun KEVLAR and NOMEX non-woven mats, and infusing them with all of the above resins. A detailed analysis will include understanding the role of fiber volume fraction, the change in index of refraction due to wet or dry lay-up before infusion, and the limits on transparency due to fiber diameters.

### **References**

- (1) Kearns, J, Hsieh, A, Hiltner, A, Baer, E, *Journal of Applied Polymer Science*, **2000**, 77, 1545-1557
- (2) Bergshoef, MM, Vancso, GJ, *Advanced Materials*, **1999**,11, 1362-1365
- (3) Deitzel, JM, Kleinmeyer, J. Harris, D, Beck Tan, NC, *Polymer*, **2001**, 42, 231-272

## **SUPER TOUGH NANOTUBE COMPOSITE FIBERS FOR ARTIFICIAL MUSCLE AND ELECTRONIC TEXTILE APPLICATIONS**

Alan B. Dalton, Steve Collins, Edgar Muñoz, Joselito M. Razal, Von Howard Ebron, John P. Ferraris, Jonathan N. Coleman, Bog G. Kim and Ray H. Baughman  
Department of Chemistry and The NanoTech Institute  
The University of Texas at Dallas  
Richardson, Texas 75080, USA

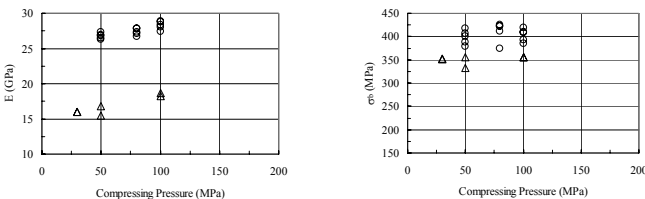
We describe spinning hundred-meter-long carbon nanotube composite fibers having a higher toughness than spider silk or any other natural or synthetic fiber, as well as high tensile strength (1.8 GPa) and modulus (80 GPa). Normalized to density, the strength and modulus is twice that of steel wire. The energy needed to break these fibers is over five times higher than the best spider silk, and at least fifty times the energy to break the same weight steel wire. We make fiber supercapacitors from our spun fibers and weave them into textiles. Long cycle life is demonstrated, as well as a gravimetric energy storage density that approaches that of large supercapacitors operated over the same one-volt potential range. These nanotube composite fibers, which are easily woven or sewn into textiles, are quite interesting for artificial muscles and other electronic textile applications - such as distributed sensors, electronic interconnects, electromagnetic shielding, antennas, and batteries. Such applications and the origin of the attractive fiber properties will be discussed.

# Bacterial cellulose: the ultimate nano-scalar cellulose morphology for the production of high-strength composites

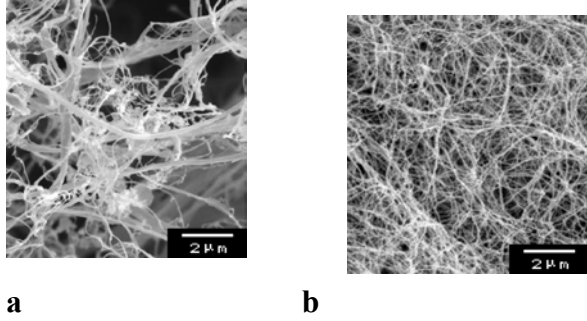
A. N. Nakagaito, S. Iwamoto, H. Yano  
Research Institute for Sustainable Humanosphere  
Kyoto University

Cellulose, being one of the commonest polymers available, is the main cell wall component of almost all plants. The smallest structural units of such cells are called microfibrils, which are comprised of stretched cellulose chains and exhibiting remarkable mechanical properties on a par with aramid fibers. In previous works [1, 2], the present authors produced high-strength isotropic biocomposites utilizing a kind of cellulosic material known as microfibrillated cellulose (MFC), a morphology obtained through the fibrillation of kraft pulp fibers. The bending strength of these composites achieved outstanding values of up to 370MPa, added to an excellent toughness, comparable to those of commercial magnesium alloy. It was found also that the strength of such composites does not vary linearly with the degree of fibrillation of kraft pulp, but rather changes in a stepwise mode, indicating that the fibrillation level is a sine qua non requisite to achieve such high-strength. Notwithstanding, the Young's modulus achieved was somewhat low, at around 19GPa, quite far from the potential provided by the modulus of microfibrils (140GPa) [3].

In the present study, high-strength bio-composites were produced utilizing bacterial cellulose (BC) as a starting material. BC presents as pellicles consisting of a networked structure of a random assembly of ribbon shaped fibrils less than 100nm wide. Although composed of the same cellulose as plants, BC is produced in a way opposed to MFC, as bundles of microfibrils are built from cellulose synthesized and secreted by bacteria. BC sheets were obtained by slight compression of BC pellicles to remove water and oven dried. Sheets were impregnated with phenolic resin, stacked in layers and compressed. The Young's modulus and bending strength as a function of compressing pressure of BC composites are compared to those of MFC composites in Fig. 1, and SEM images of the micro-scale structures of MFC and BC are shown in Fig. 2. The Young's modulus of BC composites achieved values up to 28GPa. There were also a considerable raise in bending strength but not as remarkable as in modulus. The results suggest that the high modulus of BC composites is likely related to the micro-scale order structure of BC, characterized by a continuous network of relatively straight and dimensionally uniform fibril bundles, while the structure of MFC presents as sinuous fibril bundles with a broad dimensional distribution.



**Fig. 1** Young's modulus ( $E$ ) and bending strength ( $\sigma_b$ ) against compressing pressure of: ○ BC-based composites and △ MFC-based composites. Resin content of all BC composites were 12.4%; of MFC composites were 10.3% ~ 12.5%.



**Fig. 2** Scanning electron micrographs of: **a** MFC, and **b** BC pellicle.

#### **REFERENCES**

1. A. N. Nakagaito, H. Yano: Appl. Phys. A, DOI: 10.1007/s00339-003-2225-2
2. A. N. Nakagaito, H. Yano: Appl. Phys. A, 78, 547 (2004)
3. T. Nishino, K. Takano, K. Nakamae, J. Polym. Sci. Pol. Phys., **33**, 1647 (1995)

## **Practical Applications of Thermal Analysis for Fiber-Related Industries**

P. Peter Shang, Bill Haile

Eastman Chemical Company  
Kingsport, TN 37662-5150

### **ABSTRACT**

Polyesters and copolyesters are widely used in fibers, textiles and nonwovens. One of the most useful techniques for characterizing fibers and fibrous materials is thermal analysis. It is not only a tool for R & D activities, but more often is a valuable one for complaint analysis and problem solving. In this paper, we will discuss how to apply thermal analysis, especially differential scanning calorimetry (DSC), to fiber products. It can characterize the crystallization behavior of the polymer before and after extrusion; measure the thermal properties at different stages of the process, such as monitoring the conditions for drawing and heatsetting. It can also be used as a quality control tool to screen the incoming raw materials. With a proper set of sample encapsulation, the effect of moisture on the glass transition temperature of the sample can be determined. Lastly, more recent advanced developments in thermal analysis, like Modulated DSC, Micro TA, Modulated TGA along with Modulated TMA, will be mentioned.

## **Comparison of Effects of Ultraviolet and $^{60}\text{Co}$ Gamma Ray Irradiation on Nylon 6 Mono-filaments**

**Mika Ohtsuka**

Ohtsuka Textile Design Institute, 10, Suga-cho,  
Shinjuku-ku, Tokyo, JAPAN

**Yoshino Suzuki**

Kyouritu Women's University, 2-2-1, Hitotsubashi, Chiyoda-ku, Tokyo, 101, JAPAN

**Tetsuya Sakai**

Kyoritsu Women's University, 2-2-1, Hitotsubashi, Chiyoda-ku, Tokyo, 101, JAPAN

**Anil N. Netravali**

Fiber Science Program, Cornell University, Ithaca, New York 14853, USA

It is well known that high-energy irradiation of polymeric materials generally gives rise to molecular chain scission and/or cross-linking reactions, mainly in the amorphous regions of the specimens. The extent of these reactions depends on the type of polymer. In this paper, the effect of UV and  $^{60}\text{Co}$  gamma radiations on the physical and mechanical properties of nylon 6 mono-filaments with different draw ratios has been studied. Specimens were exposed to either up to 25 Mrad of gamma or up to 168 hrs of intense UV irradiation. The results show that nylon mono-filaments exposed to gamma rays, with much higher quantum energy than UV, undergo a larger extent of molecular chain scission. Higher irradiation dose also results in the production of insoluble, macroscopic three-dimensional cross-linked network structure. The amorphous regions with a lower density of cohesive energy (lower molecular orientation) show a higher extent of cross linking reaction whereas amorphous regions with a higher density of cohesive energy (higher orientation) show higher extent of chain scission reaction, irrespective of UV ray or gamma ray irradiation.



# **Perspectives on Testing Methodology for Fibers and Fiber-Reinforced Rubber-Matrix Composites**

**Dr.A.G. Causa,**  
R&D Fellow (retired)

The Goodyear Tire & Rubber Company, Corporate Research Division, Akron, Ohio, U.S.A.

The objective of this presentation is to provide a brief discussion of the basic principles of predictive testing of fibers, cords and cord-rubber composites. A filament, the most elementary component of a fibrous assembly, can be tested to yield results of important scientific interest (Kawabata et al.) Recent approaches illustrate the use of basic principles of mechanics to the prediction of fiber strength based on its microstructure (Northolt et al.)

In the tire industry most fiber reinforcing materials are utilized in the form of a cord since this type of structure can readily be varied to provide a rather wide range of alternative selections of strength, stiffness (modulus) and fatigue (Hearle et al.) Cords are tested to provide stress-strain behavior as well as creep, stress relaxation and shrinkage force measurements over a temperature range. Most importantly, viscoelastic properties must be obtained under periodic excitation (sinusoidal, pulse, random) at various temperatures, strain amplitudes and frequencies. These measurements give us the values of the cord dynamic complex modulus, its elastic and loss components and the heat generation rate. Classical viscoelastic mechanical models (Maxwell, Kelvin and combinations there of) are useful and provide an elegant mathematical representation of the mechanical behavior. Under fatigue testing conditions interesting micro-structural changes have been observed in polyester fibers (Bunsell et al.)

When cords are embedded in rubber to form a composite structure, the testing and the interpretation of the results become more complex. We have now to consider, besides the cord and rubber properties, the cord-rubber interphase and the critically important geometrical parameters, such as the cord angles and the ply stacking sequence. Some selected examples of all the basic points stated above will be discussed in this presentation.

Important conclusions from this review are:(1) the principles involved in designing and conducting valid predictive test methods cross the lines of many disciplines, such as mechanical engineering, physics, physical-chemistry, statistics, reliability engineering and others. A multidisciplinary approach is required;(2) there is a place for a harmonious coexistence of a deterministic as well as a stochastic approach, as well as phenomenological and microstructural studies, and (3) experimental mechanics must be complemented by finite element analysis, and whenever possible, by analytical closed-form solutions.

## Section C

### Spectroscopic Detection of Cyanide in Water Using Porphyrin Dyed Cotton Fabrics

Huantian Cao, H. James Harmon, Jinhee Nam, Donna H. Branson  
Oklahoma State University, Stillwater, OK 74078

This research is to integrate chemical detection sensor components into textiles, such that the fabric will serve as the platform for the sensors to detect toxic chemicals. This chemical detection smart textile is based on the spectral shift of some colorants when bound with specific chemicals[1, 2]. When dyed onto textile fabric, the colorants have solid phase chemical detection capability. During the first phase of this research, sodium cyanide (NaCN) was selected as the target toxic chemical and two groups of colorants, porphyrins and phthalocyanines, were investigated their detection capabilities.

Phthalocyanines are widely used as textile dyes. The absorbance spectra of six commercial phthalocyanine direct and reactive dyes as well as pure chemical Iron(III) phthalocyanine chloride in the absence and presence of NaCN in solution were measured. No spectral shift was detected in the presence of NaCN for all those phthalocyanines. So, phthalocyanines are not used as candidates for cyanide detection.

In aqueous solution, two porphyrins, meso-tetra(4-carboxyphenyl)porphine (CTPP<sub>4</sub>) and zinc meso-tetra(4-carboxyphenyl)porphine (ZnCTPP<sub>4</sub>), have spectral shifts in the presence of NaCN. The difference spectrum (CTPP<sub>4</sub>+NaCN)-CTPP<sub>4</sub> has a peak at 408nm and a trough at 415nm, and (ZnCTPP<sub>4</sub>+NaCN)-ZnCTPP<sub>4</sub> has a peak at 430nm and a trough at 422nm. For both CTPP<sub>4</sub> and ZnCTPP<sub>4</sub>, there is a linear relationship between change in absorbance and NaCN concentration, which suggests the formation of NaCN-porphyrin complex. In solution, NaCN can be detected at 10ppb level by CTPP<sub>4</sub>, and at 100ppb level by ZnCTPP<sub>4</sub>.

Medium weight, plain weave 100% cotton fabric was slack mercerized by 20% NaOH solution at room temperature for 3 minutes [3]. Solvent dyeing, with 75% ethanol as solvent, was used to dye (immobilize) CTPP<sub>4</sub> onto mercerized cotton fabric. ZnCTPP<sub>4</sub> was base titrated by 1N NaOH solution to dissolve in water and then dyed onto mercerized cotton fabric. There are substantial (visible) amounts of CTPP<sub>4</sub> and ZnCTPP<sub>4</sub> remaining on cotton fabrics after soaked in 1M NaCl solution and 50% ethanol solution, which suggests good immobilization capability. CTPP<sub>4</sub> dyed mercerized cotton fabric has a peak absorbance of 0.28 at 422.5nm, and ZnCTPP<sub>4</sub> dyed mercerized cotton fabric has a peak absorbance of 0.88 at 419nm. In the presence of NaCN, both CTPP<sub>4</sub> dyed and ZnCTPP<sub>4</sub> dyed mercerized cotton fabrics have a spectral shift. The difference spectrum (CTPP<sub>4</sub>+NaCN)-CTPP<sub>4</sub> has a peak at 423nm and a trough at 447nm, and (ZnCTPP<sub>4</sub>+NaCN)-ZnCTPP<sub>4</sub> has a peak at 421nm and a trough at 406nm. Similar to porphyrins in aqueous solution, for both CTPP<sub>4</sub> and ZnCTPP<sub>4</sub> dyed cotton fabrics, there is a linear relationship between change in absorbance and NaCN concentration, which suggests the formation of NaCN-porphyrin complex in solid phase. When dyed onto cotton fabric, NaCN can be detected at 100ppb level by either CTPP<sub>4</sub> or ZnCTPP<sub>4</sub>.

The future work in this research includes identifying suitable porphyrins and/or phthalocyanines that have spectral shift when bound with organophosphates such as parathion or diazinon. Those colorants will be dyed onto textile fabrics and their organophosphate detection capabilities will be investigated. Suitable light source, fiber optics and light detector will be found and embedded into textiles. Chemical detection smart textile prototypes will be developed.

#### Acknowledgement

This work is jointly supported by National Science Foundation and the Intelligence Community through Approaches to Combat Terrorism (ACT) Program under grant 0346448.

#### References

1. Harmon, H. J., *Proceedings of Joint Conference on Point Detection for Chemical and Biological Defense*, Williamsburg, VA, 2000, pp. 505-514.
2. Legako, J. A., White, B. J., and Harmon, H.J., *Sensors and Actuators B. 91 (2003)*, 128-132.
3. Mori, R., Haga, T., Takagishi, T., *Journal of Applied Polymer Science. 65 (1997)*, 155-164.

# Fiber structure development in high-speed melt spinning of *atactic*-PS/*syndiotactic*-PS bicomponent fibers with various cross-sectional configurations

Yoshiaki Hada, Yuta Hoshino, Hiroshi Ito, and Takeshi Kikutani  
Department of Organic and Polymeric Materials,  
Graduate School of Science and Engineering, Tokyo Institute of Technology  
2-12-1, O-okayama, Meguro-ku, Tokyo 152-8552, Japan  
Phone +81-3-5734-2468, Fax +81-3-5734-2876, e-mail: [tkikutan@o.cc.titech.ac.jp](mailto:tkikutan@o.cc.titech.ac.jp)

## Introduction

In comparison with the widely used amorphous polymer, *atactic*-polystyrene (*a*-PS), syndiotactic polystyrene (*s*-PS) is a crystalline polymer and exhibits interesting properties such as high melting temperature, low density and good resistance to chemicals. In applying *s*-PS for the production of fibers, significant development of fiber structure is necessary for the enhancement of mechanical and thermal properties.

On the other hand, it has been reported that bicomponent spinning is a useful method for the control of fiber structure development in the high-speed melt spinning process. In this study, high-speed melt spinning of the bicomponent fibers of *a*-PS and *s*-PS with various cross-sectional configurations were carried out, and structure and properties of the as-spun fibers were investigated. Use of two polymers consisting of the same monomer unit but having different degree of tacticity was with the expectation of gaining high interfacial shear strength between the two polymers.

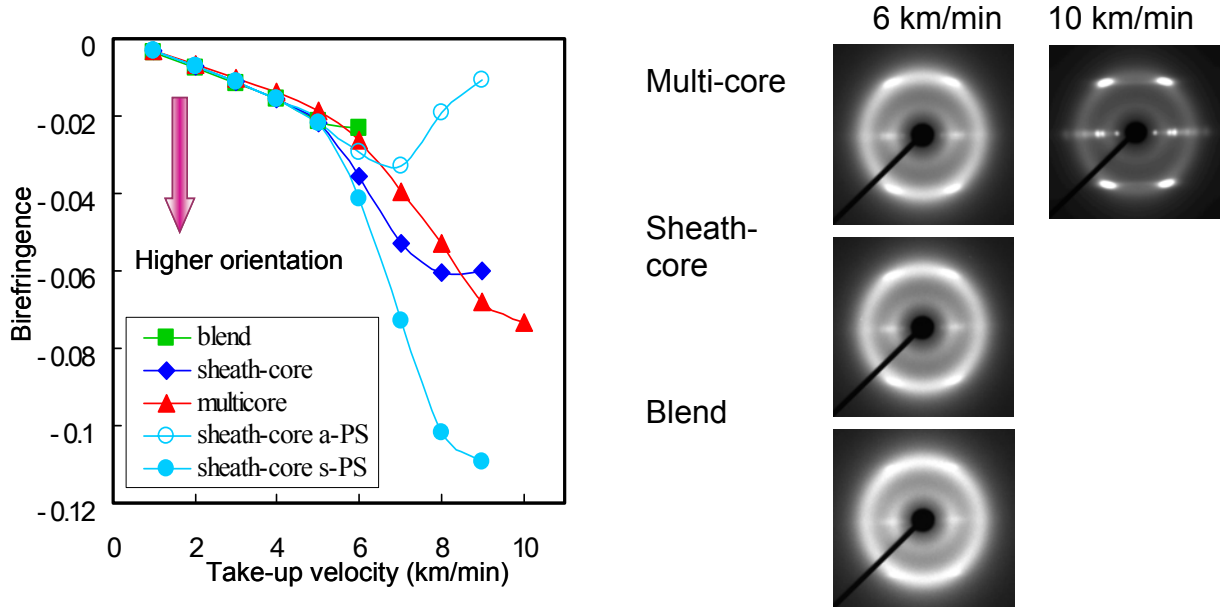
## Experimental

Three different cross-sectional configurations of the bicomponent fiber adopted in this study were blend, sheath-core, and islands-in-the-sea (multi-core) types. The blend type bicomponent fiber was extruded by feeding the mixture of *a*-PS and *s*-PS pellets to a single screw extruder equipped with a metering pump. On the other hand, the sheath-core type and the multi-core type bicomponent fibers were prepared by extruding the melts of *a*-PS and *s*-PS using two different extrusion systems, each of which is consisting of an extruder and a metering pump. Extrusion temperature was set to 290°C. Total throughput rate was 6 g/min, and *a*-PS:*s*-PS composition was 1:1. In the sheath-core type and multi-core type bicomponent fibers, *a*-PS was used as the sheath and the sea component, whereas *s*-PS was used as the core and multi-core component. For comparison, single component melt spinnings of *a*-PS and *s*-PS were also carried at the same extrusion temperature and total throughput rate. For the analysis of the structure and properties of as-spun fibers, birefringence and wide-angle X-ray diffraction (WAXD) pattern measurements, differential scanning calorimetry (DSC) and tensile test were conducted for as-spun fibers. For the better understanding of the mechanism of fiber structure development, measurement of the diameter profile along the spinning line was also carried out using a diameter monitor.

## Results and Discussion

In comparison with the single component spinning of respective polymers, in which attainable highest take-up velocities were 4 and 5 km/min for *a*-PS and *s*-PS respectively, spinnability was significantly improved in bicomponent spinnings. Maximum take-up velocities of 6, 9 and 10 km/min were attained in the bicomponent spinnings of blend type, sheath-core type and multi-core type bicomponent spinnings, respectively.

Dependences of the birefringence of the three types of bicomponent fibers on take-up velocity are shown in Fig. 1. In the sheath-core type bicomponent fibers, it was possible to measure the birefringences of the *a*-PS and *s*-PS components separately. Up to the take-up velocity of 5 km/min, it was difficult to distinguish the two components in the bicomponent fibers under an optical microscope indicating that the two components have similar degree of molecular orientation and also that the *s*-PS component is amorphous. From 6 km/min, absolute value of birefringence started to increase steeply in the sheath-core and multi-core type fibers. Results for the sheath-core type fibers suggested that the molecular orientation of the *s*-PS component increased steeply, whereas that of the *a*-PS component was suppressed significantly in this velocity region. This phenomenon was speculated to be caused by the starting of the orientation-induced crystallization of the *s*-PS component, which was confirmed from the WAXD measurement of the as-spun fibers, in that the bicomponent fibers started to show crystalline reflections from 6 km/min. WAXD patterns of the three types of bicomponent fibers obtained at 6 km/min are compared in Fig.2. WAXD pattern of multi-core type fiber prepared at 10 km/min is also shown in the figure. If structure and mechanical properties of the fibers obtained at the attainable highest take-up velocities were compared, bicomponent high-speed melt spinning could yield fibers with enhanced structure and mechanical properties than the single component spinning of *s*-PS. Among the three types of bicomponent fibers, the multi-core type fiber showed the highest degree of fiber structure development of *s*-PS component, which was represented by the highest values of molecular orientation, melting point and tensile modulus.



**Fig.1** Birefringence vs. take-up velocity for various bicomponent fibers.

**Fig.2** WAXD patterns of high-speed spun bicomponent fibers with various cross-sectional configurations.

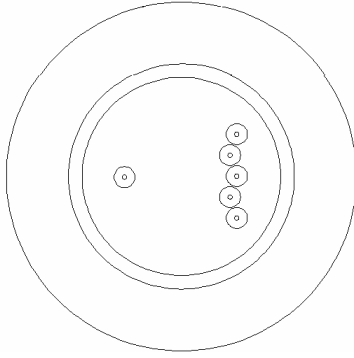
## **Real Time Evolution of Fiber Structure During Melt-Spinning**

K. Stevens (Center for Advanced Engineering Fibers and Films, Clemson University), G. Lickfield (School of Materials Science & Engineering, Clemson University), P. Lopes (Chemistry, Clemson University), S. Varkol (Materials Science and Engineering, Clemson University).

The objective of this research is to investigate the development of fiber structure during the melt-spinning process in real time. To fully understand the development of structure it is important to realize that fiber structure is directly responsible for the resulting fiber properties. Currently there is limited information relating the evolution of fiber structure to the actual spinning process. In an attempt to understand the evolution of fiber morphology in the spin line, additional data is necessary. Numerous studies have been undertaken to investigate characterization of this process on-line. In an attempt to understand how the development of fiber morphology occurs in the spin line, on-line x-ray patterns as a function of distance from the spinneret have been measured by other workers using synchrotron radiation. However, the use of synchrotron radiation restricts the utilization of larger extruders, i.e., on a scale similar to those utilized industrially. Additionally, reported studies using synchrotron radiation were not able to access the region close to the spinneret (within 30 cm of exit) and the take-up speeds were usually low (less than 60 m/min) or in a limited range. Our equipment is designed to overcome both of these obstacles. The advantage that this research group has is the capability to measure a number of parameters simultaneously and on-line. By coupling velocity, diameter and temperature measurements with the x-ray information obtained a more complete picture of the process is produced. Velocity and diameter measurements enable the selection of the appropriate region of the spin-line for x-ray analysis. The temperature profile may also highlight the region of the spin-line where crystallization is most severe. The ultimate structure and therefore properties of the fiber is a consequence of the processing conditions and as such a number of conditions were studied.

Suitable melt spinning temperature profiles were established and a matrix of experiments prepared. The Center for Advanced Engineering Fibers & Films ( CAEFF) team designed a novel spinneret to allow isolation of a single filament (Diagram 1). A six hole spinneret configuration was selected as preliminary experiments had already been carried out using a spinneret with 6 centrally aligned holes. The research team also fabricated suitable fixtures for the optimum positioning of the instruments around the spin-line. The platform can be positioned with millimeter accuracy and as such the relative positions of the instrument are accurately maintained.

The diameter measurements have provided results similar to those expected. As anticipated the diameter is at its smallest when the platform is at its lowest position, i.e. furthest away from the spinneret exit. There is also a region of the spin-line where the diameter varies considerably. This is assumed to be the area where necking is taking place, as this position is known to fluctuate, thus giving a higher variability in the average diameter values obtained.



The use of this novel spinneret design enabled a suitable sample volume to be focused in the x-ray beam consequently improving the quality of the x-ray diffracted signal when compared to a single hole configuration. This allowed shorter exposure times (from 4 hours to 1 hour), and contributed to an increase of the sample to background signal ratio. The separation of the sixth filament provides the isolation necessary for diameter and temperature measurements.

Diagram 1: *Novel Spinneret Design*

The Fiber Temperature Measurement System (FTMS) utilizes a system based on two-color pyrometry using cryogenic IR detection systems. This instrument is intended to map the temperature variation along the spin-line.

The method utilized for in-situ determination of structure development during processing was on-line, real time x-ray diffraction (XRD) during the fiber formation process. The crystalline material, characterized by long-range order, is amenable to measurement by wide-angle X-ray diffraction (WAXD). The orientation of the crystalline regions is also obtained using this analytical method.

The unique ability to combine these simultaneously obtained data allows full characterization of the spin-line as the polymer undergoes transformation from molten amorphous material as it exits the spinneret to semi-crystalline fiber. Essentially the spin-line is mapped and the point at which the metamorphosis is the greatest can be observed in relation to the spinning conditions utilized. Ultimately this data is used to confirm mathematical models being developed here at Clemson in the Center for Advanced Engineering Fibers and Films.

Results from the on-line study of isotactic polypropylene (*i*PP) using a variety of selected processing conditions, including wind-up speeds, extrusion temperatures and flow rates, at various points along the thread-line during fiber production will be presented.

# Characterization of the Dissolution Power of Organic Polar Solvents at High Temperatures for Wet-spinning of Stereoregular Isotactic Poly(acrylonitrile) by Using Raman Spectroscopy

Masatomo Minagawa,<sup>\*†</sup> Tomochika Matsuyama,<sup>‡</sup> and Nobuhiro Satoh<sup>‡</sup>

Department of Polymer Science and Engineering, Faculty of Engineering, Yamagata University, Yonezawa 992-8510; and Research Reactor Institute, Kyoto University, Kumatori 590-0494, Japan

## ABSTRACT:

As a preliminary study for the preparation of high-quality carbon fiber, solvent properties of six kinds of dipolar aprotic solvents toward stereoregular isotactic poly(acrylonitrile) (PAN) prepared by urea clathrate polymerization at low temperatures were studied by using a laboratory constructed laser-optical instrument and Raman spectroscopy. The dissolution temperature ( $T_{sol}$ ) of a series of stereoregular PAN samples with different isotacticities (ca. 25-83%) was determined. The value of  $T_{sol}$  was from  $-60^{\circ}$  to  $+180^{\circ}$  according to the difference of stereoregularity of PAN. Plots of  $T_{sol}$  against the inverse value of isotacticity were linear, from which two empirical parameters characterizing the dissolution power of these solvents toward isotactic PAN were derived. This was in the following order: dimethyl sulfoxide (DMSO) > ethylene carbonate (EC) > N,N-dimethylformamide (DMF) >  $\gamma$ -butyrolactone (G-BuL) > tetramethylene sulfone (TMS) > N,N-dimethylacetamide (DMAc). The intermolecular interaction between solvent and nitriles was evaluated by Raman spectra. Based on these results, the best solvent was determined, and the specific dissolution mechanism of isotactic PAN in these solvents at high temperatures was discussed.

<sup>†</sup>Yamagata University. <sup>‡</sup>Kyoto University.



# ELECTROSTATIC PRODUCTION OF NANOFIBERS: PHYSICS AND APPLICATIONS

S. V. Fridrikh<sup>1</sup>, J. H. Yu<sup>1</sup>, M. P. Brenner<sup>2</sup>, G. C. Rutledge<sup>1</sup>

<sup>1</sup>Department of Chemical Engineering  
Massachusetts Institute of Technology  
77 Massachusetts Avenue, Cambridge, MA 02139

<sup>2</sup>Division of Engineering and Applied Sciences  
Harvard University  
29 Oxford Street, Cambridge, MA 02139

Electrostatic production of fibers as small as 100nm (nanofibers) known as electrospinning has recently become an object of intensive experimental research due to potentially broad markets for the nanofibers. The understanding of the physics of the process and the fundamental model thereof are still lacking. We present here the theory of electrospinning accounting for non-linear effects such as the thinning of the jet and strain hardening. The model predicts the amplitude of the whipping instability causing the formation of nanofibers to saturate and the jet to reach the terminal diameter controlled by the surface tension, surface charge repulsion and solvent evaporation.

The model is tested extensively for various systems covering a broad range of material properties such as conductivity, zero shear rate viscosity, concentration and polymer molecular weight. The fiber diameters are shown to be in very good agreement with predictions. Our experimental data also proves that zero shear viscosity affects the stretching rate of the jet but not the final fiber diameter.

The role of fluid elasticity in formation of uniform fibers was investigated experimentally. It is known that even very viscous Newtonian fluids such as glycerol are prone to Rayleigh instability and break into the droplets during electrospinning. A similar effect is observed when polymer solutions with no pronounced elastic effects are electrospun. We demonstrate that elastic properties of the fluid are crucial to its processability into uniform fibers by electrospinning. The product of molecular relaxation time and the strain rate appears to be one of the key parameters controlling transition from spinning of uniform fibers to the regime when beaded fibers are produced. Experiments with Boger fluids at polymer concentrations as low as 0.1 C\* allow us to conclude that elasticity of the fluid, but not necessarily entanglement, is crucial for the formation of the uniform fibers

The need for nanofibers from materials that can not be electrospun on their own, such as natural silk and various conducting polymers, prompted further advancement of the electrospinning technology to process these materials. The common feature of the difficult to process materials is usually their weak elasticity. We have developed a method which compensates for this lack of elasticity by simultaneously spinning two polymer solutions in a co-axial configuration. The jet comprises a core fluid, that may consist of difficult-to-process material, and a shell fluid, consisting of some electrospinnable elastic fluid. The resulting fiber is uniform and exhibits a

core-shell morphology. The shell serves as a process aid to the core material and can be removed in post-processing. Using this co-spinning technology we have successfully produced uniform fibers from silk worm silk and conducting polymer (PANi). The method also allows for electrospinning of low concentration solution leading to production of smaller fibers. We have produced PAN fibers with diameters of 50nm, three times smaller than those produced by a single fluid electrospinning technique.

# Flow behavior in electrostatically driven jets of polymer solution

J. M. Deitzel<sup>1</sup>, C. Krauthauser<sup>1</sup>, J. Kleinmeyer<sup>2</sup>

<sup>1</sup>Center for Composite Materials  
University of Delaware  
Newark, Delaware 19716

<sup>2</sup>Xiotech Corporation  
8516 Springway Rd  
Ellicott City MD 21043.

## Abstract

In recent years there has been an explosion of interest [1,2,3] in electrospun polymer fibers. These fibers generally range from 10 nm to a micron in diameter, depending on processing variables such as solution viscosity, electric field strength and feed rate. The fibers are obtained through use of an electrostatically driven jet of polymer solution which is collected on an electrically ground target. Electrospun fabrics are generally characterized by high surface area and small pore size, making the materials excellent candidates for filtration and barrier applications. These materials are also of interest for a variety of other applications including nanoelectronics, biomedical applications, and optical devices.

Although the number of potential applications for electrospun fibers is growing exponentially, the influence of solution properties and processing variables on the stability of the electrospinning jet are still only dimly understood. Many of the proposed applications involve the use of additives to the polymer solution, which will provide additional functionality to the electrospun fabric in terms of conductivity, mechanical properties, or chemical sensitivity. These additives range from carbon nanotubes to biological molecules, which may further complicate the properties of the polymer solution in terms of viscosity, conductivity, and phase behavior, all of which influence the stability of the electrospinning jet. Recent [4,5,6] attempts at modeling an idealized electrospinning process have met with limited success. The majority of these modeling efforts have focused on describing the onset and growth of the “bending instability” inherent in the electrospinning process. However, there is very little experimental data obtained from direct observation of the electrospinning jet, to which the results of these models can be compared.

The purpose of the current work is to use real time imaging techniques at high magnification to begin to understand how these additives affect jet stability and fluid flow in the electrospinning process. The current work uses conventional and high speed imaging techniques to study the motion of particles in the linear portion of electrostatically driven jets Polyethylene oxide/water solutions. Observation of the motion of carbon particles using conventional video reveals the presence of eddy currents in the meniscus from which the jet originates. High-speed video of the motion urethane particles in the liquid jet has been used to measure jet velocities, which range from 2-4 meters/second depending on initial processing conditions. The effect of solution viscosity, field strength, and flow rate on jet velocity will be discussed in detail. Additionally, the effect of polymer concentration on jet initiation has been observed and will be discussed.

## References

- (4) Gibson, PW, Shreuder-Gibson, HL, *AICHE*. **1999**, *45*, 190-194.
- (5) Deitzel, JM, Kleinmeyer, J. Harris, D, Beck Tan, NC, *Polymer*, **2001**, *42*, 231-272
- (6) Larsen, G, Velarde-Ortez, R. Minchow, K, Barrero, A, Loscertales, IG, *J. AM. CHEM. SOC.*, **2003**, *125*, 1155
- (7) Feng, JJ, *Physics of Fluids*, **2002**, *14*, 3912-3926
- (8) Hohman, MM, Shin, M, Rutledge, G., Brenner, MP, *Physics of Fluids*, **2001**, *13*, 2221-2236
- (9) Yarin, AL, Koombhongse, S, Reneker, DH, *Journal of Applied Physics*, **2001**, *90*, 4836-4846

## **Spinning of Nanofibers by Electron Injection**

D.R. Salem<sup>1</sup>, A.J. Kelly<sup>1</sup>, K. Kornev<sup>2</sup> and S.K. Kurtz<sup>3</sup>

<sup>1</sup>Charge Injection Technologies Inc., <sup>2</sup>TRI/Princeton, <sup>3</sup>Pennsylvania State University

Conventional, ‘needle’ based electrospinning of nanofibers has two fundamental limitations that have impeded commercial use. The first is that the polymer spinning rates that can be achieved are very low. The second is that the system being spun must have sufficient conductivity. Electron injection technology overcomes the spinning rate limitations inherent in needle based electrospinning of nanofibers and can also be applied to non-conductive systems of commercial importance.

The first part of the paper describes the principles of dispersing liquids by two distinct electron injection methods, both of which can be applied to the production of polymer nanofibers at high throughput rates. Scanning electron microscope images are presented, showing nanofiber webs produced from different polymer systems at throughput speeds in the region of 1-4 g/s per orifice and the web morphologies are discussed.

In the second part of the paper, an effort is made to understand the physics of electron-injection fiber formation. Previous analyses in the literature have been focused on conventional electrospinning phenomena, in which an external electric field is applied. In the present study, we analyze the basic principles of fiber formation in the injection mode where the liquid polymer emerges from the orifice in a charged state and where electrons are not restricted to the surface of the filaments, but are distributed throughout their cross-section. Using a thermodynamic approach to the phenomenon, the conditions for liquid break-up and fiber formation are predicted.

## **Building Novel Functions on Ultra-Fine Fiber Surfaces**

You-Lo Hsieh

Fiber and Polymer Science  
University of California at Davis  
One Shields Avenue  
Davis, CA 95616

The intrinsic/inherent physical characteristics of fibrous materials including porosity, high surface to volume ratio, and flexibility, give unique advantages over other solid forms of materials. Full exploitation of these physical attributes, such as reducing fiber sizes, altering cross-sectional features and modifying fiber arrangements, further expand these advantages. Chemical properties of fibers are generally more limited in comparison to the much wider range of chemistry among polymers. This paper reports the most recent work in our laboratory in the areas of increasing surface reactivity and adding chemical functionalities to fibers. Our effort includes approaches directed toward devising the fiber formation processes as well as the chemical reactions and polymer syntheses. Activation of fiber surface has been demonstrated via chemical reactions, attachment of polymerizable structures, enzyme catalyzed reactions and redox initiated grafting. Design of various linear and crosslinked structures at molecular level to macroscopic extents can be accomplished via reaction control. Novel properties such as hydrophilic, hydrophobic, ionic and chelating, amphiphilic, electrolytic, and stimuli-responsive behaviors have been demonstrated. Improved wetting and transport, controlled release of compounds, temperature and/or pH responsive pore size control, and enzyme stabilization against the environmental factors further exemplify the potential of these novel chemical functionalities.

### Acknowledgement:

Findings for this presentation have been drawn from experimental work conducted by Drs. Yuhong Wang, Hong Chen, Jiangbing Xie and Haiqing Liu. The financial supports for this research from National Textile Center and the University of California at Davis are greatly appreciated.

# **PRODUCTION OF CROSSLINKED PET NANOFIBER/ MICROFIBER STRUCTURES VIA ELECTROSPINNING**

Philip J Brown and Darren A Baker

School of Materials Science and Engineering  
Clemson University, Clemson SC 29634  
Email [pjb@Clemson.edu](mailto:pjb@Clemson.edu)

## **Abstract**

Appropriate azide crosslinking agents have been synthesized and used as additives in polymer solutions that can be electrospun to produce nanofiber and microfiber substrates. These azides essentially react to crosslink, functionalize and covalently bind PET polymer chains. Electrospinning mixtures of PET with these additives allows for fiber modification during or after the electrospinning process as heat can be used to initiate the crosslinking reaction. Modification of nanofiber/microfiber substrates in this study was done by thermal post-spin treatments. This study demonstrates the effectiveness of the technique in modifying 100% PET electrospun substrates. The study shows how the process inherently changes the properties of the electrospun fibers including fiber T<sub>g</sub>, melt temperature and how different azides over a series of concentrations effect the fundamental thermal properties of the fibers.

## Preparation of Conducting Nylon 6 Electrospun by *in situ* Polymerization of Polyaniline

Tae Jin Kang<sup>1</sup>, Kyung Hwa Hong<sup>1</sup>, Kyung Wha Oh<sup>2</sup>

<sup>1</sup> School of Materials Science & Engineering, Seoul National University, Seoul 151-742, Korea

<sup>2</sup> Department of Home Economics Education, Chung-Ang University, Seoul 156-756, Korea

### Abstract:

Thin fibers provide unexpected high surface area to volume ratios and are of interest for many applications ranging from textile to composite reinforcement. For this reason, many scientists and engineers are attracted by the nanofibers these days. Particularly if conducting polymers were manufactured as a form of nanofibers, their conducting properties would be enhanced and so their applications would be more effective. In this study we prepared the Polyaniline (PANI)-nylon 6 composite nanofibers web (electrospun) by using the electrospinning process and *in-situ* polymerization of PANI. The conductivities of PANI-nylon 6 composite electrospuns were usually superior to those of other PANI coated materials such as PANI-nylon 6 plain weave fabrics due to their high surface area to volume ratios. On the other hand, the surface conductivities of PANI-nylon 6 composite electrospuns were increased but their surface conductivities were decreased with increasing the diffusion time in aniline diffusion bath. The PANI-nylon 6 composite electrospuns were also characterized by FT-IR, ESCA, and their morphologies.

**Key words:** electrospinning, nanofiber, polyaniline (PANI), conductive polymer, nylon 6.



# Field-responsive Magnetic Composite Nanofibers by Electrospinning

M. Wang, H. Singh, T.A. Hatton, G.C. Rutledge\*

Institute for Soldier Nanotechnologies and Department of Chemical Engineering

Massachusetts Institute of Technology, Cambridge, MA, 02139, U.S.A.

## Abstract

Magnetic composite fibers, in which magnetic nanoparticles are embedded into a polymeric fiber matrix, can be expected to exhibit interesting magnetic field-dependent mechanical behavior with potential applications in a range of areas such as protective clothing for military and first-response personnel. In a uniform external magnetic field, such magnetic nanoparticles within the fibers would be expected to align with their magnetic moments in the direction of the magnetic field such that when the fiber is deformed, extra energy is needed to disrupt the alignment of the nanoparticle chains within the fiber, resulting in its increased stiffness. In a nonuniform magnetic field, the magnetic nanofibers should also deform or bend in the direction of the gradient of the magnetic field. These changes in stiffness and shape should be completely reversible. The relative magnitude of these effects is expected to increase as the diameter of the embedding polymer fiber is reduced.

In this study, magnetic polymeric nanofibers ranging in diameter from 140 to 400 nm were produced via an electrospinning technique from colloiddally-stable suspensions of magnetite nanoparticles with diameter in 7.5 nm in polyethylene oxide and polyvinyl alcohol solutions. The particles of this size are superparamagnetic, exhibiting strong paramagnetic properties with large susceptibility. The magnetic composite nanofibers were characterized by transmission electron microscopy (TEM), super conducting quantum interference device (SQUID) test, and atomic force microscopy (AFM) nanoindentation. The nanoparticles were observed to align within the fibers in columns parallel to the fiber axis direction, apparently induced by the electrospinning process. The nanofibers were superparamagnetic at room temperature, and responded to an externally-applied magnetic field by deflecting in the direction of increasing field gradient. Nanoindentation tests showed that magnetite nanoparticles reinforced the mechanical properties of nanofibers, although the significant amount of short-chain polymer adsorbed to the nanoparticles to ensure their suspension stability increased the inelastic deformation of the nanofibers.

A mathematic model was also developed to predict the changing stiffness or shape of nanofibers in response to external uniform or nonuniform magnetic fields. These changes in stiffness and shape were found to be correlated closely with the sizes of the particles in the nanofibers. The deflection of nanofibers containing particles with diameter of 7.5 nm in an external nonuniform magnetic field was conducted and the experimental results were compared favorably with results predicted by the model.

## Section D

### Numerical model of the fiber flow in compact spinning

Daniel Gantner, ETH Zurich, Institute for Manufacturing Automation, CH-8092 Zurich, Switzerland

Compact spinning is becoming an important system in short staple spinning because it is advantageous for high tenacity and low hairiness. Compact spinning is used for fine cotton yarn less than 20 tex. It works with a combination of different forces acting on the fibers. The model proposed in this paper enables to simulate the fiber flow in the draft zone including the binding-in of fibers by twist.

The behavior of fibers under the impact of mechanical forces and air-flow is treated by concurrent simulation of a multitude of single fibers. The model is 3-dimensional and incorporates the binding-in of fibers by twist. The migration of an individual fiber can be followed through its creation in the drafting and yarn forming process. The interaction of fibers is taken in account by the friction existing between their bodies. This model reveals the basic differences between alternative solutions for the air flow induced compaction of the fiber flow in the draft zone.

The fiber model proposed in this paper is the concatenated mass point model (compare the bead-elastic rod model [1]). The fiber is assumed to be a chain consisting of  $n$  mass points connected by  $n - 1$  connecting rods. The mass of a mass point is  $m$ . The connecting rods are without mass, they are straight and lengthwise elastic.

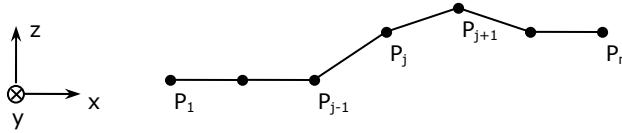


FIGURE 1: Schematic of fiber model

The fiber motion depends on several forces. When the fiber flow immersed in the air flow, it is subjected to air drag. The air-flow is approximated by a flow generated by a superposition of (2-dimensional) analytical solutions of the Poisson equation with different locations of several sinks according to the potential-flow theory [2]. The resulting force (fiber  $i$ , mass point  $j$ ) is:  $F_{af,ij}$ . The chain is elastic and flexible, for it can change its length by changing the distance between adjacent mass points, and can bend by changing the angle between successive connecting rods. By moving the mass points of a fiber out of its equilibrium position, a restoring force is exerted on the mass points. If the distance between two adjacent mass points is stretched, the following force has an effect on the mass point:  $F_{e,ij}$ . If the path of successive connecting rods is out of its equilibrium position, the following force has an effect on the mass point:  $F_{b,ij}$ . The friction between two mass points, and between mass point and external mechanical bodies, is leading to a frictional force:  $F_{r,ij}$ . Furthermore, in the case of a twisting motion, a centrifugal force acts on the mass points:  $F_{c,ij}$ .

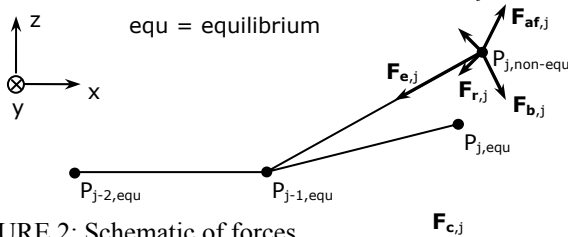


FIGURE 2: Schematic of forces

Thus, the system has to satisfy the equilibrium equations of all the mass points of all fibers:

$$m \frac{\partial^2 \mathbf{r}_{ij}}{\partial t^2} = \mathbf{F}_{af,ij} + \mathbf{F}_{e,ij} + \mathbf{F}_{b,ij} + \mathbf{F}_{r,ij} + \mathbf{F}_{c,ij}$$

where  $\mathbf{r}_{ij}$  is the position of mass point  $j$  of fiber  $i$ , and  $m$ ,  $\mathbf{F}_{af,ij}$ ,  $\mathbf{F}_{e,ij}$ ,  $\mathbf{F}_{b,ij}$ ,  $\mathbf{F}_{r,ij}$ ,  $\mathbf{F}_{c,ij}$ , are forces on the mass point as defined earlier.

Fiber to fiber interactions takes place if two mass points are positioned in a minimum distance representing mechanical contact. The friction force  $\mathbf{F}_{r,ij}$ , as defined earlier, is the first part of this fiber to fiber interaction. In addition, a mass point may push another mass point. This interaction is based on the principle of linear momentum (elastic impulse).

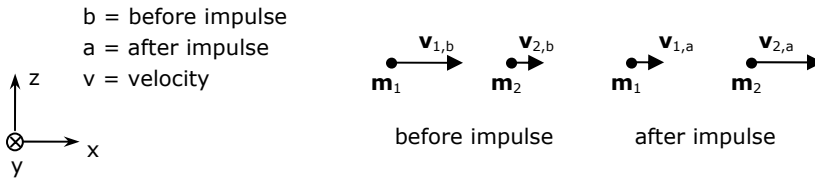


FIGURE 3: Principle of linear momentum (1-dimensional)

The equations are (1-dimensional,  $m_1 = m_2 = m$ ):

$$v_{1,a} = v_{1,b}, \quad v_{2,a} = v_{1,b}$$

In order to model fiber to fiber interactions, a discrete grid is used for calculation. Mass points are assumed a place in one of these discrete points.

To solve the problem, a numerical simulation is used. First, initial conditions of newly-created fibers, including an initial position of each mass point of the fiber, are set at time  $t$ . Second,  $\mathbf{F}_{af,ij}$ ,  $\mathbf{F}_{e,ij}$ ,  $\mathbf{F}_{b,ij}$ ,  $\mathbf{F}_{r,ij}$  and  $\mathbf{F}_{c,ij}$  of each mass point are calculated. Third, fiber to fiber interactions are taken in account. Fourth, new coordinates of  $\mathbf{r}_{ij}$  and the velocity  $\mathbf{v}_{ij}$  are calculated at time  $t + \Delta t$ . Fifth, by repeating the procedure from the first to the fourth step, the motion of all mass points is calculated.

By comparing the basic findings, like migration of mass points in the fiber flow, or the hairiness of the resulting yarn, the computation results coincide well with the experimental observations. Hairiness and compactness of the resulting yarn as well as the amount of lost fibers at the spinning triangle can be taken from the yarn exiting the simulation model. Thus, alternative ways of air flow induced compaction can be compared.

Literature cited:

- [1] Zeng, Y. C., and Yu, C. W., Numerical Simulation of Fiber Motion in the Nozzle of an Air-Jet Spinning Machine, *Textile Res. J.* **74**(2), 117-122 (2004).
- [2] Wilcox, D.C., *Basic Fluid Mechanics*, DCW Industries, La Cañada, CA, 331-390 (1997).

# Strain Localization during Adiabatic Extension of Nylon Filaments

Thomas A. Godfrey

*Natick Soldier Center  
US Army RDE Command  
Natick, Massachusetts 01760-5020, U.S.A.*

## Introduction

It has long been recognized that thermo-mechanical coupling and thermal softening have a significant affect on the adiabatic deformation of thermoplastics (Vincent, 1960a, 1960b). In the particular case of thermoplastic fibers, which differ from bulk thermoplastics in that the polymer is highly oriented, early investigators observed that when certain fibers were extended to failure at high-strain rates, the broken fiber ends exhibited a characteristic mushroom shape that appeared to be a melted blob of polymer (Holden, 1959). Hearle et al. (1998) studied high quality SEM images of such mushroom-shaped fiber breaks resulting from high rate tests of polyester fibers. They concluded that the failure process begins with localized adiabatic straining at the eventual rupture site. After rupture, the locally heated polymer near the break expands due to entropic forces driving the oriented polymer to an amorphous state, and the expansion generates the observed end swell and mushroom cap. Haward (2003) investigated the adiabatic extension process in polyester and nylon fibers and has shown that the softening effect due to increase in temperature exceeds the opposing influence of strain hardening, so that nominal stress falls continuously with increasing strain. Haward interpreted the falling stress condition using the Vincent-Considerere criteria (Vincent, 1966) as leading to localization and fracture, corroborating the theory given by Hearle and co-workers (1998) for the generation of mushroom fractures.

In this paper, the conditions leading to adiabatic strain localization are studied from the standpoint of the equations of motion and energy balance for a fiber extended at a high rate. The stability of homogeneous straining motion is investigated using a perturbation approach, where an initial small disturbance is assumed, making the strain distribution along the fiber slightly non-uniform. The analytical model suggests that, for fibers with particular thermo-mechanical and constitutive properties, initial nominally uniform strain distributions along the fiber will tend to become non-uniform, with localization of axial strain into a thermally softened region. To assess the usefulness of the model in predicting and interpreting fiber behavior, a commercial nylon filament is investigated experimentally. Nylon filaments are extended to break at a low, isothermal strain rate ( $0.0015 \text{ s}^{-1}$ ) and at a high, adiabatic strain rate ( $70 \text{ s}^{-1}$ ). A dimensionless *strain localization parameter* (SLP), used to characterize the nylon filament in the framework of the model, predicts strain localization to occur during extension at the  $70 \text{ s}^{-1}$  strain rate. Experimental load-extension curves exhibit a sharply reduced elongation-to-break at the high strain rate, consistent with the predicted occurrence of localized, versus uniform, straining. In addition, the transition from homogeneous to localized straining appears to occur at elongations that correspond with the SLP attaining a critical value for onset of localization.

## Stability Analysis

The equations of motion and energy balance are formulated for the fiber undergoing high constant rate of extension. The fiber is assumed to exhibit linear strain hardening and linear thermal softening for a short period following an arbitrary moment in time at which the stability of uniform straining is in question. Equations are obtained for the behavior of perturbed displacements and temperatures reflecting a small disturbance from the nominal state of increasing homogeneous strain and temperature. For values of a dimensionless *strain localization parameter* (SLP) less than one, the perturbations are found to decay, with some oscillation, to stationary values less than their initial values. Therefore, homogeneous straining motion is stable for SLP values less than one. For values of the parameter greater than one, the perturbations grow in time, suggesting a trend toward localized straining. It is likely that, for SLP values greater than one, adiabatic strain localization will continue until rupture of the fiber, due to the onset of elastic unloading of the fiber outside of the strain localization band. During elastic unloading, strain energy from outside the band drives further strain localization within the band. The SLP is written as,  $SLP = \frac{a\eta p_0}{b\rho cAT_0}$ , where  $a$  is the thermal softening coefficient,  $b$  is the strain hardening coefficient,  $p_0$  is the fiber load,  $\eta$  is the fraction of plastic work dissipated as heat,  $\rho$  is density,  $c$  is specific heat,  $A$  is fiber cross-sectional area, and  $T_0$  is the temperature.

## Experiments

A commercial nylon filament, about 140  $\mu\text{m}$  in diameter, sold for use as monofilament sewing thread, was investigated. Filament specimens, nominally 60 mm long, were extended to break at a strain rate of  $0.0015\text{ s}^{-1}$  using an Instron test machine, and at a strain rate of about  $70\text{ s}^{-1}$  using a simple drop weight test device. Typical high-rate and low-rate load-elongation curves are exhibited in Fig. 1. It can be seen that specimen breaks at a lower elongation in the high-rate test as compared with the low-rate test. The experimental distributions for elongation-to-break in the high-rate and low-rate tests were compared and found to have very little overlap. Mean high rate and low rate elongation-to-break were 0.25 and 0.32, respectively.

## Discussion and Conclusion

Typically in localization phenomena, regions of increasing deformation become contained in narrow bands, as elastic unloading occurs outside the bands (Bazant and Cedolin, 1991). In filament specimens of length far greater than the filament diameter, it is reasonable to expect that the localization band will be a small fraction of the specimen length. Rupture of the specimen should occur soon after the development of the localization band, and the elongation-to-break of the specimen should be very close to the elongation at which strain localization initiates. Fitting constitutive parameters using the low rate tests and additional elevated temperature tests, we estimate the value of the high rate SLP as the specimen is extended. The estimates were calculated based on five typical low-rate load-extension curves and are exhibited in Fig. 2. At the beginning of plastic extension, the estimated value of the strain localization parameter is about 0.18. The value of the SLP steadily increases with increasing extension, attaining a value of one at elongations ranging from 0.23 to 0.27. These estimates for the onset of strain localization in high-rate extension compare favorably with the high-rate elongation-to-break results (mean: 0.25). The good agreement supports the above interpretation of the localization and failure process, and corroborates the stability analysis.

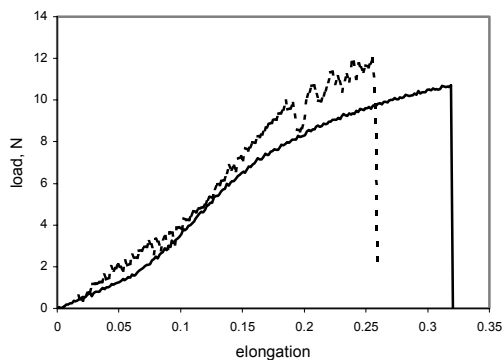


Fig. 1 Typical low rate (solid line) and high rate (dotted line) load-elongation curves.

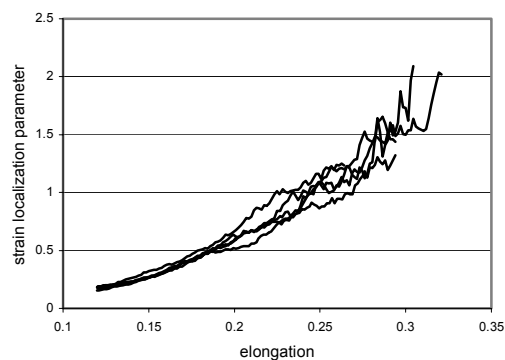


Fig. 2 Estimated SLP with increasing elongation using data from five typical low rate tests.

## References

- Bazant, Z.P., and Cedolin, L., 1991, "Stability of Structures," Oxford University Press, New York, p. 845.
- Haward, R.N., 2003, The Adiabatic Fracture of Thermoplastic Fibres, *J. Mater. Sci.* 38, 2155-2160.
- Hearle, J.W.S., Lomas, B., and Cooke, W.D., 1998, "Atlas of Fibre Fracture and Damage to Textiles," C.R.C., Boca Raton.
- Holden, G., 1959, Tensile Properties of Textile Fibres at Very High Rates of Extension, *J. Textile Inst.* 50, T41-54.
- Vincent, P.I., 1960a, The Necking and Cold-Drawing of Rigid Plastics, *Polymer* 1, 7-19.
- Vincent, P.I., 1960b, The Tough-Brittle Transition in Thermoplastics, *Polymer* 1, 425-444.
- Vincent, P.I., 1966, "The Physical Basis of Yield and Fracture," Oxford, p. 155.

# AIRFLOW MODELING IN NOZZLE TO REDUCE YARN HAIRINESS IN WINDING

Asis Patnaik, R.S. Rengasamy, V.K. Kothari, A. Ghosh and H. Punekar<sup>1</sup>  
Department of Textile Technology, Indian Institute of Technology Delhi  
Hauz Khas, New Delhi 110016

<sup>1</sup>Fluent India Private Limited, Pune 411000, India  
E-mail: patnaik\_asis@yahoo.com

## Abstract

Reduction of yarn hairiness in winding by nozzle is a novel approach because of high production rate of winding and the above process itself increases yarn hairiness [1, 2].

Modeling of the airflow pattern inside the nozzle provides some insight into the mechanism of hairiness reduction. Because, previous work hardly reports any information about this aspect, so, the present work is aimed at studying the hairiness reduction through modeling of airflow pattern inside the nozzle, placed at a distance of 10 cm above balloon bracket in the winding machine. A CFD (computational fluid dynamics) model has been developed to simulate the airflow pattern inside the nozzle using FLUENT 6.1 software, to solve the three-dimensional flow field. The parameters viz. velocity profile and air particle path line trajectory obtained from this CFD analysis gives important information for further analysis. In this study, an air-nozzle having a spiral angle of 50° and diameter of 2.2 mm was used for simulation studies. To create a swirling effect four air holes of 0.4 mm diameter are made tangential to the inner walls of the nozzle. Fig.1 shows the front view of the nozzle.

The flow inside the nozzle is turbulent and hence the standard k-ε model of turbulence along with standard wall functions is used. The Reynold's averaged momentum and continuity equations along with energy equation, turbulent kinetic energy equation and ε equation are solved in coupled implicit solver [3]. For simplification, we assume that the process is adiabatic with no heat transfer, so the model used was viscous, compressible airflow. We use the following series of equations to solve a compressible turbulent flow during airflow modeling using FLUENT 6.1 software.

Mass conversion equation:

$$\frac{\partial \rho}{\partial t} + \frac{\partial \rho u_i}{\partial x_i} = 0$$

Momentum conversion equation:

$$\frac{\partial}{\partial x_i} (\rho u_i u_j) = - \frac{\partial p}{\partial x_i} + \frac{\partial}{\partial x_j} \left[ \mu \left( \frac{\partial u_i}{\partial x_j} + \frac{\partial u_j}{\partial x_i} - \frac{2}{3} \delta_{ij} \frac{\partial u_l}{\partial x_l} \right) \right] + \frac{\partial}{\partial x_j} (- \rho \overline{u'_i u'_j})$$

Turbulent Kinetic Equation

$$\frac{\partial (\rho k u_i)}{\partial x_i} = \frac{\partial}{\partial x_j} \left[ \left( \mu + \frac{\mu_t}{\sigma_k} \right) \frac{\partial k}{\partial x_j} \right] + G - \rho \varepsilon$$

Rate of Dissipation of the Turbulent Kinetic Energy

$$\frac{\partial (\rho \varepsilon u_i)}{\partial x_i} = \frac{\partial}{\partial x_j} \left[ \left( \mu + \frac{\mu_t}{\sigma_\varepsilon} \right) \frac{\partial \varepsilon}{\partial x_j} \right] + c_1 \frac{\varepsilon}{k} G - c_2 \rho \frac{\varepsilon^2}{k}$$

\*Where symbols have their usual meaning.

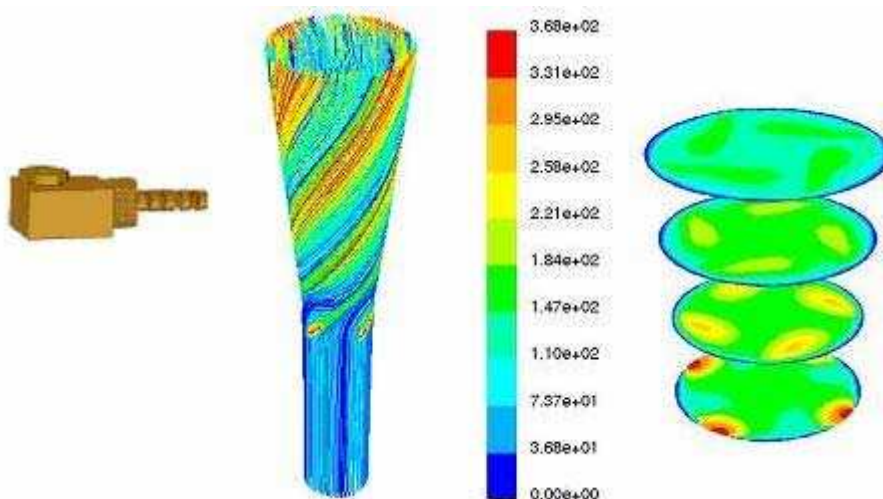


Fig. 1. Front view of the nozzle

Fig. 2. Air particle path lines

Fig. 3. Contours of total velocity (m/s)

The airflow in the nozzle is against yarn movement. 30 tex Z-twisted ring spun yarn was first converted into pirn and this yarn was passed through the nozzle, to wind at a speed of 1000 m/min. The air pressure in the nozzle was kept at 0.5 bar. 800m of yarn were tested for hairiness using Zweigle G 566. The reduction in S3 values (hairs  $\geq 3$  mm) of the yarn wound with the nozzle is about 28 % less than the spun yarn and 54 % less than the pirn wound yarn, while both the yarn types show little difference in evenness and tensile properties.

Fig.2 shows the path lines of air particles, released from air inlet holes and bottom plane of the nozzle. Air velocity is resolved into 3 components viz. axial, tangential and radial. This swirling action is created by the tangential and axial velocity component of air velocity. Absence of staggering in the location of air entry holes helps to generate perfect swirling flow. The yarn passes through the center of the nozzle. Average air velocity in the nozzle is 150 m/sec, which can be seen from Fig. 3, is much higher than yarn speed, which is in the order of 17 m/sec. From Fig. 3, it is observed that four vortices arise adjacent to the wall of the nozzle, which are rotating in anti-clockwise direction. Due to action of the vortices, yarn body is untwisted at the core of the nozzle and because of the false twisting action, original twist in the yarn is restored. This process leads to the wrapping of protruding hairs, in a direction opposite to the direction of twist, hence reduces yarn hairiness. In addition, straight path lines in the lower half show the suction air rushing in without any swirl, but with high axial velocity. This air is also responsible to push down the hairs to the yarn body, thereby reducing the hairiness.

In conclusion, airflow modeling of the nozzle gives a better insight into the mechanism of hairiness reduction in winding.

#### References

1. Wang, X., and Miao, M., *Textile. Res. J.* **67** (7), 481- 485 (1997).
2. Chellamani, K.P., Chattopadhyay, D., and Kumarasamy, K., *Ind. J. Fibre Textile Res.* **25** (12), 289-294 (2000).
3. FLUENT 6.1, User Guide Vol. I., (2003).

## Section E

### Nanostructuring Polymers with Cyclodextrins to Alter Their Conformations and Properties

Tamer Uyar, Jyotsna Vedula, Todd A. Bullions, Min Wei, Cristian Rusa,  
Mariana Rusa, Xingwu Wang, and Alan E. Tonelli

Fiber & Polymer Science Program  
North Carolina State University  
Campus Box 830, Raleigh, NC 27695-8301

#### Abstract

Polymer guests may be non-covalently complexed with host cyclodextrins (CDs) to form crystalline inclusion compounds (ICs). In polymer-CD-ICs, the guest polymer chains are constrained to occupy narrow channels (0.5-1.0nm in diameter) formed by the stacked CD hosts. As a consequence, the guest polymers are restricted from assuming all but the most highly extended of their conformations. CD-IC restriction of included guest polymer conformations has at least two important consequences: i.) Coalescence of guest polymers from their CD-ICs by removing the host CDs, without disruption of the extension and orientation of the included polymer chains, can result in consolidated bulk polymer samples with morphologies and even polymer chain conformations that differ dramatically from those achieved by consolidation from their disordered, randomly-coiling, and entangled solutions and melts; and ii.) Polymerization of monomers that reside as guests in the narrow channels of their CD-IC crystals can lead to polymers with microstructures that are distinct from those achieved during homogeneous polymerizations, because certain microstructures resulting from homogeneous polymerizations are prevented by conformational restrictions placed on them by the narrow CD-IC channels. We will describe the effects on the conformations, morphologies, and thermal characteristics of PET samples produced by coalescence from their  $\gamma$ -CD-IC crystals. In addition, when styrene monomer included and constrained in the narrow channels of its  $\gamma$ -CD-IC crystals is polymerized, we suggest, on the basis of the conformational modeling of stereoisomeric polystyrenes (PSs) confined to the narrow  $\gamma$ -CD channels ( $\sim$ 0.8-1.0nm), that the resulting PS is likely to have a novel stereochemistry characterized by alternating meso and racemic diads (...mrmrmmr...). The stereochemistry of PS obtained by the constrained free-radical polymerization of styrene in its  $\gamma$ -CD-IC crystals is compared to that expected from conformational modeling and observed for PS free-radically polymerized in solution.



## **NANOLAYER SELF-ASSEMBLIES: CUSTOMIZABLE FIBER SURFACES**

Juan P. Hinestroza, Ph.D.  
Fiber and Polymer Science Program  
Department of Textile Engineering, Chemistry and Science  
North Carolina State University  
Raleigh, NC 27695  
Tel: 919-515-9426 Fax: 919-515-6532  
Juan\_Hinestroza@ncsu.edu

The use of electrostatic self-assembled nanolayers offers a unique solution for adding functionality to the surface of textile fibers. This technique is particularly appealing as the thickness, homogeneity and sequence of these nanolayers can be precisely controlled by means of molecular architecture, self-assembly and electrostatic interactions. In addition, the self-healing capability of the electrostatic self-assembly method makes this technique particularly tolerant to defects.

While glass, silicon wafers, gold coated particles, quartz and mica have dominated the choice of substrates for the electrostatic self-assembly of nanolayers, the use of textile fibers has been rarely considered. Cotton, in particular, offers a unique challenge to the deposition of nanolayers because of its unique cross section as well as the chemical heterogeneity of its surface.

In this project we deposited nanolayers of poly(sodium 4-styrene sulfonate) (PSS) and poly(allylamine hydrochloride) (PAH) over cotton fibers. The first step involved the preparation of the cotton substrate by using 2,3-epoxypropyltrimethylammonium chloride producing in this way a cationic cotton. The deposition of nanolayers required the repeated sequential dipping of the charged textile fibers into solutions of PSS and PAH with rinsing between each deposition step. Thermal analysis equipment (DSC and TGA) were used to characterize the textile fibers. A UV spectrophotometer was used to monitor the adsorption kinetics of the nanolayers by following the absorbance versus deposition cycles. A high resolution scanning electron microscope SEM was used to verify the homogeneity and quality of the nanolayer ensembles.

In summary, the use of the electrostatic self-assembly technique offers the possibility to tailor the surface of textile fibers at the molecular level by depositing nanolayers of biocidal, charged nanoparticles, non-reactive dyes, and polyelectrolytes in a controlled manner. The thickness and sequence of the nanolayers will tailor and enhance the selectivity, diffusivity and permeability of the textile fibers while maintaining their comfort and physical properties.

## **Preparation and Incorporation of Reactive Nanoparticles Suitable for Use in Textiles for Protection against Chemical and Biological Warfare Agents**

Shyamala Rajagopalan\*, Marc Finley, Olga Koper, John Rasinski, and Scott Toerber  
NanoScale Materials, Inc., Manhattan, KS, 66502

Holly Axtell and Thomas Pease  
Gentex Corporation, PO Box 315, Carbondale, PA, 18407

The goal of this study is to investigate the untapped potential of highly adsorbent and reactive nanoparticles in the area of protective garments manufacturing. When dealing with situations involving hazardous materials, released either by accident or on purpose, protective clothing is critical to guard against the effects of toxic or corrosive products that could enter the body through inhalation or skin absorption, causing adverse effects. More specifically, this collaborative project between NanoScale Materials, Inc., and Gentex Corp. seeks to establish the feasibility of incorporating highly adsorbent and reactive nanoparticles into Gentex's current carbon bead laminate system and to evaluate the resultant fabric's utility as protective clothing against chemical and biological warfare agents.

## Evaluation of Shape Memory Effects on Fabrics

Jinlian Hu, (Associate Professor)  
Siuping Chung, Susanna Li and Laikuen Chan

Institute of Textiles and Clothing  
The Hong Kong Polytechnic University  
Hong Kong  
e-mail: [tchujl@inet.polyu.edu.hk](mailto:tchujl@inet.polyu.edu.hk)

### Abstract:

Shape-memory polymer is a new product that has been created by utilizing the shape memorizing mechanism of elastomers of the polyurethane family. These materials exhibit novel properties such as sensing (thermal, stress, optical, chemical), actuation, high damping, adaptive responses, super-elasticity capability, and air permeability. Recently, they are being used in textiles and garments. In order to know and measure the ability and effectiveness of the fabrics and garments, methods for characterizing shape memory fabrics need to be developed.

To define whether a fabric has a shape memory effect, we would say if a fabric can fix the deformation without external loading and recover to their original shape by a recovery process involving changing the surrounding temperatures of the fabrics, then the fabric has a shape memory effect. There are many reports on studies that have been conducted on shape memory polymers in textiles. Hayashi, Kobayashi et al. [1, 2] developed shape memory film, foam, sheet and fibres that could enhance the fixity and shape recovery of materials.

In order to know the thermo-sensitivity of the polymers in the fabrics, methods of characterizing shape memory fabrics are needed to evaluate the shape memory effects. Since shape memory fabrics are responsive to changes in temperature in some controlled environments such as water, a special experimental design for the recovery stage of the fabrics is necessary for evaluating the fabrics.

The purpose of this study is to introduce methods of characterizing shape memory fabrics so that some properties of shape memory fabrics can be evaluated. These methods include subjective evaluations of the recovery of a flat appearance, the ability to retain creases and an objective evaluation of shape memory angles. Thus, the recovery performance of shape memory fabrics can be known. The shape memory effects from subjective evaluations and the objective evaluation will be discussed and compared.

Therefore, a series of experiments are designed so that shape memory fabrics can be processed in water under a controlled temperature environment. In order to characterize the effects of shape memory fabrics, experimental designs can be drawn up according to subjective evaluations of the fabric's recovery of a flat appearance, the fabric's ability to retain creases, and to an objective evaluation of the shape of the fabric's angles. The designs of the equipment involve a

temperature-controlled water tank for providing a temperature-controlled environment, some fabric-drying devices for the fabric recovery process, and some weights for the fabric deformation process, in which we can measure the abilities and effectiveness of the shape memory fabrics.

Some existing evaluation methods of evaluating shape memory can thereby can be applied and modified. They are: 1) Appearance of Fabrics after Repeated Home Laundering (AATCC 124-2001), 2) Retention of Crease in Fabrics after Repeated Home Laundering (AATCC 88C-2001), 3) Wrinkle Recovery of Woven Fabrics: Recovery Angle (AATCC 66-1998).

We used a piece of plain woven cotton fabric, one that had not been finished with shape memory polymers, and others that had. Different shape memory polymers are used to finish one type of woven cotton fabric. We will compare the results with defined shape memory effects in terms of subjective rankings on the recovery of a fabric's flat appearance and crease retention. The subjective results will be compared to the shape memory angles on cottons in order to determine their shape memory capability.

The investigation provides new methods of defining and evaluating shape memory fabrics according to the functions of retaining creases and recovering a flat appearance, and to the fabric recovery angles. The basis for characterizing shape memory fabrics is to establish methods of evaluating the responses of shape memory fabrics to changes in the temperature of water. It is hoped that new methods of evaluation can contribute to future research and create advantages for industrial sectors in the characterization of the effects on shape memory fabrics.

1. Hayashi, Kobayashi et al., Shape fixity and shape recovery of polyurethane shape-memory polymer foams. *Journal of Materials-Design and Applications*, 217 (L2): 135-143, 2003
2. Hayashi, Kobayashi et al., Thermo mechanical constitutive model of shape memory polymer, *Mechanics of Materials*, 33(10), 545-554, October 2001

# Optical device for the characterization of the surface state and the deformation of periodical surfaces

Michel TOURLONIAS\*, Marie-Ange BUENO\*, Laurent BIGUÉ\*\*and Marc RENNER\*

\* Ecole Nationale Supérieure des Industries Textiles de Mulhouse – University of Mulhouse  
11, rue Alfred Werner – 68093 Mulhouse Cedex - France

\*\* Laboratoire Intelligence Processus Systèmes – Ecole Supérieure des Sciences Appliquées  
pour l'Ingénieur de Mulhouse, University of Mulhouse  
12, rue des Frères Lumière – 68093 Mulhouse Cedex - France

## Summary

In this study, the same optical method has been developed in order to evaluate a change of the state of surface or the deformation of periodical fabrics or nonwovens during a tensile test. This method is sensitive to a change at the macroscopic scale (fabric or nonwoven structure) and at the microscopic scale (hairiness). This method is global and integrates these both aspects. The principle consists in highlighting a surface with a rotating optical probe and a Fourier analysis allows to obtain the relief periods and the surface state or a change in these periods.

## 1 Experiments

### 1.1 Materials

Materials have to present small periods or patterns like woven or knitted fabrics, therefore non periodical or periodical fabrics with large periods, as structured jacquard or damassé fabrics for instance, are not taken into account in this study. Nonwovens with small dots patterns can also be used. At present, the system allows periods from about 0.3 mm to about 3 mm.

In this study, for the strain measurement, we used a plain woven fabric for skirt and a spunbonded nonwoven for medical uses. For the surface state characterization, a twill woven fabric for a pair of jeans before and after different kind of sanding process had been used, and a spunbonded nonwoven for medical uses with a change in calendering adjustments.

### 1.2 Principle

We studied the reflection of a bright small rotating line on the surface. The small line scans the surface in a ring. The reflection is imaged onto a photodetector and the resulting output, i.e. a 1-D temporal signal, is processed by a digital Fourier Transform. The spectrum obtained shows some peaks of frequency. The frequency of these peaks depends on the surface periods; the magnitude and energy of these peaks are linked to the height of the surface asperities. Therefore, in order to measure a change in the state of the fabric surface, the peak energy is considered. In the other case, in order to measure the surface strain during a tensile test for instance, the frequency variations are measured.

## 2 Results

An illustration of surface state measurement results is displayed in Figure 1. The influence of nonwoven calendering on results is highlighted.

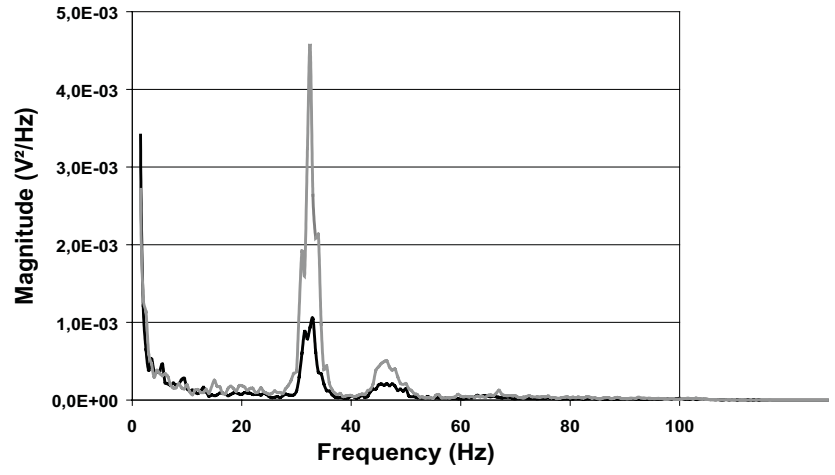


Figure 1 : Spectrum of a spunbonded nonwoven with a strong (in grey) and a light calendaring (in dark).

The strain measurement during a tensile test is illustrated in Figure 2.

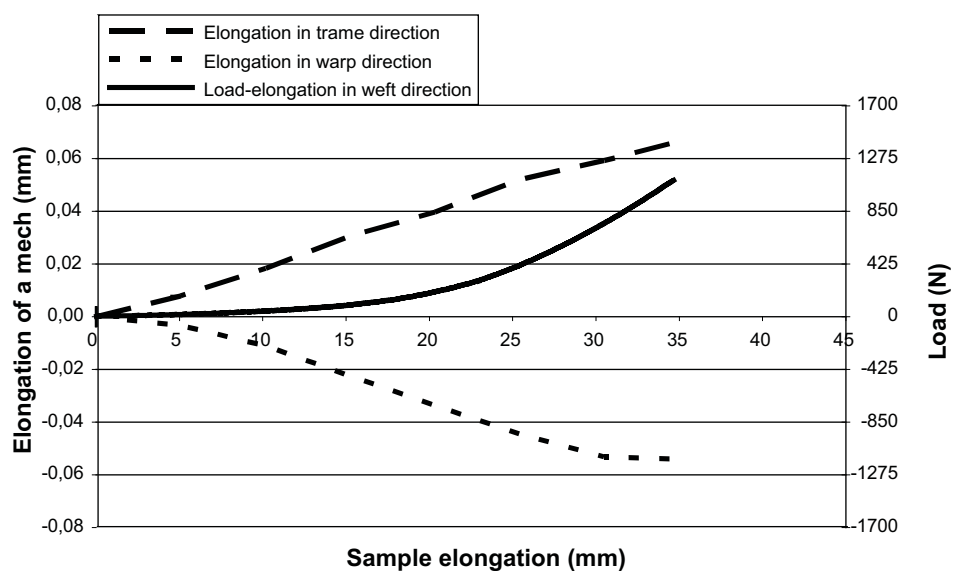


Figure 2 : Load-elongation and strain curves during a tensile test in weft direction of a plain woven fabric.

### 3 Conclusions and future prospects

The same principle is used in order to measure the strain of a periodical fabric and a change in the state of this surface without any contact. The difference between these two applications stands in the signal processing.  
 In the future, a special device must be designed for each measurement in order to optimize the system in regard to the use.

## Rheological aspects of spinning high performance fibres from liquid crystalline solutions (Twaron®, cellulose)

*H. Boerstoel, Teijin Twaron, Velperweg 76, P.O. Box 9600, 6800 TC Arnhem,  
[Hanneke.Boerstoel@Twaron.com](mailto:Hanneke.Boerstoel@Twaron.com)*

Para-aramid fibers (Twaron® and Kevlar®) were the first commercial yarns, spun from liquid crystalline solutions<sup>1,2</sup>. More recently PBO<sup>3</sup> (Zylon®, Toyobo) and PIPD<sup>4</sup> (M5®, Magellan) fibers were developed according to the same dry-jet wet-spinning technique. Also, cellulose (Acordis) can be spun analogously<sup>5,6</sup>.

In dry-jet wet-spinning, or air gap spinning, use is being made of the orientation that forms spontaneously due to the rigid character of the polymer chains. The elongational flow field in the air gap brings about the overall high orientation necessary for forming high modulus yarns. Picken et al. developed a model for describing this process<sup>7</sup>.

Twaron yarns are being produced by spinning the rigid polymer poly-para-phenylene terephthalamide from liquid crystalline sulfuric acid solutions. Cellulose can directly be spun from liquid crystalline phosphoric acid solutions, giving gives rise to high modulus, high tenacity yarns<sup>8</sup>.

In this paper various rheological aspects, occurring during processing of Twaron and cellulose, will be treated.

Both shear flow and elongational flow have been studied. The Twaron shear viscosity has been determined over 5 orders of magnitude using both cone and plate rheometry and capillary rheometry. In shear flow Twaron shows the well known three regions, as described by Onogi and Asada<sup>9</sup>.

The elongational flow field in the air gap has been studied for both Twaron and cellulose. By Laser Doppler anemometry the velocity profiles in the air gap have been determined. By also measuring the force to draw the material the elongational viscosity has been determined. The elongational viscosity appeared to be much higher than the shear viscosity, the Trouton ratio exceeding the value of 3 by far. The Laser Doppler technique has been combined with a birefringence measurement. This revealed that when the solution exits the spinneret capillaries the die swell gives rise to a collective desorientation, which is quickly repaired by subsequent drawing.

### References

1. S.L. Kwolek, NL6908984
2. L. Vollbracht, NL157327
3. J. Wolfe, WO8401162
4. D.J. Sikkema, V.L. Lishinski, WO9425506
5. S.J. Picken, H. Boerstoel, M.G. Northolt, processing rigid polymers to high performance fibers, Encyclopedia of Materials: Science and Technology, pp 7883-7887
6. H. Boerstoel, Liquid crystalline solutions of cellulose in phosphoric acid for preparing cellulose yarns, PhD thesis, Rijksuniversiteit Groningen, The Netherlands, 1998
7. S.J. Picken, S. van der Zwaag, M.G. Norhtolt, Polymer **33(14)**, 2998 (1992)
8. H. Boerstoel, B.M. Koenders, J.B. Westerink, WO9606208
9. S. Onogi, T. Asada in "Rheology", eds. G. Astarita, G. Marrucci, L. Nicolais, Vol 1, 421 (1980)

## Preparing New Polymers That Interact With Cotton

Nicolette Prevost, Oliver Dailey, Alexander Lambert, and Navzer D. Sachinvala\*  
Southern Regional Research Center, USDA-ARS, New Orleans, Louisiana.

In this talk we will show that sucrose and polyethylene and polypropylene glycols are excellent starting materials for monomers, prepolymers, thermosets, and cycloaddition polymers that interact well with cotton to improve performance properties (Figures 1, 2, and 3). Herein we will discuss the synthesis, structural and biological characteristics of the new polymers; explain their curing behavior with cotton fabrics; and show enhancement of tensile, tear, and abrasion resistance properties.

Figure 1: Sucrose-based Monomers for Reactions With Cotton

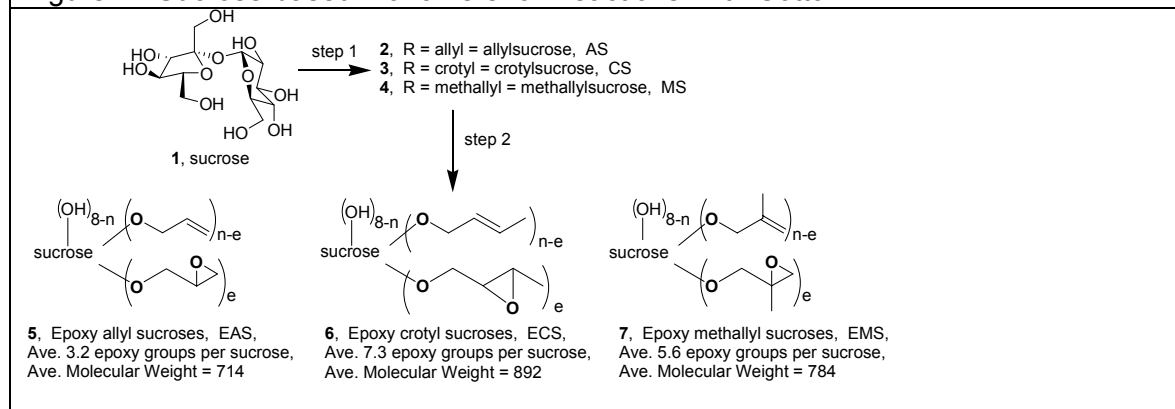


Figure 2: Polyethylene and Polypropylene oxide polymers, PEO and PPO respectively

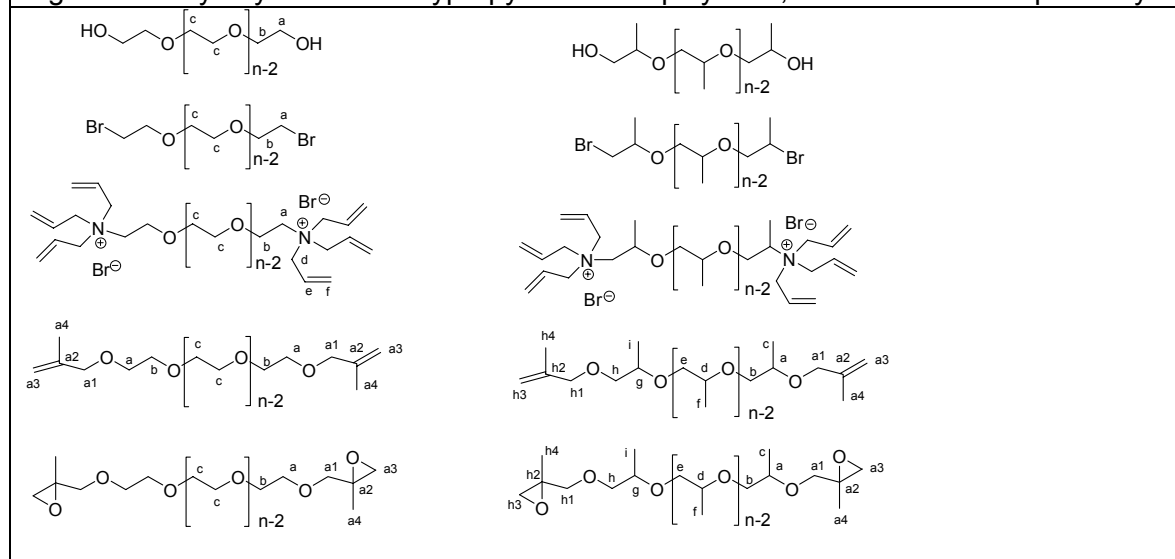
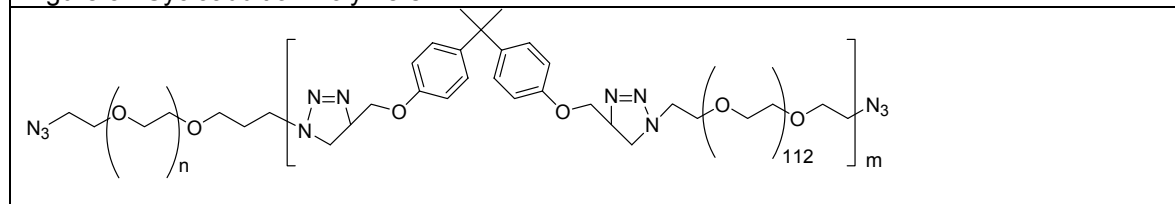


Figure 3: Cycloaddition Polymers



\*Address correspondence to N. Sachinvala: [Nozar@src.ars.usda.gov](mailto:Nozar@src.ars.usda.gov)



## **Biopreparation of Cotton and Linen Fabrics**

EMÍLIA CSISZÁR

*Budapest University of Technology and Economics*

*Department of Plastics and Rubber Technology*

*H-1521 Budapest, Hungary*

e-mail: emi@muatex.mua.bme.hu

Cotton and linen fibers containing different amounts of non-cellulosic constituents, are prepared by subjecting the fibers to scouring and bleaching under different conditions. Conventional preparation is based on a treatment with an aqueous solution of either caustic soda or sodium carbonate/caustic soda followed by bleaching with an aqueous sodium hypochlorite or hydrogen peroxide. Enzymatic scouring of cotton and linen fabrics prior to bleaching is an encouraging alternative environmentally-friendly process. Enzymes such as pectinases, cellulases, hemicellulases, ligninases, etc. can be used to remove or break-down the non-cellulosic constituents which mainly are pectin, lignin, waxy materials and hemicelluloses. Enzymatic scouring results in fabrics with excellent and uniform water absorbency and can improve the efficiency of the subsequent bleaching process as well. It also enables the simplification of technological processes and the elimination of energy consuming steps.

Degradation of pectic substances is one of the most essential processes in bioscouring of celluloses. Pectin generally builds up from D-galacturonic acid residues and covalently links to hemicellulose or to cellulose as well as interacts itself forming calcium cross bridges. Removal of calcium ions can accelerate the degradation of calcium-rich pectic substances. It was demonstrated recently that application of chelating agents increased the efficiency of microbial-retting and bioscouring significantly. Comprehensive research works have also shown that ethylenediaminetetraacetic acid (EDTA) is the most efficient chelator in improving the enzymatic pretreatment of celluloses. Recently we have shown that addition of EDTA markedly enhances the apparent enzyme activity in cotton bioscouring. EDTA improves the effectiveness of the commercial xylanase and pectinase enzymes, as well as accelerates both the removal of the impurities from cotton fabric and the degradation of seed-coat fragments. Application of EDTA in the enzyme solution has also significant effect on the efficiency of the subsequent chemical process.

In this presentation we show how the EDTA can improve the efficiency of the enzyme process in cotton and linen bioscouring. The main goals of this study are the quantitative characterization of the enzyme activities in the presence of EDTA, and comparison of the degradation efficiency of the non-cellulosic constituents of cotton and linen in bioscouring with or without EDTA. Influence of EDTA in different concentrations on the enzyme activities i.e. filter paper (cellulase), 1,4- $\beta$ -endoglucanase,  $\beta$ -glucosidase, xylanase and pectinase, is investigated. Degradation of seed-coat fragments – the most resistant impurities of greige cotton - is characterized in cotton bioscouring by weight loss and reducing sugar liberation, as well as by changes in metal ion content.

**Key Terms:** Bioscouring, Cotton, Linen, EDTA, Enzyme activity, Seed-coat fragments, Metal ion content

## **Student Paper Competition Final Presentations**

### **Mechanical and structural properties of melt spun polypropylene/nylon 6 alloy filaments**

**Mehdi Afshari**

Department of Textile Engineering, Yazd University, P. O. Box 89195-741, Yazd, Iran

#### **Abstract**

Investigated in the present study are the physical properties, morphology and structure of PP/N6 alloy filaments (10, 20 wt% N6) made with or without PP-g-MAH as compatibilizer. The alloy filaments produced at the take-up speeds of 300 and 800 m/min were drawn with draw ratio of 3.5 and 2, respectively. Stress-strain curves of PP and alloy filaments show ductile and brittle behavior, respectively. It is suggested that the brittle behavior of alloy filaments is due to the presence of micro-voids or micro-pores at the interface of PP and N6; these lead to stress concentration and thus to a decrease in tenacity, modulus and elongation at break. Effects of the blending of N6 with PP on birefringence and crystalline and amorphous orientation factors of the composite filaments are studied. The amorphous orientation factor,  $f_{am}$  of PP was found to increase with an increase in the amount of N6. The alloy filaments behaved like iso-strain materials and most of the force in spinning and drawing was born by the PP phase. The presence of N6 fibrils helped to orient PP chain molecules in amorphous regions. However, the crystalline factor,  $f_c$  of PP decreased with increase in nylon fraction. This means the presence of the crystals of N6 caused a decrease in the orientation of the PP crystals. LSCM micrographs of the filament showed the presence of matrix-fibril morphology with the N6 fibrils oriented along the axis.

# **Mathematical Modeling and Experimental Investigation of Yarn Strength as a Stochastic Process<sup>\*)</sup>**

Dipayan Das

Department of Textile Structures, Technical University of Liberec, Halkova 6, Liberec 1,

Czech Republic-461 17, E-mail: [dipayan.das@vslib.cz](mailto:dipayan.das@vslib.cz)

## **ABSTRACT**

The standard measurement of yarn strength is carried out at 500 mm gauge length. However, in practice, yarns experience stresses at different lengths. Therefore, it is necessary to estimate the descriptive statistical parameters as well as frequency distributions of yarn strength at different lengths. In this present work, a theoretical model on yarn strength as a stochastic process is developed and based on the results of actual strength measurement corresponding to short gauge length, the response of yarn strength at any gauge length is simulated by using computer. The results of computer simulation are also verified with the actual strength results and compared with F. T. Peirce's strength equations. In order to better understanding of the distribution of strengths along the yarn, autocorrelation function is used to analyze the strength values of adjacent yarn sections.

# **Fabrication, Structures and Properties of Thermo-regulated Polyacrylonitrile-Vinylidene Chloride Fibers**

<sup>a</sup>Zhang Xing-xiang<sup>1,2</sup>, Tao Xiao-ming<sup>1</sup>, Yick Kit-lun<sup>1</sup>

*1-Institute of Textiles and Clothing, The Hong Kong Polytechnic University, Hung Hom, Hong Kong, China*

*2-Institute of Functional Fibers, Tianjin Polytechnic University, Tianjin 300160, China*

## **ABSTRACT**

Thermo-regulated Polyacrylonitrile-Vinylidene Chloride (PAN/VDC) fibers containing 4-40wt% of MicroPCMs were wet-spun. In this study, fibers containing less than 30wt% of microencapsulated n-octadecane can be spun smoothly. The structures and properties of the fibers were investigated by using FTIR, SEM, DSC, WAXD, DMA and TG etc. The microcapsules are intact and evenly distributed inside the polymer matrix. The tensile strengths of the fibers with titers in the range of 1.9 to 10.9dtex are 0.7 to 2.0cN/dtex. The elongation of the fibers is approximately 7%. The heat absorbing and heat evolving temperatures of the fibers increase slightly with the increasing content of MicroPCMs. The enthalpy of the fiber containing 30wt% of MicroPCMs is approximately 30J/g, and the enthalpy rises steadily as the content of MicroPCMs increase. The glass transition temperature of the fiber is 89-108°C which decreases with the increase of MicroPCMs content, and the melting and decompose temperatures of the fiber are approximately 190°C and 220°C, respectively. The fibers have a value of LOI higher than 26% and are permanent flame retardant.

## Section F

### Thermal Insulation Layers for Working Clothes

Bayar Myagmar\*, Dominique C. Adolphe\*\*, Altantsetseg Chuluun\*

\*Mongolian University Science and Technology –Ulaanbaatar, Mongolia

\*\* Ecole Nationale Supérieure des Industries Textile de Mulhouse, France

#### I. Introduction

In the frame of research program between Mongolian University of Sciences and Technology and ENSITM, a study on natural fiber nonwoven applied as insulation layer has been carried out. The choice of natural fiber has been done in regard to economical aspects. In fact, one goal of this work is to re-used waste fibers issued of the animal hair based industries.

In this study, the lap structure will be analysed in order to select the one which will present the best quality to be included as an insulation layer in a worker garment. The thermal properties and the air permeability will be here studied and analyzed.

The first obtained results, on blend, will be presented; conclusions and perspectives will be drawn out.

#### II. Aim of the study

In Mongolia, the temperature difference between the colder and the hotter season varies between  $-38^{\circ}\text{C}$  to  $+32^{\circ}\text{C}$  and, clearly, textile clothing has to provide satisfactory protection and comfort under such climate conditions. In the same time, agriculture produces raw wool fibers (20125 tons/year) which are mainly used in carpet industry. During the carpet production process, some coarse fibers are eliminated and composed waste material.

The global aim of this study is to know if this waste material can be used as insulation layer for worker clothes. In this step, first experiences have been carried out and based on these results, other investigations could be envisaged.

#### III. Experimental part

Analyzes of the raw material in terms of fiber contain, kind of fiber and percentage in the blend are presented in table 1.

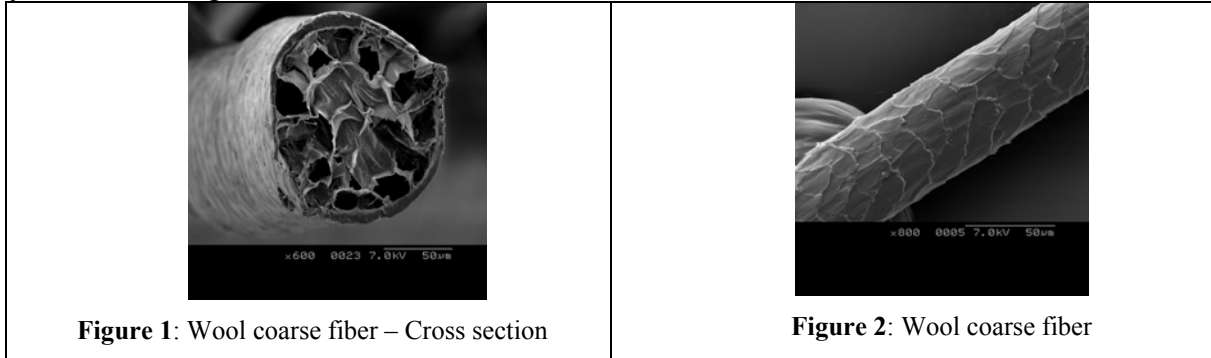
Type of wool fiber	Down	Intermediate	Long Hair	Coarse
Diameter	22.3 $\mu\text{m}$	32.4 $\mu\text{m}$	49.5 $\mu\text{m}$	120.8 $\mu\text{m}$
Composition of sample	47.53%	4.47%	9.91%	35.84%

The difference between the obtained total and 100% is due to the dust material.

**Table 1:** Composition of the used blend

The raw material have tested and analyzed in terms of fiber structure [1]. It appears that the coarse fibers present an alveolar structure (figure 1&2) different of the other kind of material.

Therefore, in order analyze the effect of this structure over the thermal and insulation properties, materials have been tested separately in order to evaluate their capability to be used as isolation layers for working clothes.



The thermal conductivity and the insulation ratio have been evaluated thanks to KES Thermo Lab devices. Analyses of the fiber morphology have been carried out and highlighted the alveolar structure of the coarse fibers.

#### **IV. Results and discussion**

The obtained results permit to discuss about the more efficient choice of the kind of fibers dedicated to insulation layers materiel. In this analysis, the economical data have to be taken into account in order to answer completely to the initial assertion that is to say “As waist material issued of the animal hair based industries can be valorized in the garment industry?”

#### **References**

- [1] B. Myagmar, D. C. Adolphe, A. Chuluun ; “Natural fibers as Insulation Layer – Case of Mongolian Wool  
Fiber Society Spring Conference – 17-20 may 2004 - Saint Louis –MO - USA

# The Effect of Pattern Construction on Tactile Feeling as Determined Using Tactile Sensory Analysis

S. BENSAID, JF. OSSELIN, L. SCHACHER, D. ADOLPHE  
Ecole Nationale Supérieure des Industries Textiles de Mulhouse  
11, rue Alfred Werner 68093 MULHOUSE Cedex, France  
Tel.: 33 (0)3 89 33 63 20 - Fax: 33 (0)3 89 33 63 39 - e-mail: s.bensaid@uha.fr

**Key words:** Sensory evaluation, tactile feeling, pattern, woven fabric, weave

**Introduction:** The ability to test with instruments the tactile feeling of fabrics in a reliable and meaningful manner very often met with failure. However, customer's choices are more and more based on multisensorial feature, and particularly on touch. In order to overcome this problem, it becomes essential to be able to take "tactile quality" of a textile product into account in the product development process and to predict sensory perception of textile fabrics on the basis of physical properties: material, construction or treatments.

This paper investigates the effect of different woven construction parameters of cotton fabrics on tactile feelings. Sensory analysis methodologies were applied to obtain Quantitative Descriptive Description (QDA) of fabrics woven on Jacquard loom with the same yarn, but with different patterns.

**Experimental:** Nine adults between 20 to 40 years old participate in sensory trials conducted in an environmentally controlled room. The subjects have been trained according to previously established methodology [1][2] to be able to dissociate complex tactile stimulus in simple information and verbally it. Sensory rating was done using a set of 15 individual sensory perceptions (attributes) on a 0-10 non structured scale.

Nine fabrics were selected for the trial. They were created with nine classical patterns using the same yarn (warp & weft): plain weave; 3-twill, 4-twill (Z direction); broken twill (weft effect); 4-satin, 5-satin, 6-satin, 12-satin (horizontal weaved effect), crêpe.

**Results and discussion:** By using statistical methods of factor analysis, 5 non-relevant attributes were removed and sensory attributes were abstracted into two sensory independent factors which explain 45%, 34% of total variance, respectively: *elastic*, *crumple-like* and *rigid* opposed to *pillous* and *falling*; and *thick*, *granulous* and *grooved* opposed to *soft* and *slippery*. Principle Component Analysis (PCA) on the mean score of the panel across replication allows visualization and interpretation of the results, even if part of the information in the data set is lost during the abstraction process. Based on the obtained results, we can conclude that, as expected, weave parameters strongly affects tactile feeling and mainly surface attributes. But for complete tactile evaluation, subjects use three-dimensional exploration and full-hand attributes are also concerned. Plain fabrics and broken twill appear as strongly different and they strongly structure the product space. They have to be removed for more subtle analysis.

**Conclusion:** A study of the influence of texture on the touch quality of fabrics was interesting in order to predict which parameters can directly induce a specific touch. Several parameters of texture can be studied; the most important of them is the weave. Sensory evaluation, method applied in fields where emotional feature of the consumer and his preferences are taken into

account like cosmetic and food industries, is well adapted to evaluate the tactile feeling of textile fabrics.

**Literature cited**

[1] Philippe, F. *Contribution à l'analyse sensorielle tactile des produits textiles par analyse sensorielle*. Thèse de doctorat en Sciences pour l'Ingénieur - Université de Haute-Alsace - Mulhouse (France) - Jan. 2001

[2] Chollakup, R. *Mélanges soie-coton en filature fibres courtes caractéristiques des fils et analyse sensorielle des tricots*. Thèse de doctorat en Sciences pour l'Ingénieur - Université de Haute-Alsace - Mulhouse (France) - Dec. 2003



## Methods for Measuring and Predicting the Thermal Comfort of Clothing

Elizabeth McCullough, Kansas State University

To adequately predict the thermal comfort of people wearing protective clothing ensembles, the thermal insulation and evaporative resistance of the entire ensemble should be measured on a heated, sweating manikin. These values can then be used in biophysical models to predict the thermal responses of people in different environments. However, sweating manikins are rare, and the tests are expensive to perform. This paper will describe methods for 1) measuring the insulation value and evaporative resistance of materials used in garments, 2) predicting these values for an entire clothing ensemble, and 3) predicting the thermal comfort responses of people wearing the ensemble under different environmental conditions at different activity levels.

**Clothing Thermal Model.** First, the thermal resistance and evaporative resistance values for all of the fabrics used in garments in an ensemble are measured on a hot plate according to ISO 11092 or ASTM F 1868. These values are estimated for footwear, or the footwear can be omitted from the ensemble. Then the garments are put on a life-size manikin one by one, and the percent of each body segment that remains uncovered and/or covered by different garment layers is documented. Then subsegments of uniform coverage are identified. In addition to the distribution of garment layers, the radial dimension of the fabrics is measured for successive layers of garments by measuring the circumference of each body segment with and without the garment layers. The thickness of the air layers between the manikin and the first garment layers and between additional garment layers is determined by subtracting the fabric thickness and smaller radius from the larger radius. The model basically treats the body as a set of cylindrical segments with uniform surface temperature and wettedness. Each clothing layer is treated as a uniform cylinder around the body cylinder. If a segment is not uniformly covered with clothing, the segments are further divided into subsegments until each subsegment is uniformly clothed. The heat loss from each segment is then treated as a one-dimensional radial heat flow problem. Finally, the resistances on all of the parts of the body are determined and summed.

**Physiological Model.** The physiological model combines a transient version of the clothing model described above with a transient segmented model of the human body. The transient clothing model includes the effects of condensation and evaporation of sweat in the clothing and also sorption and desorption of moisture by textile fibers in addition to heat and moisture transport. The human body model is a segmented version of the Gagge two-node model widely used in thermal comfort and heat stress analysis. The segmented model allows the calculation of local heat and moisture loss and local sweat accumulation on the skin as well as overall body heat and moisture dissipation. The focus of the development of this model was to accurately model the heat and moisture transport processes and the resulting physiological responses of the human body. Specific predictions include 1) thermal sensation – the overall feeling of warmth or coolness of a person, 2) sweat rate, 3) body core temperature, 4) sweat accumulation, and 5) local sweat accumulation. The combined clothing-body model has been validated experimentally for a range of transient environmental conditions, activities, and clothing ensembles in a previous study.

**Applications.** The advantage of this approach is that apparel designers can substitute a new material in a garment or part of a garment and model the impact on thermal comfort without producing a prototype and testing it. The models would provide manufacturers with a quick, simple, and inexpensive method for predicting the thermal comfort responses of people wearing a specific type of garment (surgical gown) with a standard set of garments (scrub suit, gloves, face mask, head cover, etc.) under different environmental conditions and activity levels.

## PERCEPTIONS OF FIT CRITERIA

Elizabeth Bye  
Karen LaBat  
University of Minnesota

Fit plays a crucial role in the product development process. It is the main component in producing a quality garment that will ultimately translate into sales and satisfied customers (DesMarteau & Speer, 2004). Catalogue and web retailers continue to be challenged by the high rate of return due to poor fit (Langer, 2004). With most apparel production occurring overseas or in remote domestic locations, the methods of communicating the product development process have changed. The fit session is the main evaluation point of the process, so issues surrounding the preparation, execution, and follow-up of these fit sessions are critical to the quality of the final product.

Responsibility for the decisions made during a fit session is divided among several employees including technical designer, patternmaker, designer, buyer, product manager and fit model. These employees have varied backgrounds and responsibilities in the technical, aesthetic, and sales issues of product development. However, all have a common goal, to bring a garment to market that will satisfy consumers and generate a profit. The purpose of this study is to define apparel fit criteria as perceived by professionals in the apparel industry. Understanding the dynamics of a fit session will provide insight to the training needs of current employees and curriculum needs for current students. Sixty questionnaires will be distributed to employees with job descriptions that include participation in fit sessions at two major apparel retailers who develop private label apparel. Questionnaires address participants' experience in fit analysis, criteria they use to evaluate fit and procedures used in the preparation, execution and follow-up of a fit session. The fit session is the main evaluation point of the product development process, so clearly defining and understanding fit criteria from multiple perspectives is crucial.

A pre-study was conducted at both companies (Target 1998 and Nike 2003) using an open-ended interview method to acquire basic knowledge of fit evaluation processes. Data are currently (Spring 2004) being collected. Data analysis will be completed and results ready to present in the fall of 2004.

DesMarteau, K. & Speer, J. K. (2004). Sizing up the tech design position. *Apparel*, April, 39-44.

Langer, W. (March 31, 2004). Poor size, fit drain profits for catalogs, web retailers. Retrieved April 14, 2004 from [http://www.apparelmag.com/bobbin/headlines/viewpoints\\_display.jsp?vnu\\_content\\_id=1000475612](http://www.apparelmag.com/bobbin/headlines/viewpoints_display.jsp?vnu_content_id=1000475612).

## Title: Evaluation of Apparel Drape in Virtual Environment

Traci May-Plumlee<sup>+</sup>, Jeffrey Eischen<sup>+</sup>, Pradeep Pandurangan<sup>+</sup>, Narahari Kenkare<sup>+</sup>  
David Bruner<sup>++</sup>

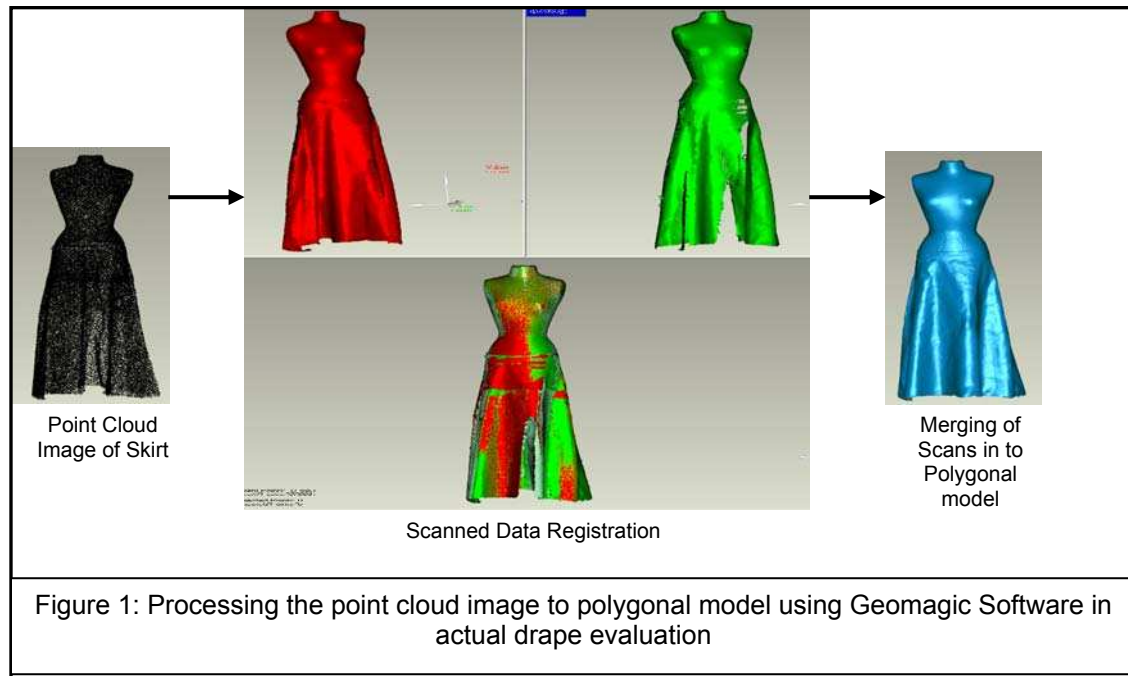
<sup>+</sup>North Carolina State University, Raleigh, N.C

<sup>++</sup> Textile/Clothing Technology Corporation [TC]<sup>2</sup>, Cary, N.C

### ABSTRACT:

The objective of this research was to develop techniques for accurate comparison and evaluation of virtual drape with the actual drape in a virtual environment. Virtual draping of apparel on a digitized 3D model was devised by considering variations in fabric mechanical properties. The goal initially was to develop methods and metrics for measuring virtual draping accurately for simple forms such as circles and squares, and then to extend the developed techniques to garments. We initially developed methods for evaluating drape simulations for simple forms with virtual drape results showing the match of 80-90% to the actual drape parameters of the fabrics.

A broad spectrum of structures such as; Plain, twill, sateen, single jersey, rib and interlock structures were selected for drape analysis. Skirts were constructed from these selected fabrics. The skirt was draped over a mannequin in the [TC]<sup>2</sup> three-dimensional body scanner. Since it was difficult to capture the complete configuration of a drape in a single scan, a number of scans were captured for the purpose of evaluation in the virtual environment.



The point cloud data from the body scanner was processed using *Geomagic* software to get the actual drape (Figure 1) of the skirt. In *Geomagic* software the point cloud image was cleaned for any extraneous points after which the multiple images captured using the body scanner were merged into one complete image. The scans were subjected to a registration process in order to apply a surface to the point cloud image. The final polygonal model developed by registering and surfacing image was used for characterizing drape parameters of the selected apparel.



Figure 2 : Polygonal model of Skirt used in characterizing drape parameters

The Polygonal model (Figure 2) of a skirt was used for characterizing drape parameters. The ratio of the area within the boundary of the cross sectional area of the supporting mannequin and the boundary of the draped form was used to calculate the drape coefficient. The average values from three readings were used to calculate the drape coefficient of the apparel. Volume of the image was also utilized along with drape coefficients and number of nodes in evaluation of drape parameters of apparel.

In the virtual method; the pattern for the skirt was designed using 'Optitex -PDS' software and exported to 'Modulate' Software that incorporates the principal of a particle model for simulating cloth. The skirt pattern for the virtual simulation was constructed in PDS software based on the measurements of the actual skirt. The input values from the actual fabrics are input into the software property

window of the *Modulate* software. The input to the *Modulate* software was based on bending, weight and frictional value of the fabrics from Kawabata evaluation system.

The fabric properties for the skirt, predetermined resolution, and the location of the pattern were selected prior to the simulation. In the simulation mode, the skirt was placed on the mannequin in the virtual environment. The drape simulation was run on *Modulate* particle model software. The simulation was repeated for few times before getting final configuration of the drape. The simulated image was then exported for processing on *Geomagic* software. The image was processed to create a polygonal model with the procedure similar to that of processing the point cloud image in the actual drape technique. The performance parameters were tabulated and analyzed. The image volume, drape coefficient and node numbers were evaluated and compared among fabrics.

Future research will look into verifying the developed method for skirts for varied shape and dimensions.

# Garment Pattern Unfolding with Bijective Pattern Map

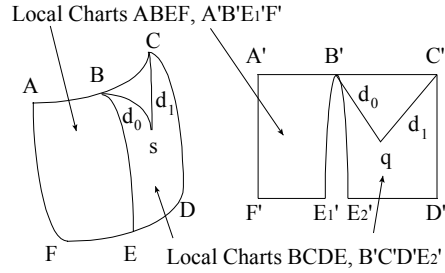
Roger Ng  
 Institute of Textiles and Clothing  
 Hong Kong Polytechnic University

## Introduction

Traditional 2-D garment pattern CAD systems allow users to design the flat patterns to be projected onto the virtual 3-D mannequin for viewing of visual effect. Commercial systems, such as Asahi, support interactive marking of style lines and reference lines, which can be exported back to the flat pattern CAD system. Yet, ideally, 3-D fashion design CAD system should support interactive 3-D virtual garment, which can then be unfolded directly without the use of intermediate flat pattern to simulate the virtual draping. In this article, the author reports a non-finite element technique, known as the Bijective Pattern Map.

### Definition of Bijective Pattern Map

On a 3-D surface  $S$ ,  $ABCDEF$ , any point  $s$  on be mapped bijectively (one-to-one and onto) another flat surface  $S'$ ,  $A'B'C'D'E'F'$ , to the  $q$ , by maintaining the geodesic distance  $d_0$  (between  $s$  and  $B$ ) and  $d_1$  (between  $s$  and  $C$ ), that straight line distance between  $q$  and  $B'$  is well as that between  $q$  and  $C'$  is  $d_1$ . Such function is known as Bijective Pattern Map is a triple  $(B, C, s)$  to  $(B', C', q)$ . Explicitly,



$S$  can  
 to  
 point  
 so  
 $d_0$  as  
 and

Figure 1 Bijective Pattern Map

$$\begin{aligned} BPM[B, C, s] &= \{geodesic[B, s], geodesic[C, s], orientation3[B, C, s]\} \\ &= \{d_0, d_1, -1\} \end{aligned} \quad (1)$$

where the  $geodesic[p, q]$  is the geodesic distance between point  $p$  and  $q$ , and  $orientation3[p, q, r]$  indicating whether point  $r$  lies above or below the geodesic curve connecting  $p$  and  $q$ .

$$geodesic[p, q] = \text{minimum arc length connecting } p \text{ and } q \text{ along } S \quad (2)$$

### Properties of BPM

- (1)  $BPM$  is a partial isometric mapping, meaning that distance is maintained among  $B$ ,  $C$ , and  $s$ . Distortion exists for other points on the surface. Some of the distortion properties of  $BPM$  on bicubic Bezier tensor product surface have been reported by Ng (1997, 1999).
- (2) If the surface  $S[u, v]$  is continuous and developable, the geodesic is reduced to a straight line on the  $uv$ -plane. The  $BPM$  and the inverse of  $BPM$  is exactly the same.
- (3) If the surface  $S$  contains the conjugate point(s) of  $B$  or  $C$ ,  $BPM$  fails to map in a one-to-one manner. This problem can be reduced by the proper choice of boundary.
- (4) The shape of the pattern varies according to the choice of reference points.
- (5) Unlike finite element method, the accuracy of  $BPM$  does not depend on the resolution of the grid, but rather on the choice of the boundary.

### Application of BPM on Continuous Surface

The BPM has been tested on virtual mannequin (Ng 1995) composed of an atlas bicubic Bezier surface patches. A man's top bodice is unfolded (Figure 2) into flat pattern, which resembles the draped pattern. choice of the reference points is critical as final shape of the pattern do vary according the reference points.

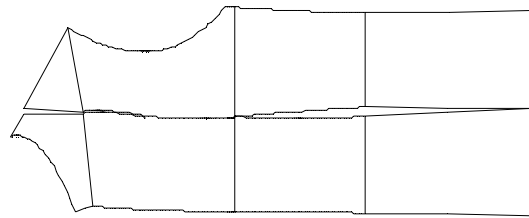


Figure 2 Unfolded Garment Pattern

of  
The  
the  
to

### Application of BPM on Discrete Surface

During the 3-D scanning, one can only obtain a set of data cloud, which is a discrete approximation of the continuous physical surface. To compute the geodesic curve on a discrete surface, one can follow any existing methods as such Zantout and Zheng (1994).

### Improvement of BPM

The present form of BPM is purely geometric based. The Generalized BPM (GBPM) is an improved version of BPM which takes the fabric properties, such as shearing and tensile into consideration. The geodesic curve on the deformed fabric surface can be mapped back to the relaxed state before processing by BPM.

### Conclusion

This article presents an alternative method of 3-D garment pattern unfolding method, besides the finite element method. This method is partially isometric with improved version being capable of handling the fabric properties. Its properties have been reported with illustration on the continuous surface. Bijective Pattern Map can be applied on discrete surface, such as 3D data cloud to unfold the garment surface to flat pattern.

### Reference

- (NG 1999) NG, Roger, CHAN, C.K., PONG, T.Y., AU, Raymond, "Distortional Properties of the Bijective Pattern Map (Part II: Change of Reference)", *Journal of China Textile University, English Edition*, 1999, Vol. 16, No. 1, Page 70-73.
- (NG 1997) NG, Roger, CHAN, C.K., PONG, T.Y., AU, Raymond, "Distortional Properties of the Bijective Pattern Map (Part I: Distortion in Length)", *Journal of China Textile University, (English Edition)*, 1997, Vol. 14, No.3, page 28-33.
- (NG 1995) Ng, R., Chan, C.K., Pong, T.Y., Au, R. *Algebraic Mannequin: The First Order Approximation. Conference Proceeding of the 3<sup>rd</sup> Asian Textile Conference*, Hong Kong, pp 734-742, 19-21 Sept 1995
- (Zantout 1994) Zantour, R.N., Zheng, Y.F., "Determining geodesics of a discrete surface", *Proceeding of the 1994 IEEE International Conference on Multisensor Fusion and Integration for Intelligent System (MFI'94)*, Las Vegas, NV, Oct. 2-5, 1994, pp 551-558.

# **Comparison of Sitting and Standing 3D Body Measurements of the Lower Body**

Suzanne Loker, Susan Ashdown, Katherine Schoenfelder, and Adriana Petrova  
Department of Textiles and Apparel  
Cornell University

The three-dimensional body scanner is a promising new research technology that will contribute to revolutionary changes in the conception, design, manufacture, and distribution of apparel. Currently, the quantification of body size and fit is complex and ambiguous. Traditional objective methods taken with a tape measure are inadequate to properly describe fit in its entirety. Body scanning provides multi-dimensional anthropometric data that have the potential to provide new insights into sizing and grading systems.

Anthropometric measurements for clothing are generally taken in only a standing position and there is limited knowledge about how these body dimensions change when the body is placed in other positions. The sitting position is of particular interest because it is frequently assumed in everyday life. This research was initiated to compare typical apparel body dimensions between the standing and sitting positions to determine how morphology and size impacts soft tissue displacement and its impact on the fit and design of pants.

A pilot study of nine subjects was conducted to investigate protocol and data collection methodologies. This pilot protocol was further refined and developed to study 49 subjects across various sizes. Cluster analysis results performed on body measurements from a larger study were used to ensure that a sufficient number of subjects of various body types were included in the subject population. Six 3D scans were taken of each subject: two standing and four sitting. Adhesive landmarks were used to mark sitting breadth, waist, hip, and thigh so to be visible for the appropriate 3D scan. Early results based on the pilot study indicated that waist, hip, and thigh increased and crotch lengths decreased with size. The pilot also indicated that changes in measurements may be linked to body size, with larger women exhibiting greater increase or decrease. Measurement extraction for the 49 subject main study is ongoing as multiple measurements can be extracted from the scans as different questions are posed.

# A Study of Ease Distribution and Garment Style

Zhaohui Wang<sup>1</sup>, Roger Ng<sup>1</sup>, Edward Newton<sup>1</sup>,

Weiyuan Zhang<sup>2</sup>

<sup>1</sup>Institute of Textiles and Clothing, Hong Kong Polytechnic University

<sup>2</sup>Institute of Fashion Design, Donghua University

## Introduction

In Pattern Generation process, style ease must be integrated into basic block according to the characteristics of style. Therefore, the relationship between garment style and ease distribution is crucial to the pattern alteration process. Since the distribution of ease in the garment is uneven and nonlinear, it is traditionally estimated mainly by the experiences of pattern makers.

## Objective

The objective of the current study is to evaluate the distribution of radial ease allowance of garment at different cross-sections of body.

## Methodology

Both the 3D surface data from mannequin with and without garment are digitized. The shape of cross-section is reconstructed by using the cubic-spline curves. By comparing the cross-sectional curves of body and garment, the ease at different location can be derived. To predict the ease distribution in garments of different volume for a particular body shape, a mathematical model of ease distribution is developed by surface fitting approach. This pilot study is based on ten draped garments of X-line style (hour-glass silhouette).

### *Definition of Radial Ease Allowance (REA)*

Within a cross-section of body with garment, radial ease allowance of the garment is the radial distance from the body surface to clothes' surface with respect to an artificial coordinate system. This definition is different from the girth ease allowance, which is the extra measurement along the circumference of a cross-sectional body shape. Furthermore, other concept of ease allowance, expressed in terms of distance, area and volume between body and garment can be found in the literature (Miyoshi 2001, Ng 1996). In this study, the radial definition is used because it can easily be expressed as equation (1) in polar coordinate system:

$$E = r_g - r_b$$

(1)

where  $E$  denotes the radial ease allowance,  $r_g$  denotes the radial distance of the garment from O to B, and  $r_b$  denotes the radial distance of the body from O to A as shown in Figure 1.

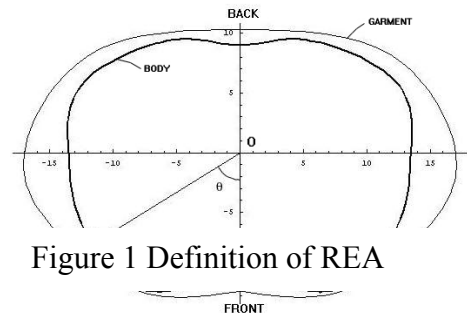


Figure 1 Definition of REA



## Analysis and Result

The cross-sectional view of the garments and the mannequin is displayed in Figure 2.

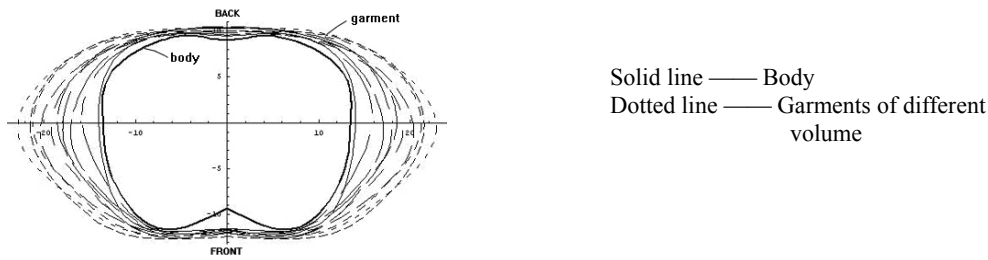


Fig 2 Bustline Cross Section Figure of Garment of Different Volume

Since the distribution is expected to be periodic with respect to angle  $\theta$ , and varies as the volume changes, the distribution function  $F$  is assumed to be of the form of Equation (2), with independent variables of  $\theta$  and volume parameter  $y$ , which is expressed as integers indicating the different sizes of the garments. Then, the distribution of radial ease allowance is modeled by fitting a surface of the form:

$$F(\theta, y) = \sum_{i=0}^4 \sum_{j=0}^5 \{a_i \cos[\theta]^{2i} \cdot y^j\} \quad (2)$$

Consequently, the distribution surface is shown in Figure 3.

### Conclusion

This study reveals the relationship between the ease allowance and garments of different volume. This relationship is crucial to the pattern alteration. Based on this distribution of radial ease allowance, one can easily generate the garment. By measuring the extra arc length on the garment respect to any given pair of angles, one can determine the segmental distribution of girth ease allowance, as well as the correct position of style lines. It is part of the effort in advancing the flat pattern theory.

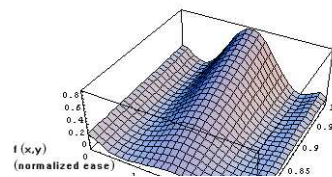


Figure 3 Distribution of REA

radial  
This  
process.  
surface.  
with

### Reference

- (Miyoshi 2001) Miyoshi M., Hirokawa T., Study on the Method of a Vacant Space Distance in a Worn Jacket for Clothing Pattern Design, *Journal of the Japan research association for textile end-uses*, 42, 4, pp233-241.
- (Ng 1996) Ng, R., Chan, C.K., Pong, T.Y., Au, R., Objective Measurement Of The “Fit” Of An Apparel. *Proceeding, Textile Institute 77<sup>th</sup> World Conference*, Tampere, Finland, 21-24 May 1996, pp 347.

# POSTER PRESENTATIONS

## Section I

### Synthesis and characterization of shape memory polyurethanes

Hu Jinlian\*, Yang Zhuohong, Ji Fenglong, Yeung Lapyan

*Institute of Textile and Clothing, The Hong Kong Polytechnic University, Hung Hum, Kowloon, Hong Kong*

#### 1. Introduction

Based on our previous work, a series of shape memory polyurethanes (SMPUs) were prepared from polycaprolactone diol 4000, 1,4-butanediol, dimethylol propionic acid (DMPA), triethylamine, 4,4'-diphenylmethane diisocyanate (MDI), methyl ethyl ketone (MEKO) and some additives such as PEG 200, Bisphenol A, PCL 530 were also blended with PCL 4000. Their mechanical, thermomechanical, thermal, and shape memory properties were investigated using DSC, FT-IR, DMA, and tensile testing.

#### 2. Experimental

##### 2.1. Synthesis of SMPUs

A series of shape memory polyurethanes were prepared according to the components listed in Table 1. The solid content of the product is about 15 ~ 20%.

Table 1. The formulation of shape memory polyurethanes (content in mol)

No.	MDI	PCL 4000	Additives	BDO	DMPA	Blocking agent MEKO	Tm
a	16 mmol	3 mmol	--	5 mmol	2 mmol	12 mmol	43.1
b	12 mmol	2 mmol	PEG 200, 4 mmol	2 mmol	2 mmol	4 mmol	47.3
c	12 mmol	3 mmol	PCL 530, 3 mmol	2 mmol	2 mmol	4 mmol	50.8
d	12 mmol	3 mmol	PEG 200, 3 mmol	2 mmol	2 mmol	4 mmol	44.3
e	14 mmol	4 mmol	PEG 200, 2 mmol	2 mmol	2 mmol	8 mmol	45.7
f	14 mmol	4 mmol	PEG 600, 2 mmol	2 mmol	2 mmol	8 mmol	45.3
g	14 mmol	3 mmol	BisphenolA, 2 mmol	3 mmol	2 mmol	8 mmol	43.3
h	16 mmol	3 mmol	BisphenolA, 3 mmol	2 mmol	2 mmol	12 mmol	46.5
i	16 mmol	4 mmol	BisphenolA, 2 mmol	2 mmol	2 mmol	12 mmol	46.0

\* Corresponding author: Dr. Hu J.L. (Email: tchujl@inet.polyu.edu.hk)

### 3. Results and discussion

#### 3.1. Shape memory effect

All samples were tested for DSC analysis, FT-IR and DMA analysis. Based on these results, samples **a**, **b**, **g**, and **h** were chosen to undergo to a further analysis of the shape memory effect. The results of the cyclic tensile tests to characterize the shape memory effect of these samples are shown from Figures 1 to 2. It has been found that these samples gave a higher shape recovery and higher shape retention as compared with that reported in the literature. For example, even after several cycles, sample **b** still has a shape recovery of around 88% and a shape retention of around 95%, while in literature, only about a 75% shape recovery can be obtained.

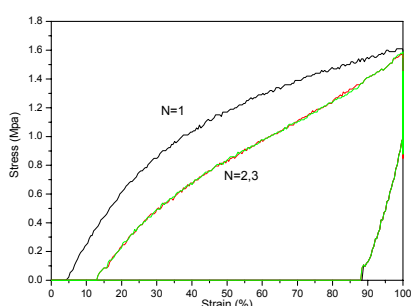


Figure 1. Cyclic tensile behaviour of **a** with 100% maximum strain.

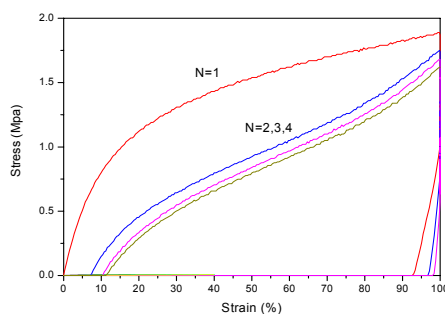


Figure 4. Cyclic tensile behaviour of **b** with 100% maximum strain.

### 4. Conclusions

In this paper, one series of shape memory polyurethanes were prepared and their thermomechanical, mechanical and thermal properties were tested. The shape memory properties of samples **a**, **b**, **g**, and **h** were also investigated. The results showed that these samples have a good shape memory effect.

#### Conference:

1. Lee, B.S., Chun, B.C., Chung, Y-C., Sul, K.I., Cho, J.W. *Macromolecules* 2001, **34**, 6431-6437.
2. Kim, B. K., Lee, S. Y., Lee, J. S., Baek, S. H., Choi, Y. J., Lee, J. O., and Xu, M. *Polym.* 1998, **39** (13), 2803-2808
3. Jeong, H. M., Lee, J. B., Lee, S. Y., and Kim, B. K., *J. Mat. Sci.*, 2000, **35**, 279-283
4. Li, F. K., Chen, Y., Zhu, W., Zhang, X., and Xu, M., *Polym.*, 1998, **39** (26), 6929-6934
5. Han, M.J., Boung, K.A., Byung K.K., *Eur.Polym.J.*, 2001, **37**, 2245-2252
6. Yang, B., Huang, W.M., Li, C., Lee, C.M., Li, L. *Samrt Mater. Struct.* 2004, **13**, 191-195

## **New Process for Spun Yarns from Producer Color Fibers**

speaker/author: Glen E. Simmonds, DuPont

other authors: William R. Corcoran Jr., David C. Visser, Roger S. Wilson, Joseph Jones all of DuPont

Gregory J. Scott, Continua Technologies;

David They, SSM

### **Introduction:**

A new process overcomes problems that severely limit the viability of producing spun yarns from producer color fibers. In addition, the process offers totally new color possibilities. Commercially available equipment was unveiled at ITMA 2003 in Birmingham, England.

### **Problems with Current System:**

Producer color staple fibers currently occupy only a small market niche due to the tremendous cost and logistical complications involved with current staple systems. In fiber production, the issues are:

- Extremely large lot size minimums if made using a CP (continuous polymerization) staple process
- Expensive color changes due to equipment cleaning
- Lot to lot color matching if made using batch processes
- More expensive fiber (vs CP produced) if made using a batch process
- Limited color range availability

In the yarn spinning mill, the issues are:

- Extensive downtime and cleaning, especially of carding machines at each color change
- Limited color range offered to customers due to change costs
- Large inventories of feed fibers with limited shelf life
- Large minimum lot size of final yarns

### **Advantages and Current Use of Producer Color Fibers:**

The major advantages of using producer color fibers are:

- Elimination of costly and environmentally harmful dyeing,
- Color fastness

For these reasons the use of producer colored fibers is growing among textured filament yarns. In addition, the problems of color changes and color matching are less imposing in POY spinning, even for mass producers using CP's instead of batch processing, thanks to new technologies like transfer line color injection.

### **Special Features of New Process:**

The new process shifts the spun yarn feed source from staple fiber to filament yarn, especially partially oriented yarn (POY). As a result, the direct conversion of POY to spun yarn opens up the field of producer color to spun yarn producers and users. Key features of the new process are:

- Access to a wider range of producer color fibers at smaller lot sizes and reasonable prices
- Very small finished yarn lot sizes possible
- No extensive cleaning or downtime with color changes
- The ability to create custom color blends without the use of mixed polymer types (such as a blend of cationic dyeable and disperse dyeable fibers).

- Yarn count flexibility, ie not limited to standard POY to Textured Yarn relationships
- A vast color palette from a relatively small number of feed yarn colors in inventory (see chart)

	No. of Feed Colors			
No. of Feed Ends	3	6	10	Min Yarn Denier
3	<b>10</b>	<b>56</b>	<b>220</b>	<b>110</b>
6	<b>28</b>	<b>462</b>	<b>5005</b>	<b>260</b>
10	<b>66</b>	<b>3003</b>	<b>92378</b>	<b>375</b>

Number of Final Spun Yarn Colors

## **Enhancement of the Environmental Stability of Polypyrrole-Coated Fabrics**

X.Y. Cheng, W.Y. Kwok, J. Tsang, X.M. Tao, M.Y. Leung, C.W. Yuen, X.Pue

Institute of Textiles and Clothing, The Hong Kong Polytechnic University

### **Abstract**

Polypyrrole (PPy)-coated fabric can be produced by means of chemical vapor deposition using pyrrole in the presence of oxidizing agent. This electrically conductive fabric are suitable for a wide range of wearable textile sensors in the application of electrical apparel that can sense temperature, humidity, heart beat rate, respiration rate, posture and movement. However, the stability is one of the most important factors determining its potential for practical applications. In this paper, emphasis is placed on studying the effect of various types of treatment on the environmental stability of the PPy-coated fabrics. The effect of various types of treatment on the enhancement of the stability of the polypyrrole-coated fabrics was investigated by monitoring the decay of conductivity. Results showed that 1) cyclic temperature treatment can obtain better stable conductive characteristics; 2) low temp exhaustion was the best in thermal sensitive recovery for the cyclic temperature property; 3) fabrics with higher hydrophobicity (such as polyester or fabrics with water repellent treated) would be the best fabrication for thermal sensing for the conductive stability in same temperature. The mechanisms are analyzed.

## **Direct electrochemical reduction of vat dyes in a fixed bed of graphite particles**

David Crettenand, ETH Zurich, Institute for Manufacturing Automation,  
CH-8092 Zürich, Switzerland

Vat dyes, especially indigo, play an important role in today's dyeing industry. In the dyeing of cellulosic fibres, vat dyes hold a large part of the dyestuff market. About 33,000 tons of vat dyes are being used annually. The situation will remain constant in the near future mainly because vat dyes yield dyed textiles of excellent all-round fastness, particularly to light, washing and chlorine bleaching.

Nevertheless, vat dyes require a somewhat complicated application procedure because they are practically insoluble in water. In order to produce a water-soluble form of the dyestuff (leuco dye) with an affinity to the cellulosic fibre, the dye molecule has to be reduced. The reducing agent generally used is sodium dithionite. Unfortunately, the disposal of dye baths and rinse water causes problems, because the reducing agents are finally oxidized into a form that can hardly be regenerated. Thus, sulphite, sulphate, thiosulphate and toxic sulphide, contaminate waste water from dyeing plants (worldwide approximately 180,000 t/a). Therefore, many attempts are made to replace the environmentally unfavourable sodium dithionite by ecologically more attractive alternatives, like organic reducing agents (e.g.  $\alpha$ -hydroxyketones), the indirect electrochemical reduction employing a redox mediator (e.g. iron complexes with triethanolamine or gluconic acid), the electrocatalytic hydrogenation, or the direct electrochemical reduction. According to this, a radical anion is formed in a comproportionation reaction between the dye and the leuco dye, and a subsequent electrochemical reduction of this radical takes place. However, until now, reactor performances are poor, operation are still expensive, and partly toxically chemicals (reducing agent, mediator) are necessary [1-5].

For ecological and economic reasons, electrochemical reduction is an attractive alternative to vatting techniques employing chemical reducing agents [6]. Here, the most challenging engineering task is to achieve a dye reduction rate and an electrolytic current efficiency, which are high enough to make electrochemical reduction industrially feasible. Unfortunately, it is not industrially feasible to reduce indigo in aqueous solution electrochemically under dye bath conditions on a planar electrode. The most limiting factor appears to be the poor contact between indigo particles and the electrode. It is therefore desirable to develop a reduction process by using a different process design for the intensification of the contact between the dye particles and the electrode. Graphite granules are used as electrode material in a fixed bed reactor. It is an attractive process, because the reactor performances are much more promising than with other electrochemical alternatives. In addition graphite is a cost effective and stable material. Hardly any decomposition of the particles has been observed throughout all experiments, and the pressure drop over the graphite material proved to be feasible [7-8].

The application of this new process has been investigated by spectrophotometric and voltammetric experiments in a laboratory plant flow through reactor with various graphite material. The electrochemical activity of the graphite appears to be connected with quinone and hydroquinone groups at the surface of the graphite material, which can be depicted as immobilised mediators. Therefore, it is possible to accelerate the relevant processes by the selective generation of quinone-like functionalities on

the surface of the graphite electrode. Oxidative pre-treatment can increase the content of oxygen-containing groups on the surface of carbon. Thus, special pre-treatment of the graphite has been investigated to enhance the reduction rate (chemical, electrochemical and plasma pre-treatment).

Another interesting approach to improve the electrocatalytic properties, the covalent binding of quinoid molecules or other mediator system onto the graphite surface, has also been investigated. Thus, electron transfer mediators, which can undergo fast electron transfer with the electrode and also with the substrate (vat dye), are immobilized on the carbon electrode.

Improvement of the cell construction will be a requirement for the successful realization of this method in textile dye houses. The measurement of the reduction rate and the current efficiency is to be optimized in dependence of relevant variables, such as concentration of the pigment, pH, temperature, current density, flow rate, etc..

The proposed process allows reducing an extensive range of vat dye (i.e. indanthrene dyes) and indigo suspensions. The electrochemical reactor performance is sufficient for the complete reduction of a stock solution in case of continuous dyeing.

The next step will be the design, planning and building of an electro-chemical pilot reactor after a scale-up procedure and practice tests in dyeing of cellulose fibres.

- [1] T. Bechtold, A. Turcanu, *J. Electrochem. Soc.* **2002**, *149*, D7.
- [2] A. Roessler, O. Dossenbach, W. Marte, P. Rys, *J. Appl. Electrochem.* **2002**, *32*, 647.
- [3] C. Merk, J. Botzem, G. Huber, N. Grund, Patent WO 01/46497, **2001**.
- [4] A. Roessler, O. Dossenbach, P. Rys, *J. Electrochem. Soc.* **2003**, *150*, D1.
- [5] A. Roessler, D. Crettenand, O. Dossenbach, W. Marte, P. Rys, *Electrochim. Acta* **2002**, *47*, 1989.
- [6] H. Schlüter, *Melliand Textilberichte* **1995**, *76*, 143.
- [7] A. Roessler, D. Crettenand, O. Dossenbach, P. Rys, *J. Appl. Electrochem.* **2003**, *33*, 901.
- [8] A. Roessler, D. Crettenand, *Dyes and Pigments* **2004**, *63*, 29.



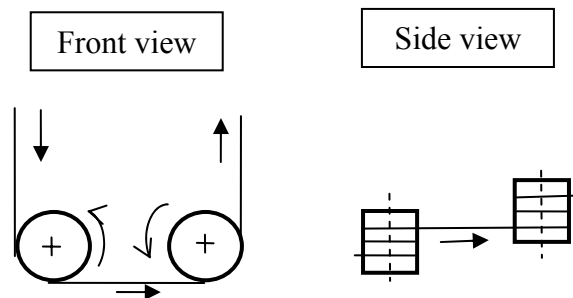
## Modeling of individually driven drafting godets

Matteo Castiglioni, ETH Zurich, Institute for Manufacturing Automation,  
CH-8092 Zürich, Switzerland

Individually driven godets are state of the art in full scale melt spinning machinery. Those godets are normally driven by reluctance motors, overrated in power, fed by inverters, without closed loop speed control.

For subsequent drafting of filament yarns in draw winding or draw texturizing machines, simple drives with a single common motor and a set of reduction gears are in common use. A resistive or inductive heater is typically mounted in those godets, in order to heat the surface.

The stretch of the partially oriented polymer chains occurs at a temperature around the glass transition temperature and is induced by a set of those godets, which in a sequence rotate at increasing speed.



The yarn path goes several times around the godets where it is heated by conduction from the hot godet surface.

The need of higher speed, finer tuning, and flexibility of the process, has brought to consider the use of smaller individual drives.

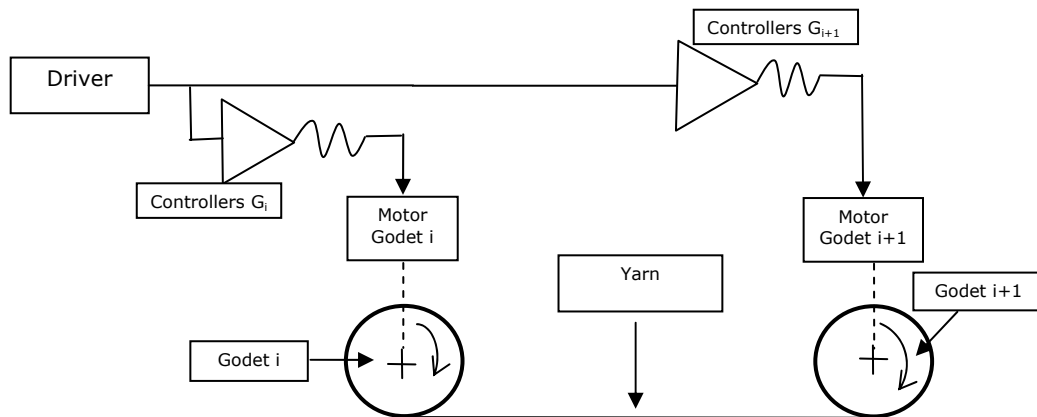
The target of the project is to develop a system made of smaller and lighter godets, each driven by a motor with a precise individual controller.

For such a light godet and sensitive control loop, the behavior of the yarn with its elasticity, dampening and plasticity properties may cause instability of the velocity control loop.

A simulation of godets with different inertias and controllers, allows finding a good compromise between an overrated system, with low efficiency and high costs, and a small-individual apparatus, which is more complex in the control but more flexible and efficient for high speed.

The model proposed in this paper is a dynamic model of a set of godets, having a given inertia, being driven by different kind of motors, controlled by either open or closed loop controls, and processing a yarn with a range of modulus and denier.

The speed and the torque of each godets, influenced by the dynamic of the yarn, is the subject of closer examination.



In a first phase of the simulation the yarn is considered an elastic coupling element between two godets and its slipping on the godet is neglected.

In the model the dynamic equations of all the elements are transformed in Laplace functions.

For each controller, inertias, type of motors as well as the yarn, a response time is calculated.

Different combinations of yarn-godet-motor-control are then studied and for each of them the possible causes of instability are found out.

The result of the simulation is a comparison of typical combinations of motor-driver: reluctance motor with inverter, brushless D.C. with closed loop control, and synchronous motor with open loop.

Following the insight gained by this model, different concepts and algorithms for open and closed loop control are discussed.

#### Literature cited:

- [1] Michael Pyra, Dieter Noss, Markus Herzberg, Barmag AG (DE), "MPS Barmag introduces new generation of texturing machines", *International Fiber Journal*, **35** (October 2003).
- [2] S.E. Bechtel, S. Vohra, K.I. Jakob, "Stretching and Slipping of Fibers in Isothermal Draw Processes", *Textile Research journal*, **72** (9), 769-776 (2002).
- [3] S.E. Bechtel, S. Vohra, K.I. Jacob, "Modeling of a two-stage draw process", *Polymer*, **42**, 2045-2059 (2000).
- [4] S.E. Bechtel, S. Vohra, K.I. Jacob, C.D. Carlson, "The Stretching and Slipping of Belts and Fibres on Pulleys", *Journal of Applied Mechanics*, **67** (3), 197-206 (2000).
- [5] A.R. Postema, A.J. Pennings, "Study of the Drawing Behavior of Poly (l-Lactide) to Obtain High-Strength Fibres", *Journal of Applied Polymer Science*, **37**, 2351-2369 (1989).
- [6] M.V. Sussman, "Incremental Drawing for Controlling Synthetic Fiber Structure, Properties, and Productivity", *Advances in Polymer Technology*, **12** (3), 291-296 (1993).

# The Preparation of High Efficiency Filter Media via Electrospinning

**Se Kwan Jeong, Dae Young Lim, Sung Won Byun and Yong Sik Chung\***

*Technical Textile Team, Korea Institute of Industrial Technology, Chonan, Korea*

*\*Department of Textile Engineering, Chonbuk National University, Cheonju, Korea*

*e-mail: chsk007@kitech.re.kr*

## Introduction

Clean rooms are widely used in the semiconductor, pharmaceutical, medical device, aerospace, food processing, disk drive and other industries where foreign matter such as particles must be kept out of the workplace. The most stringent requirements of clean room is to prevent particles greater than  $0.1\ \mu\text{m}$  which can result in device failure. To make clean room, the clean rooms are covered with HEPA or ULPA filters.

Air filtration mechanism is classified by diffusion, inertia, gravity, interception and electrostatic effect. Fine particles are removed by diffusion and inertia effect mainly. By electrostatic effect, filtration efficiency is increased more. Recently, electret filter is applied to most air filter because of the high filtration efficiency, long filter life and low pressure drop.

Glass fiber and meltblown nonwovens have been used in the area of air filtration in commercial, industrial and defense applications for more than 20 years. Nanofiber web will be a strong candidate for manufacturing a HEPA or ULPA filter media, in the near future.

In this study, we prepared the high efficiency filter media composed with fluoropolymer-based nanofiber. And, we evaluated the filtration performances.

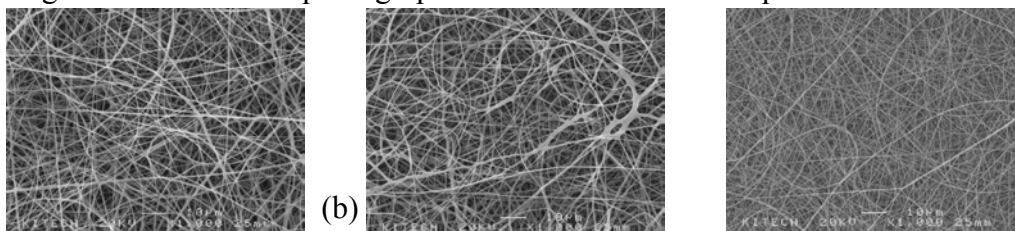
## Experimental

PVDF-HFP (Polyvinylidene fluoride-co-hexafluoropropylene) was purchased from Atofina Inc. The polymer solution for electrospinning were prepared by using mixture of solvents acetone and *N,N*-dimethyl acetamide (DMAc) in the ratio of 55/45. Electrospinning parameters are as following; applied voltage: 20~30 kV, solution concentration: 15~20 wt% and basis weight: 2~8 g/m<sup>2</sup>.

Fractional efficiency of the electrospun web evaluated by Fractional Efficiency Filter Tester (TSI 3160, TSI Inc.). Pore size and pore distribution analysis were measured by Capillary Flow Analysis (CFP 1200-AEL, Porous material Inc.). Morphology of electrospun web was measured by Scanning Electron Microscope (SEM, JSM-6400, JEOL).

## Results and Discussion

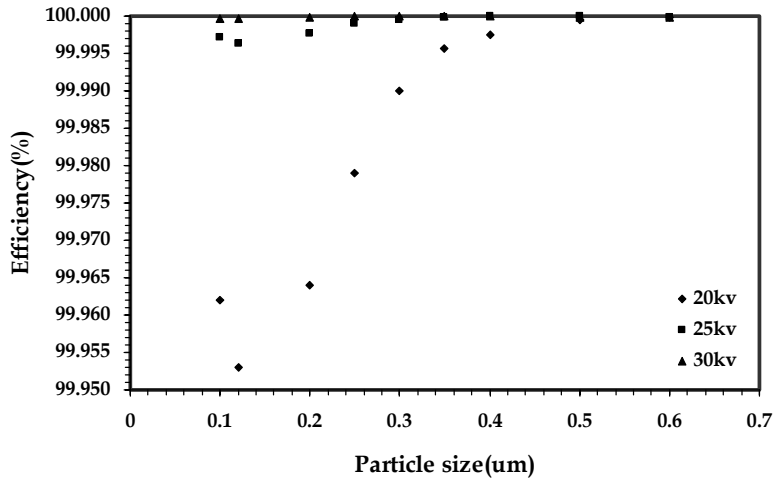
Fig. 1. show the SEM photographs of PVDF-HFP electrospun web.



**Fig. 1. SEM photographs of PVDF-HFP electrospun web (a) 20 kV, (b) 25 kV and (c) 30 kV.**

Increase in applied voltage cause the decrease in the diameter of fiber, and, finally, the decrease in the pore size of electrospun web.

Fig. 2. shows the fractional efficiency of high efficiency filter media. The value of fractional efficiency increased according to the increase in applied voltage.



**Fig. 2. Fractional efficiency of PVDF-HFP electrospun web(basis weight: 6 g/m<sup>2</sup>).**

### References

1. Donaldson company Inc., *American filtration & separation society report*. **2002**
2. New HEPA/ULPA filters for Clean-Room Technology, *filtration & separation*, volume 33, Issue 3, march **1996**, page 245-250.
3. Polymeric nanofibres exhibit an enhanced air filtration performance, *Filtration & Seperation*, Volume 39, Issue 6, July-August **2002**, page 20-22.

# Sol-Gel Synthesis of Nano-Scaled Barium Titanate Fibers via Semi-Alkoxide Routes and Electrospinning

Sung Wook Lee<sup>(1)</sup>, Boyoung Chu<sup>(2)</sup>, Do Sun Hwang<sup>(2)</sup>, Seung Goo Lee<sup>(2)+</sup>, Chang Whan Joo<sup>(2)</sup> and Yong L. Joo<sup>(3)</sup>

(1) Research Institute of Advanced Materials, Chungnam National University, Daejeon, 305-764, Korea

(2) Department of Textile Engineering, Chungnam National University, Daejeon, 305-764, Korea

(3) School of Chemical & Biomolecular Engineering, Cornell University, 340 Olin Hall, Ithaca, NY 14853, USA

+ : Corresponding author: [lsgoo@cnu.ac.kr](mailto:lsgoo@cnu.ac.kr)

## Abstract

Nanosopic Barium titanate( $\text{BaTiO}_3$ ) fibers with diameters of 100 to 300nm were prepared by calcining the electrospun precursor fibers. These precursor nanofibers were obtained from semi-alkoxide route of  $\text{Ba}(\text{OH})_2$  and titanium (IV) isopropoxide(TiP) by using the electrospinning with PVAc as gelator or binder to help spinnability. The sintered nanofibers were characterized by using the XRD, SEM, FTIR, and thermal analysis.

## Introduction

One dimensional structures with nanoscaled diameters are of great potential for understanding the fundamental concept about the roles of dimensionality and size in optical, electrical, and mechanical properties of materials.<sup>1-5</sup> Ceramics that have  $\text{ABO}_3$  type structure can be applied to various electronic devices because of its piezoelectric, ferroelectric, thermoelectric and optical properties. Recent advances in nanotechnology such as MLCC, MEMs, and DRAM have resulted in the miniaturization of devices. These require nanosize inorganic fibers such as  $\text{TiO}_2$ ,  $\text{BaTiO}_3$  and etc. with high surface area.

Since the discovery of carbon nanotubes, the preparation of one dimensional structures of nanotubes and nanowires have attracted a wide attention.<sup>2</sup> In recent year, there has been intense interest surrounding the fabrication of nanofiber of oxides have also been synthesized with the sol-gel method via an electrospinning technique.<sup>6</sup> In the present work, the formation of  $\text{BaTiO}_3$  nanofibers using sol-gel semi-alkoxide route and electrospinning technique was studied.

## Experimentals

$\text{Ba}(\text{OH})_2$  and isopropoxide(TiP) sol mixture was produced by hydrolysis and condensation by dropwise addition of aqueous HCl to solution with vigorous stirring at room temperature for 2h. And 10wt% PVAc solution that is dissolved to acetone was slowly added into the mixture under vigorous stirring to give the final electrospinning solution. A transparent solution was obtained by this method. Electrospinning of the prepared solution was conducted under the following condition: 15cm of the tip-to-collector distance(TCD) and 15kV of the applied electric field. The electrospun precursor fibers were calcined at 800, 1000, and 1200°C in air for 3h to get the  $\text{BaTiO}_3$  polycrystalline nanofibers. The morphology, crystalline structure, and chemical

composition etc. of the electrospun fibers were characterized with SEM, XRD, and FTIR, respectively

### Results and Discussion

Figure 1 shows a SEM photograph of electrospun BaTiO<sub>3</sub>/PVAc composite nanofibers. The results revealed that the the fine fibers had diameters varying from 100 to 300 nm. It can be seen that the surface of BaTiO<sub>3</sub> composite fibers was smooth due to the amorphous nature of PVAc. After the BaTiO<sub>3</sub> composite nanofibers were calcined at several temperatures of 800, 1000, and 1200°C, amorphous peak of PVAc disappeared, and intense reflection peaks corresponding to pure cubic BaTiO<sub>3</sub> appeared. The formation of Barium titanate nanofibers is further supported by IR spectra. Morphological changes of nanofibers, crystal structures, and the coordination of BaTiO<sub>3</sub> after sol-gel synthesis were investigated by using SEM, XRD, and FTIR analysis, respectively.

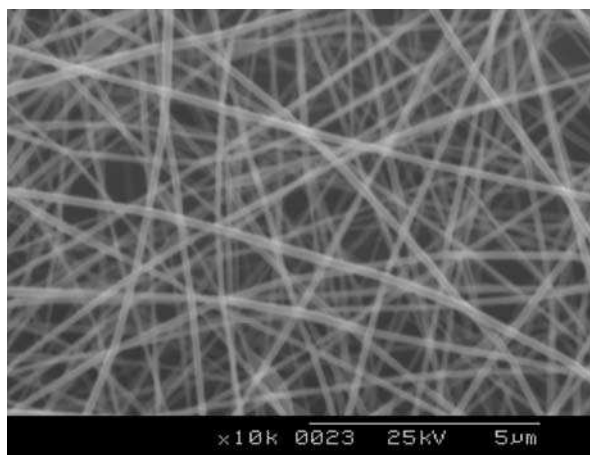


Fig. 1. SEM photograph of the electrospun BaTiO<sub>3</sub> nanofibers.

Conclusively, BaTiO<sub>3</sub> nanofibers were obtained from semi-alkoxide route of Ba(OH)<sub>2</sub> and titanium (IV) isopropoxide(TiP) by using the electrospinning. In this study, we will discuss about the physical properties, morphology, structure, and applications of nanoscopic BaTiO<sub>3</sub> fibers, with the various instrumental analysis

### Acknowledgement

This work was supported by Korea Research Foundation Grant (KRF-2001-005-00037).

### References

1. P. Yang, and C. M. Lieber, *J. Mater. Res.*, **12**, 2981 (1997).
2. Z. W. Pan, Z. R. Dai, and Z. L. Wang, *Science*, **291**, 1947, (2001).
3. M. H. Huang, E. Weber, and P. Yang, *Adv. Mater.*, **13**, 113 (2001).
4. H. Z. Zhang, Y. C. Kong, Y. Z. Wang, and S. Q. Feng, *Solid State Commun.*, **109**, 677 (1999).
5. Z. R. Dai, Z. W. Pan, and Z. L. Wang, *Solid State Commun.*, **118**, 351 (2001).
6. H. Guan, C. Shao, S. Wen, B. Chin, X. Yang, *Inorg. Chem. Commun.*, **6**, 1302, (2003).

## Structures and Properties of Wet Spun Thermo-regulated Polyacrylonitrile-Vinylidene Chloride Fibers

<sup>1,2</sup>Zhang Xing-xiang, <sup>1</sup>Tao Xiao-ming, <sup>1</sup>Yick Kit-lun, <sup>2</sup>Wang Xue-chen  
(*1-Institute of Textiles and Clothing, The Hong Kong Polytechnic University, Hong Kong, China; 2-Institute of Functional Fibers, Tianjin Polytechnic University, Tianjin 300160, China*)

Thermo-regulated Polyacrylonitrile-Vinylidene Chloride (PAN/VDC) fibers containing 4-40wt% of MicroPCMs were wet-spun. The spinnability tends to decrease gradually with the increasing contents of MicroPCMs in the mixture. Mixtures containing less than 30wt% of MicroPCMs can be spun into fiber readily. The structures and properties of the fibers were investigated by using FTIR, SEM, DSC, WAXD, DMA and TG etc. The microcapsules are intact and evenly distributed inside the polymer matrix (Fig.1). The tensile strengths of the fibers with titers in the range of 1.9 to 10.9dtex are 0.7 to 2.0cN/dtex. The elongation of the fibers is approximately 7%. The modulus of the fiber decreases with the increase of MicroPCMs content (Fig. 2). The heat absorbing and heat evolving temperatures of the fibers increase slightly with the increasing content of MicroPCMs. The enthalpy of the fiber containing 30wt% of MicroPCMs is approximately 30J/g, and the enthalpy rises steadily as the content of MicroPCMs increase (Table 1). The glass transition temperature of the fiber is 89-108°C which decreases with the increase of MicroPCMs content, and the melting and decompose temperatures of the fiber are approximately 190°C and 220°C, respectively. The fibers have a value of LOI higher than 26% and are permanent flame retardancy.

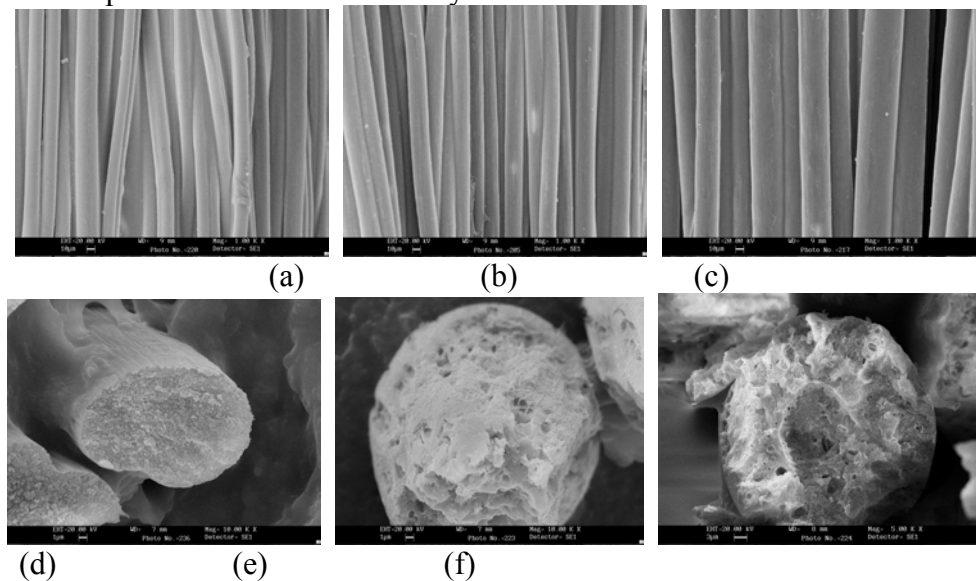


Fig. 1 SEM micrographs of PAN/VDC fibers: A0 side surface (a) B9 side surface (b) B20 side surface (c) A0 profile (d) B17 profile (e) profile (f).

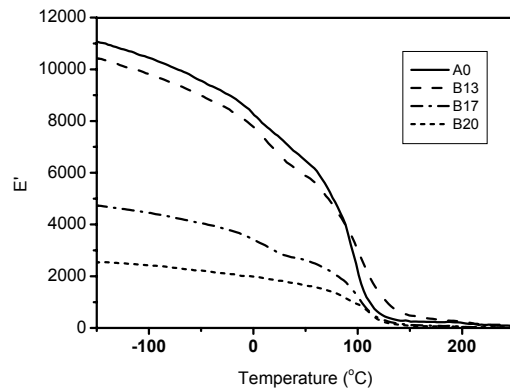


Fig. 2 Modulus and temperature curves of the thermo-regulated fibers

Table 1 Phase change properties of thermo-regulated PAN/VDC fibers

Sample No	MicoPCMs Content/wt%	Efficiency of Enthalpy, %	Tm <sup>a</sup> , °C		$\Delta H_m^d$ , J/g	Tc <sup>e</sup> , °C		$\Delta H_c^h$ , J/g
			Tmo <sup>b</sup>	Tmp <sup>c</sup>		Tco <sup>f</sup>	Tcp <sup>g</sup>	
A0	0	-	-	-	-	-	-	-
B4	4	67	19.3	24.5	3	14.5	8.7	-4
B9	7	67	20.5	25.9	5	16.9	9.6	-7
B11	10	67	21.0	25.7	4	14.9	20.8	-10
B13	15	72	23.2	29.5	14	24.1	21.8	-16
B15	18	71	26.0	30.6	14	26.4	21.9	-19
B17	20	71	25.3	30.3	20	25.0	22.6	-21
B20	30	67	24.3	30.7	27	24.0	20.2	-30
B23	35	65	25.4	30.9	30	25.8	22.0	-34
B25	40	74	26.1	31.2	43	26.1	22.1	-44
C0	10		27.6	33.3	145	26.3	22.2	-149

<sup>a</sup>Tm-melting temperature on the DSC heating curve. <sup>b</sup>Tmo-the melting starting temperature.

<sup>c</sup>Tmp-the melting peak temperature. <sup>d</sup> $\Delta H_m$ -melting enthalpy. <sup>e</sup>Tc-crystallization temperature on the DSC cooling curve. <sup>f</sup>Tco-the crystallization starting temperature. <sup>g</sup>Tcp-the crystallization peak temperature. <sup>h</sup> $\Delta H_c$ -crystallization enthalpy.

## References

1. Bryant, Y. G., and Colvin, D. P., U.S. 4756985 (1988).
2. Bryant, Y. G., American Society of Mechanical Engineers, Bioengineering Division BED, 14-19 November 1999, Nashville, TN, USA
3. Bryant, Y. G., *2.0 New Textiles-New Technologies, Techtexile Symposium*, Frankfurt, Germany, 1(1992).
4. Zhang, X. X., Tao, X. M., Yick, K. L., and Wang, X. C., *Colloid & Polymer Sci.*, 88(2), 330-336 (2004).



## **Characterization of Polymer Solutions Intended for Electrospinning**

Andrew Hawkins, Gisela Buschle-Diller, Textile Engineering Department, Auburn University,  
AL 36849

An attempt has been made to predict the potential for fiber formation via an electrospinning process by characterizing the polymer solution. Examples for easy-to-electrospin polymers include poly(vinyl alcohol), polyacrylate and poly(vinyl pyrrolidone). Different concentrations of the polymer solutions were prepared. Their characteristics regarding viscosity, surface tension, conductivity and drying were studied and compared to solutions of difficult-to-spin polymers, such as chitosan. Electrospun products were characterized by scanning electron microscopy.

## **Development of fibrous materials for Micro-electromechanical Systems (MEMS)**

Shahyaan Desai and Anil N. Netravali  
Fiber Science program, Dept. of Textiles and Apparel,  
Michael O. Thompson  
Dept. of Materials Science and Engineering,  
S. Leigh Phoenix  
Dept. of Theoretical and Applied Mechanics,  
Cornell University, Ithaca, NY 14853

### **Abstract:**

The micro-electromechanical System (MEMS) technology, as it exists today, has been developed primarily using isotropic materials, and processes developed by the semiconductor industry. Fundamental limitations in the mechanical properties of semiconductor materials such as silicon, which forms the backbone of the majority of MEMS structures, have prevented the progress of dynamic micro-mechanical devices. It is therefore essential to investigate and explore the behavior of alternative materials with more versatile and anisotropic mechanical properties better suited for micro-mechanical applications.

Fibrous materials as yet remain unexplored for MEMS applications. We have developed a novel MEMS materials technology based on such materials and have demonstrated the fabrication of fibrous micro-mechanical structures using conventional semiconductor processing. Dynamic characterization has shown that in sub-mm lengths, the reduction in defects per length enhances the mechanical and physical properties of  $\mu\text{m}$  diameter fibers considerably beyond corresponding macroscopic lengths and bulk materials. Such behavior promises to have tremendous implications in incorporating fibrous materials in MEMS structures where their superior mechanical behavior and observed fatigue resistance can be exploited.

# Mechanical Behaviors of Woven Fabrics

Huiyu Sun\*

Division of Textiles and Clothing, University of California, Davis, CA 95616, USA

## Abstract

This paper introducing some recent research progress consists of two parts: the shear deformation analysis and Poisson's ratios for woven fabrics. The analytical methods of the shear moduli and Poisson's ratios for woven fabrics will enable more rigorous studies on such important issues of fabric bending and draping behaviors.

A new mechanical model is proposed in this paper to evaluate the shearing properties for woven fabrics during the initial slip region. Compared to the existing mechanical models for fabric shear, this model involves not only bending but also torsion of curved yarns. Analytical results show that this model provides better agreement with the experiments for both the initial shear modulus and the slipping angle than the existing models.

Furthermore, another mechanical model for a woven fabric made of *extensible* yarns is developed to calculate the fabric Poisson's ratios. Theoretical results are compared with the available experimental data. A thorough examination on the influences of various mechanical properties of yarns and structural parameters of fabrics on the Poisson's ratios of a woven fabric

is given.

*Keywords:* Plain-weave fabrics; Shear deformation; Undulation geometry; Poisson's ratios; Extensible yarns

## Section II

### Liquid Ammonia Treatment of Linen Fabrics

<sup>1</sup>\*EMÍLIA CSISZÁR, <sup>1</sup>BARBARA DORNYI, <sup>2</sup>PÉTER SOMLAI, <sup>2</sup>ANIKÓ BORS

<sup>1</sup>*Budapest University of Technology and Economics, Department of Plastics and Rubber  
Technology, H-1521 Budapest, Hungary;*

<sup>2</sup>*Pannon-Flax Linen Weaving Corp., H-9027 Győr, Hungary*

\*e-mail: emi@muatex.mua.bme.hu

Recent fashion trends have increased demands for natural bast fibers in general. The best known of them is linen, which is utilized widely in wearing apparel and household textiles. Linen, with a more environmentally-friendly image than cotton, has several extremely advantageous features like excellent tensile properties, high tenacity, “cool-handle” attribute, good comfort and appearance. Along with the many positive qualities, linen fabrics have some disadvantages, such as low wrinkle recovery, dimensional instability, poor abrasion resistance, as well as high stiffness and low resilience. Various finishes developed for linen can compensate for some of these less desirable qualities. Blending of linen with cotton or synthetic fibers may also help to improve the negative properties. Liquid ammonia treatment can also give significant improvement in the mentioned negative properties of linen.

Liquid ammonia treatment induces intracrystalline swelling of cellulose and it has considerable influence on the rate and degree of conversion of the subsequent heterogeneous cellulose reactions. Two alternative technologies exist for liquid ammonia treatment today. They differ from each other especially in the procedure used to remove ammonia after the swelling stage. In the water-based process ammonia is removed from the swollen substrate by means of hot water. In the dry-steam process ammonia is removed by dry volatilization followed by steaming. The removal techniques alter both the physical properties and fine structure of the substrate. The commercial processes are generally applied to cotton products. Improvements that are conferred to cotton textiles by liquid ammonia treatment are widely documented in the literature. It is very effective in enhancing certain end-use properties, such as dimensional stability, tensile strength, resistance to abrasion, crease recovery, as well as handle and appearance. Although a number of shorter studies and comprehensive reviews have been published regarding the swelling with liquid ammonia, most of them concentrated on cotton and only a very few publications focused on liquid ammonia treatment of linen and linen-containing fabrics. Our starting assumption is that liquid ammonia treatment can be an appropriate technology for manufacturing of linen and linen containing woven fabrics with excellent easy-care and wearing properties, as well as for producing of high quality and luxurious tablecloths and apparel textiles from linen.

The objective of this work is to evaluate the influence of liquid ammonia treatment on the properties of linen and linen/cotton fabrics. 100 % linen and cotton/linen (warp/weft) woven fabrics from different stages of the finishing process, were treated with liquid ammonia in large-scale production. Removal of the liquid ammonia was performed by water. Research discussed in this paper is concerned first with the improvement of easy-care and wearing properties; second

with the changes in abrasion resistance, fabric structure, tensile properties and fine structure; third with the comparison of behavior of cotton and linen constituents during the swelling process; and finally with the evaluation of the finishing step applied prior to liquid ammonia treatment.

**Key Terms:** Liquid ammonia treatment, Linen fabrics, Linen-cotton fabrics, Easy-care properties, Mechanical properties, Fine structure

# **Alkalization of natural fibers. Influence of batch conditions and exposure times on their physical behaviour**

Piedad Gañán <sup>1</sup>, Aitor Arbelaiz, Rodrigo Llano-Ponte and Iñaki Mondragon <sup>2\*</sup>

<sup>1</sup> Assistant Professor of New Materials Group  
Universidad Pontificia Bolivariana  
Circular 1, # 70-01. Medellin (Colombia)

<sup>2</sup> Professor of Chemical Engineering. Head of ‘Materials + Technologies’ Group  
Dpto. Ingenieria Quimica y M. Ambiente, Escuela Univ. Politecnica  
Universidad del Pais Vasco/Euskal Herriko Unibertsitatea.  
Pza. Europa, 1. 20018 Donostia - San Sebastian (Spain)  
e-mail: iapmoegi@sc.ehu.es

## **ABSTRACT**

The fiber/matrix interface has an important influence on mechanical and physical properties of composite materials. In the case of composites reinforced with natural fibers, it is a source of problems owing to the low compatibility between hydrophilic natural fibers and hydrophobic polymeric matrices. Different alternatives have been investigated to enhance the natural fiber/polymeric matrix interfacial adhesion, such as: chemical and physical fiber modification, matrix modification and coupling agent addition as well. One of the most common fiber treatment employed is alkalization. This fiber treatment has an important influence on structure, morphology and properties of alkalized fiber bundles. In this study, natural fiber bundles have been subjected to different treatment conditions, that include bath temperature, solution concentration and exposure time. The changes registered on morphology and structure of alkalized natural fibers were studied by optical microscopy (OM) and atomic force microscopy (AFM). These changes have an important influence on tensile properties of treated fibers. Fourier transform infrared spectroscopy (FTIR) spectra showed that strong chemical variations of treated fibers occur at high temperature conditions.

## **Hierarchical microordering of banana fibers**

Piedad Gañán<sup>1</sup>, Robin Zuluaga and Iñaki Mondragon<sup>2\*</sup>

<sup>1</sup> Assistant Professor of New Materials Group  
Universidad Pontificia Bolivariana  
Circular 1, # 70-01. Medellin (Colombia)

<sup>2</sup> Professor of Chemical Engineering. Head of 'Materials + Technologies' Group  
Dpto. Ingeniería Química y M. Ambiente, Escuela Univ. Politécnica  
Universidad del País Vasco/Euskal Herriko Unibertsitatea  
Pza. Europa, 1. 20018 Donostia - San Sebastian (Spain)  
e-mail: iapmoegi@sc.ehu.es

### **ABSTRACT**

Nowadays, different natural fibers have been studied as a potential alternative for composites, especially as replacement of glass fibers in functional structures. Natural fibers present important technical and economical advantages such as: low density, low cost, medium mechanical and thermal properties, ease processing, biodegradability and high disposability. In this sense, fibers can be obtained from different resources such as plant cultivated oriented to fiber production as in the case of flax or sisal fibers, or fiber derived from other growing as pineapple leaf or banana fibers. On the other way, different fiber extraction methods can be employed, such as hand or decorticator method, biological natural retting, chemical retting or degumming. In this study, banana fiber bundles have been extracted from bunch wastes (Colombian region) by biological natural retting. This method has demonstrated its appropriateness to obtain banana fiber bundles. However, the most important result of this work is associated with the elucidation of the structure of this fiber type. Hierarchical microstructuration is the key for both fiber bundle integrity and inner region orientation of microfibrils.

Fourier transform infrared spectrophotometry (FTIR) has been employed to establish the chemical composition of fibers. The main variations observed at different times of exposure correspond to the decrease in the absorptions of hemicellulose and pectin bands. Hierarchical helicoidal ordering in the bundle surface as well as orientation on the longitudinal axis of the bundle have been observed by optical microscopy (OM) and scanning electron microscopy (SEM) for 3-4  $\mu\text{m}$  surface microfibrils and 10-15  $\mu\text{m}$  inner microfibrils, respectively. By increasing exposure time, fiber bundle walls lose their integrity, which is reflected on their mechanical behavior.

## **Spatial Mapping of the Structural Properties of Paper and other Fibrous Webs using Non-Contact Laser Profilometry and $\beta$ -Radiographic Transmission Imaging**

**D. Steven Keller**

*Faculty of Paper Science and Engineering,  
Empire State Paper Research Institute  
SUNY College of Environmental Sci. &  
Forestry  
Syracuse, NY USA*

Choong-Hyun Ham and Hak-Lae Lee

*Department of Forest Product,  
Seoul National University, Seoul  
South Korea*

The performance characteristics of paper, and other non-woven materials comprised of stochastic distributions of fibers, depend extensively on the apparent density of the fibrous structure. Most of the key properties associated with mechanical strength, optical response and fluid transport are directly influenced by the distribution of fibers and pores within the web. Non-uniformity of the apparent density within the principal plane of the web may yield production and converting runnability problems. It may also result in quality defects such as poor formation (distribution of opacity), various print mottles (print density and gloss) or excessive dimensional instability (cockle). The uniformity of apparent density is usually approximated by the in-plane distribution of mass (formation) measured by transmission radiography, due to the difficulty in measuring local volume or true local thickness.

This presentation will focus on the development and application of a non-contact laser based profiling instrument useful in characterizing various aspects of web structure. Through simultaneous scanning of the topography of both sides of the specimen by opposing range sensors, the surface contour of each side, the local thickness, and the out of plane deformation were determined. By fusion of the thickness map with the distribution of mass measured by  $\beta$ -transmission radiography, the local apparent density was calculated. The application of this method to various aspects of the manufacture and end use of paper will be discussed, including the influence of compressive steps (calendering and wet pressing) and hygroexpansivity, and the influence on local apparent density and surface roughness will be addressed.



# Effect of environmental conditions on the biodegradation of cellulose fibers

**C. H. Park, Y. K. Kang and S. S. Im<sup>†</sup>**

Seoul National University, Dept. of Clothing & Textiles, Korea.

<sup>†</sup>Hanyang University, Dept. of Textile Engineering, Korea.

## Abstract

Based on the correlation analysis result of preceding research, the biodegradabilities of cellulose fibers were closely related to the moisture regain of the samples, which reflects the hydrophilicity and internal structure of the fibers. In addition to this factor, it was expected that the biodegradation conditions influence on the biodegradability of fibers.

In this study, widely used cellulose fibers including cotton, rayon, and acetate were used. The biodegradabilities of cellulose fibers were measured by soil-burial test, and then the degradation behaviors based on each condition were compared. Moreover, the effects of degradation conditions such as humidity of the soil were investigated. Changes in internal structure of samples were also observed by X-ray analysis according to the biodegradation time. The biodegradabilities of the specimens by soil burial test were similar in two sets of moisture condition: moisture regains less than 20% in soil and over 50%. But the X-ray intensities of cotton samples buried in soil were affected by the humidity of soil. The cotton samples buried in soil of less moisture maintained about 80% of initial crystallinity, but crystalline peak of cotton samples buried in soil of higher moisture decreased remarkably. Hence, it can be said that amount of moisture in soil influenced the internal structure of specimens, where the degrees of influence varied according to moisture regain of fibers.

External change of each specimen was observed by digital photograph. Appearances of samples were similar until 16 days. But, the samples buried in the soil of over 50% humidity have broken into smaller pieces than those in the soil of less humidity afterward.

## Adsorption of Aroma Chemicals on Fabric

Haiqing Liu<sup>1</sup>, S. Kay Obendorf<sup>1</sup>, Michael J. Leonard<sup>2</sup>, Timothy J. Young<sup>2</sup>, Michael J. Incorvia<sup>2</sup>

<sup>1</sup>Department of Textiles and Apparel, Cornell University, Ithaca, NY 14853

<sup>2</sup>International Flavors & Fragrances Inc., 1515 State Highway 36, Union Beach, NJ 07335

Distribution of aroma chemical on fiber was investigated by x-ray microanalysis. *cis*-3-Hexenyl salicylate was distributed over the entire fiber surfaces of both cotton and lyocell, with higher concentrations in surface irregularities and morphological features such as the crenulation in cotton. In contrast, CHS deposited only on isolated areas on PET fiber surfaces and no penetration into PET bulk fiber was observed. These discrepancies are most likely due to the relative smoothness of the PET fiber, its low polarity and high degree of crystallinity, and its round cross-sectional shape.

Adsorption of aroma chemicals on cotton fabric from aqueous solution with anionic surfactant sodium dodecyl sulfate (SDS) and cationic surfactant cetyltrimethylammonium chloride (CTAC) was evaluated by gas chromatography/mass spectrometry (GC/MS). The presence of surfactants SDS and CTAC increased the amount adsorbed compared to solution without surfactant; maximum adsorption was near the critical micelle concentration, i.e. 0.02 wt% CTAC and 0.05 wt% SDS. Adsorption of aroma chemical on fabric varied with surfactant concentration. Adsorption increased sharply with surfactant concentration up to the critical micelle concentration (CMC); maximum adsorption was then reached, followed by reduction in the amount adsorbed when surfactant concentration was further increased to 15 times CMC of SDS. This effect of surfactant concentration on the adsorption was similar for both anionic SDS and cationic CTAC surfactants. Adsorption increase of aroma chemical on fabric correlated with the decrease in surface tension of surfactant system. Adsorption is also affected by aroma chemical water solubility.

# Modification of cotton fabric by water-base shape memory polyurethane

Liu Yejiu and Hu Jinlian\*

*Institute of textile and clothing, Hong Kong Polytechnic University, Hong Kong, P R China*

A series of aqueous shape memory polyurethane (SMPU) were prepared by dispersing the water-base SMPU in water and were further used for treating cotton fabric. The properties of treated cotton fabric were investigated by using Wrinkle Recover Angle (WRA) and flat appearance. The results showed that better WRA and flat appearance of cotton have been got under high temperature, which means the SMPU have given the temperature sensitive property to cotton.

Shape memory polymers (SMPs) as a novel class of functional materials was developed quickly in the last decades.<sup>1-2</sup> Especially with polyurethane, the structure-property relationships are extremely diverse and controlled, and hence the shape recovery temperature can be set at any temperature between -30° and 70°, also they are easy to be molded using conventional processing techniques, including extrusion, injection, coating and blow molding, which allow a broad range of application in many fields<sup>3</sup>. For the application in textile industry, SMPU has been used to manufacture intelligent, water-proof, breathable fabric and so on by laminating or coating a layer of ultra-thin solid SMPU membrane onto fabric<sup>4-5</sup>. But there are still a huge limitation for the application of SMPU in textile industry. The main problem is that all of the reported SMPU are solvent-based and the environmental issues become increasingly important. For this reason, in this paper, variety of water-base SMPU were prepared and were used to treated cotton fabric. It was expected that the SMPU could give the temperature sensitive property to cotton without causing environmental problem.

A series of water-base shape memory polyurethane (SMPU) were obtained by a reaction of polycaprolactone diol, 1,4-butanediol, dimethylol propionic acid (DMPA), and 4,4'-diphenylmethane diisocyanate (MDI). The aqueous polyurethane were prepared by dispersing the water-base SMPU in water. Cotton fabric samples were padded through two dips and two nips in above PU solution without further dilution to a wet pickup of ca 85%. The fabric samples were dried for 3 min at 100 °C and cured for 3 min at 150 °C. The samples were then washed with acetone for 5 min. Finally, the fabrics were dried, conditioned and examined for different properties. The weight increase of PU on cotton (add-on) was calculate as showed below:

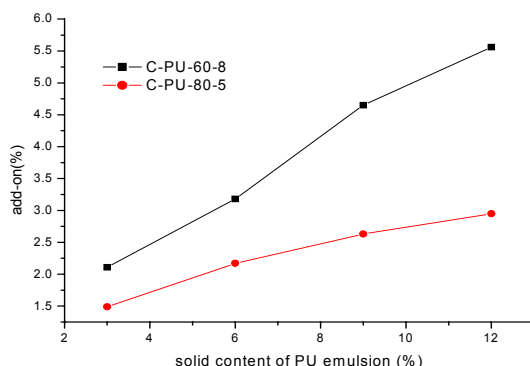
$$\text{the add-on} = (G_1 - G_0) / G_0 \times 100\%$$

$G_0$  means the weight of untreated cotton,  $G_1$  means the weight of cotton after finishing.

**Table I the relation of the particle size and the structure of SMPU**

sample code	soft content (%)	DMPA content (%)	particle size(nm)
PU-60-2	60	2	517
PU-60-5	60	5	205
PU-60-8	60	8	62
PU-70-2	70	2	690
PU-70-5	70	5	240
PU-70-8	70	8	103
PU-80-2	80	2	750
PU-80-5	80	5	301

Particle size decreases rapidly with increasing DMPA concentration (Table 1). In PU dispersions, average particle size can be controlled to some extent by emulsification conditions. However, it is mostly governed by the concentration of solubilizing groups. Therefore, average particle size should decrease with increasing DMPA concentration due to its ionic groups, viz. the carboxylate anions. On the other hand, the crystalline property of PCL soft segment has shown its effect on the PU dispersion in emulsion. Increasing PCL soft segment may lead to decrease hydrophilicity of the PU and increase the viscosity of the emulsion and at last cause high average particle size.



**Figure 1** The relation of the add-on and the solid content of PU emulsion (C-PU-60-8 means cotton treated with PU-60-8, C-PU-80-5 means cotton treated with PU-80-5)

Add-on increases almost linearly at high solid content of PU emulsion (Fig. 1). It means high solid content of PU emulsion could give thicker PU film surround cotton fiber. The particle size of PU emulsion has an effect on the add-on. Decreasing the particle size will help PU immerse into the internal of fiber or adhere tightly on the surface of fiber, which lead to high add-on.

**Table 2** The effect of SMPU on the property of cotton

cotton code	add-on(%)	Wrinkle recovery angle	Flat appearance (25°)	Flat appearance (60°)
untreated	0	188	2.5	2.5
C-PU-60-8	2.11	169	1.8	2.7
C-PU-60-8	3.18	147.5	1.5	2.5
C-PU-60-8	4.65	121	1.3	2.3
C-PU-60-8	5.56	119	1.3	2.3
C-PU-80-5	1.49	166	1.5	2.5
C-PU-80-5	2.17	157.5	1.3	2.5
C-PU-80-5	2.63	140	1	2
C-PU-80-5	2.95	136	1	2

Adding PU decreased WRA and flat appearance (Table 2) which. Maybe related to the high crystallinity of PU. But better WRA and flat appearance of cotton have been obtained under high temperature, which means that the SMPU have given the temperature sensitive property to cotton. Average particle size decreased with increasing DMPA concentration. PCL soft segment also had an effect on the PU dispersion in emulsion. High solid content and small particle size of PU emulsion gave thicker PU film surround cotton fiber. But better WRA and flat appearance was attained under high temperature, indicating that SMPU gave the temperature sensitivity.

## **Advancement in Methodology for the Use of HPLC/MS<sup>n</sup> for Dye Identification in a Forensic Setting**

Lauren M. Petrick<sup>1,2</sup> and Trevor Wilson<sup>2</sup>

*1 Chemistry Department, University of California, One Shields Avenue, Davis, CA*

*2 Sacramento County District Attorney Laboratory of Forensic Services, 4800 Broadway St., Suite 200, Sacramento, CA*

The use of a high performance liquid chromatograph mass spectrometer with an ultraviolet/visible diode array detector (HPLC/MS/UV/Vis) in forensic science is a new and potentially powerful tool, combining the flexibility of HPLC with the specificity of MS. Forensic applications of HPLC/MS exist for the analysis of controlled substances, explosives, poisons, toxins, and biologicals. However, the applicability of this instrumental technique for textile dye identification and characterization has been neglected. Current methods of fiber analysis provide chemical as well as physical characterization of fibers. Fiber dyes have been analyzed using comparative techniques such as microscopy, UV/Vis microspectrophotometry, and thin layer chromatography. The development of HPLC/MS methodology will allow an analyst to extract a reference fiber and analyze the solution with HPLC/MS/UV/Vis, uniquely characterizing the dye components and relative concentration of these components. The spectral data can then be compared to the questioned fiber, as well as a spectral database. This data will confirm or deny a forensic association between the questioned and reference fibers.

Currently, extraction techniques used in thin layer chromatography of fiber dyes utilize solvent systems which are incompatible with the MS, with the exception of basic dyes from acrylic fibers. The HPLC/MS parameters for basic dye separation and characterization were optimized for 16 basic dyes. This extraction system and the extracted dye analysis were then evaluated through the successful implementation in casework involving acrylic fibers.

The traditional extraction techniques for the removal of disperse dyes from polyester and acid dyes from nylon make use of a pyridine and water solvent system, which is not MS compatible. Therefore, HPLC and MS parameters were optimized for the separation of 13 disperse dyes, and a new solvent system was developed. A comprehensive evaluation of extraction efficiency was then performed comparing the pyridine to the new solvent system through bulk visual comparisons, quantitative analysis with the HPLC/UV/Vis, and through single fiber UV/Vis microspectrophotometer analysis.

The results establish reliable methodology for the analysis of polyester and acrylic fibers with HPLC/MS. Further methodology development for HPLC/MS analysis of all dye classes as well as the formation of a MS<sup>n</sup> and UV/Vis spectral database will provide a more specific means of dye identification and therefore allow greater discrimination for forensic fiber analysis.

## NOVEL BIOSENSOR FABRIC ASSEMBLIES FOR DETECTION OF BIOHAZARDS

Prashant Kakad and Prof. Margaret Frey Page  
Department of Textiles and Apparel  
Cornell University

This research takes advantage of the developments in biosensors and fibrous materials to create a new class of highly sensitive, robust and easy to use fibrous assemblies for quick detection of biohazards. Detection of *Escherichia Coli* (*E. Coli*) bacteria is used as a proof of concept. Biotinylated antibody that specifically attaches to the *E. Coli* antigen was incorporated into the fibrous assembly using streptavidinbiotin binding; the fibrous assembly was then treated with *E. Coli*. The specific detection of *E. Coli* captured on the fibrous assembly will be achieved by treating the assembly with a fluorescence labeled antibody (specific to *E. Coli*) and further visualizing the assembly under confocal fluorescence microscope.

This protocol represents a significant improvement over the currently available methods to detect biohazards, which require multi-step chemical assays, are extremely time consuming, expensive and not very suitable for field use.

Preliminary results including Confocal Fluorescence Microscopy images and analysis, Electron Micro Probe Analysis, SEM images and a statistical model demonstrating the binding of streptavidin to the biotin in fibers and attachment of biotinylated antibody to the streptavidin will be presented.

Ideally, several of these mats (immobilized with antibodies specific to various biohazards) can be manufactured at once and stored in the field, to be used to detect biohazards using fluorescence microscopy as and when necessary. The protocol can be extended to detect Salmonellae, Anthrax, Small Pox, Ricin and other such biohazards.

## **Biodegradable Non-woven Fabrics Electrospun from Renewable Polymers for Controlled Release Delivery of Chemicals**

Chunhui Xiang, Margaret Frey  
Department of Textiles and Apparel  
Cornell University

Electrospinning has attracted much attention in forming novel fibrous systems. The simplicity of the electrospinning process and the high absorbency of the resulting fabrics make this a promising technology for preparing useful polymer systems for controlled release delivery of chemicals.

In this study non-woven fabrics with controlled fabric structure and surface chemistry have been produced by controlling the ratio of hydrophilic and hydrophobic fibers and electrospinning conditions. Cellulose acetate and polylactic acid were electrospun and surface chemistry controlled by the initial polymer type and by deacetylating cellulose acetate non-wovens. Variations in fabric structure and surface chemistry of these non-woven fabrics have been used to control absorption and release chemicals with varying  $K_{ow}$  value. Degree of deacylation of cellulose acetate fabrics obtained cellulose non-woven fabrics have been determined analytically. Average fiber diameter of cellulose and PLA non-woven fabrics have been measured via image analysis. Mechanical properties of cellulose and PLA non-woven fabrics have been measured. Initial results on sorption and desorption of the disperse dye in relation to non-woven fabric properties will be presented.

## **Fabrication of organic-inorganic hybrid co-polymer nanofibers via electrospinning**

Alpa C Patel, Li Shuxi, and Yen Wei. Department of Chemistry, Drexel University, Philadelphia, PA 19104

Organic-inorganic co-polymer 3-(trimethoxysilyl) propyl methacrylate (MSMA), and its hybrid poly [methyl methacrylate-co-3-(tri-methoxysilyl) propyl methacrylate]-silica (PMCM) have been fabricated into nanofibers using electrospinning technique. Rapid formation of covalent bonds between the polymer and the silica components during the sol-gel reaction prevents inorganic-organic phase separation in the fibers. The fibers thus fabricated are in the form of non-woven mats with high specific surface area and mechanical strength. These fibers are excellent candidates for reinforcement of elastomers and as templates for the preparation of nanotubes. The average size of the co-polymer fibers synthesized is around 50-80 nm and that of hybrid fibers is around 300-400nm in diameter. The effect of electrospinning voltage, type of solvent used and the concentration of electrospinning solution are evaluated. The size and morphology of the fibers was characterized using environmental scanning microscope (ESCM).



## Section III

### The Evaluation of Fabric Hand by KES-F Equipment and KTU-Griff-Tester Device

Eugenija Strazdiene\*, Matas Gutauskas\*, Diana Grineviciute\*,  
Laurence Schacher\*\*, Dominique C. Adolphe\*\*

\* Kaunas University of Technology, Faculty of Design and Technologies, Studentu str. 56, Kaunas LT-3031, Lithuania

\*\* Laboratoire de Physique et Mécanique Textiles – Ecole Nationale Supérieure des Industries Textiles de Mulhouse –  
11, rue Alfred Werner – 68093 Mulhouse Cedex – France

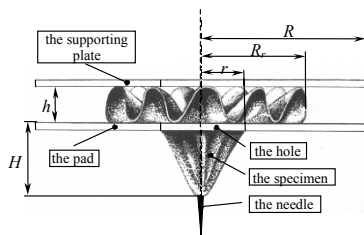
#### INTRODUCTION

Fabric handle is considered to be among the main performance properties of textiles. For many years this property was mainly defined on the basis of panel judgement results obtained after touching samples of material. More than 20 years ago KES-F and SiroFAST systems were proposed for textiles objective evaluation with the help of which textile hand could be characterise with certain accuracy [1, 2]. Meantime several groups of researchers have described methods for evaluating fabric handle that depended on the analysis of the force –displacement curve obtained when a circular fabric sample, held at its centre, was pulled (extracted) through a circular hole of appropriate diameter by using Instron Tensile Tester or other similar universal testing instrument [3 - 7]. One of them, called KTU-Griff-Tester (created at Kaunas University of Technology), differs from the others by the fact that it operates on the principle of restricted pulling (extraction), i.e. test sample is placed between two limiting plates the lower of them having centre hole [7, 9]. Thus the specimen, pulled by a small punch with its restricted movement in upward direction, experiences complicated stressed state herewith revealing the anisotropy and deformability levels of test sample together with its frictional, bending, compression and draping properties [10]. So, the aim of the presented research is to compare the results obtained by two testing basis: KES-F system and KTU-Griff-Tester device and to find dependencies between provided textiles mechanical properties, which are able to give an accurate textile hand evaluation.

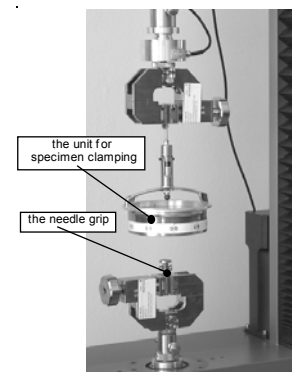
#### METHODICS

The objects of the research were textile materials (woven and knitted), investigated by KES-F equipment at Ecole Nationale Supérieure des Industries Textiles de Mulhouse (France) and by KTU-Griff-Tester at Kaunas University of Technology (Lithuania). Both investigations were performed under strict control of typical testing conditions [1, 8, 9].

Principle scheme of KTU-Griff-Tester device and its general view are presented in Figures 1 and 2. The radius of specimen was  $R = 56.5$  mm. Radius of circular hole of the lower plate ( $r = 10$  mm) and the distance between the limiting plates ( $h = 1.6$  mm) were chosen in respect to the thickness of tested material  $\delta$  and taking into account the conditions of specimen jamming between the limiting plates [7]. During testing four parameters were defined on the



**Fig. 1.** Principal scheme of textile handle evaluation in pulling process



**Fig. 2.** KTU-Griff-Tester device attached to the standard tensile testing machine

$H - P$  (pulling height – force), i.e. maximal force  $P_{\max}$ , initial slope angle  $\text{tg}\alpha$ , pulling work  $A$  and maximal pulling height  $H_{\max}$ . Thickness of tested material  $\delta$  which determines the values of  $r$  and  $h$  parameters was measured at two loading values (ratio 1:5) and presented the fifth parameter  $\Delta\delta$  next to  $P_{\max}$ ,  $\text{tg}\alpha$ ,  $A$  and  $H_{\max}$ . All these five criterions composed complex criterion  $Q$ , the value of which was expressed by the units of relative area  $S$  on the basis of polar diagram [8]. Principle scheme of KTU-Griff-Tester device and its general view are presented in Figures 1 and 2. The radius of specimen was  $R = 56.5$  mm. Radius of circular hole of the lower plate ( $r = 10$  mm) and the distance

#### RESULTS AND DISCUSSION

The results of typical textile materials obtained by KTU-Griff-Tester are presented in Table. Investigations have revealed that the behaviour of woven fabrics and knitted materials in pulling differs not only by the character of  $H-P$  curve (that is evident from the parameters presented in the Table), but essentially by their shapes (Fig. 3). Specimen of woven fabric obtains the four-leafed shape, while specimen of knitted material - the shape of Cassini oval [11]. The later phenomenon is closely related with the structure of tested materials, as well as with its anisotrophy level.

**Table.** Material properties defined by KTU-Griff-Tester device (W – woven fabrics, K – knitted materials)

Material code	Parameters					
	$P_{\max}$ , N	$\text{tg}\alpha$	$A$ , Ncm	$\Delta\delta$ , %	$H_{\max}$ , mm	$Q$
W02	$48,0 \pm 3,48$	$42,5 \pm 1,50$	$166,9 \pm 4,13$	$12,1 \pm 0,28$	$55,0 \pm 0,34$	12,5
W04	$6,9 \pm 0,22$	$6,1 \pm 0,48$	$20,0 \pm 1,05$	$16,0 \pm 0,15$	$56,1 \pm 1,23$	1,0
W08	$13,4 \pm 0,98$	$11,2 \pm 0,59$	$47,0 \pm 4,06$	$7,8 \pm 0,12$	$53,6 \pm 0,39$	2,9
K01	$7,0 \pm 0,86$	$5,5 \pm 0,44$	$20,8 \pm 2,45$	$16,7 \pm 0,24$	$54,2 \pm 1,17$	4,7
K03	$3,7 \pm 0,22$	$2,3 \pm 0,09$	$14,4 \pm 0,59$	$6,8 \pm 0,32$	$58,2 \pm 0,97$	4,1
K05	$11,6 \pm 0,83$	$6,8 \pm 0,72$	$32,2 \pm 3,34$	$3,6 \pm 0,23$	$55,3 \pm 0,79$	10,3



**Fig. 3.** Typical shapes of specimens pulled through a rounded hole

Comparative analysis of initial parameters defined by KTU-Griff-Tester device with those obtained by KES-F equipment for the whole set of tested materials (including woven and knitted) have shown that linear dependency exists between parameters  $P_{\max}$  and shear stiffness  $G$ , as well as between  $P_{\max}$  and shear hysteresis  $2HG$  and  $2HG5$ , and between  $P_{\max}$  and bending rigidity  $B$ . The same was defined for initial slope angle  $\text{tg}\alpha$  and  $G$ ,  $2HG$ ,  $2HG$  and  $B$  parameters. It must be noted that linear dependency becomes much more stronger when complex criterion  $Q$  is used instead of initial parameters of  $H-P$  curve. In such a case the coefficient of determination of linear dependency reaches even the values of  $r^2 = 0.963$ , especially for shear parameters  $G$  and  $2HG5$ . Furthermore, stronger dependency is obtained when knitted materials are excluded from the set of tested samples and this is natural because KES-F equipment originally was not orientated for knitted materials. So, for woven fabrics the linear dependencies become as follows: between  $P_{\max}$  and  $G - r^2 = 0.991$ ,  $P_{\max}$  and  $2HG - r^2 = 0.999$ ,  $P_{\max}$  and  $2HG5 - r^2 = 0.998$  and between  $P_{\max}$  and  $B - r^2 = 0.865$ . The similar can be observed for  $\text{tg}\alpha$  parameter. More strong dependencies in the case of woven fabrics can be found for complex criterion  $Q$ , i.e. between  $Q$  and tensile resilience  $RT$  ( $r^2 = 0.986$ ), between  $Q$  and compression energy  $WC$  ( $r^2 = 0.972$ ), between  $Q$  and linearity  $LT$  ( $r^2 = 0.9617$ ).

In conclusion it must be noted that the results of the investigation have shown that criterion  $Q$  obtained by KTU-Griff-Tester can be sufficiently reliable parameter able to characterise fabric hand. Besides, its advantage is that it can be defined from by one single test. Also it is evident that pulling through a hole technique should be more fully utilised for quality evaluation, especially taking into account knitted materials.

#### References

1. **S. Kawabata** The Standardization and Analysis of Hand Evaluation *The Textile Machinery Society of Japan*, Osaka, 1980
2. **D. P. Bishop** Fabrics: Sensory and Mechanical Properties *Journal of the Textile Institute*, vol. 26, no. 3, 1996, pp. 1 – 63
3. **N. Pan and K.C. Yen** Physical Explanations of Fabric Extracting Curve for Fabric Handle Evaluation, *Textile Research Journal*, vol. 62, 1992, pp. 279-290
4. **V. L. Alley** Nozzle Extraction Process and Handmeter for Measuring Handle // US pat. 4103550, 1978
5. **L. Henrich, A. Seidel, O. Rieder** Griffprüfung an Maschenwaren *Maschen-Industrie*, no. 7, 1999, pp. 46 – 47
6. **M. A. Grover, S. M. Sultan, A. Spivak** Screening Technique for Fabric Handle *Journal of the Textile Institute*, vol. 23, no. 3, 1993, pp. 486 – 494
7. **E. Strazdienė, L. Papreckienė, M. Gutauskas** New Method for the Objective Evaluation of Technical Textile Behavior // 6<sup>th</sup> Dresden Textile Conference 2002, CD ROM Page 1 – 8 of 8, <http://www.fiz-technik.de>.
8. **G. Martišiūtė, M. Gutauskas** A New Approach to Evaluation of Textile Fabric Handle *Materials Science*, Kaunas: Technologija, vol. 7, no. 3, 2001, pp. 186 – 190
9. **E. Strazdienė, V. Daukantiene, M. Gutauskas** Bagging of Thin Polymer Materials: Geometry, Resistance and Application *Materials Science*, Kaunas, Technologija, vol. 9, no. 3, 2003, pp. 262 – 265
10. **V. Daukantiene, L. Papreckienė, M. Gutauskas** Simulation and Application of the Behaviour of a Textile Fabric while Pulling of Through a Round Hole *Fibres and Textiles in Eastern Europe*, vol. 11, no. 2, 2003, pp. 38 – 42

# A Comparison of Body Surface Change to Evaluate Traditional and 3D Body Scan Anthropometric Measures for Dynamic Postures

Jeong Ran Lee, Susan P. Ashdown\*

Department of Clothing and Textiles, Pusan National University

\*Department of Textiles and Apparel, Cornell University

The efficiency of three-dimensional body scanning, from which an infinite number of measurements, body shapes, angles, and relational data can be extracted, is well known. Much research has been done on the reliability and validity of 3D anthropometric measurements for standard anthropometric positions. But there has been little published literature on the use of 3D anthropometry for measurement of dynamic postures.

This study is to verify the validity of 3D body scan measures of dynamic postures. For this purpose, body surfaces were measured using traditional anthropometric measures (manual measurement processes using a tape measure and anthropometer) and 3D body scan measures of the dynamic posture. Comparative measurements of the subject in the standard anthropometric posture were taken using both measurement methods.

Subjects were 15 females in their twenties. Subjects wore a lycra body suit during the scan process and the manual measurements. Nineteen dimensions of the upper body were measured in both a standard anthropometric posture and a posture with shoulders flexed at an angle of 135°. The VITUS whole body scanner and ScanWorX (Bodymeasure) program were used for 3D measurement. The scanning process took 12 seconds.

The results were as follows.

1. The average age, height and weight of subjects were 22.2, 165cm, 61.3kg respectively. The average bust and waist girth measurements were 88.4 and 72.5cm.

2. Measurements of the body in a posture with a shoulder flexion of 135° decreased for 11 items. The decrease of the shoulder length, interscye front and biacromion length were especially pronounced (-22%~-29%). Results were the same for the manual and 3D measures.

3. The scanned girth measurements were 0.5~1.9cm and 0.5~2.2cm larger than the manual measurements for both the standard anthropometric posture and flexed 135° posture measurements, however there is no statistically significant difference between the two measurement methods. Differences between length measurements were 0.1~0.3cm .

4. Upper body items which showed significant surface change in the dynamic position were neck base girth, bust point to underbust, bust point to waistline, waist back length ( $p \leq 0.05$ ), shoulder length, interscye front, biacromion length, interscye back, side seam ( $p \leq 0.001$ ). These items were also the same for both measurement methods.

5. When comparing all other body measurements except for bust girth, underbust girth, and waist girth (items likely to be affected by breathing), most items exhibited very similar values regardless of the measuring methods or the posture.

While more data from various dynamic postures will be needed, these results demonstrate that 3D measurements of subjects in dynamic postures have similar values to those obtained by manual methods. It is possible to collect more data in a much shorter amount of time using the 3D body scanner than by measuring using traditional manual anthropometric methods. To provide data for the design of garments that are worn in dynamic working conditions, the dimensions for a range of dynamic body positions will be investigated using the 3D body scanner.

## Visual Fit Analysis from 3D Scans

Susan P. Ashdown, Suzanne Loker, Katherine Schoenfelder, and Lindsay Lyman-Clarke  
Cornell University

3D body scanning technology has emerged as a powerful tool for measurement and analysis of population anthropometrics, and is being developed by the apparel industry for a variety of uses such as custom fitted clothing, mass customized fitting, virtual try-on, and automated size selection. Though promising, these scan uses require further development and testing of software tools. One powerful use of body scans that the technology currently supports is the use of scan visualizations for fit analysis. Visual analysis can make use of the ability of the human eye and brain to evaluate complex relationships that are more difficult to analyze using other methods.

Visual fit analysis of the 3D model is an effective method for categorizing and analyzing the complex relationship between clothing and the human body. In this study fit analysis based on the classic fit elements of ease, grain, line, balance, and set was used to analyze the fit of women's pants from 3-D scans. A panel of expert judges conducted this analysis using the scan to observe the smoothness or distortion of the hang of the garment on the body, the angle of the seams or edges, areas of constriction of the body, stress folds, and garment and body proportions.

Subjects were 155 women in Misses sizes 4 to 16 who were fitted in test garments; closely fitted ready-to-wear casual pants. Each woman was first scanned in a closely fitted body suit and again in the best fitting pair of ready-to-wear pants from the size range. The judges rated 13 critical fit locations and assigned overall ratings for the front and back using a three point scale. Ratings were assessed for reliability among the judges, and instances of extreme disagreement were identified. Judges discussed each of these instances and came to an agreement for final scores, which were compiled for analysis.

The fit ratings for the subjects were used to assess the effectiveness of the sizing system. Comparison of the fit ratings for different areas of the body showed that the fit of the pants at the thigh and hip in the front was generally very good, and that the fit in the back, particularly the crotch back, was generally bad (less than 10% of subjects had acceptable fit in the crotch back). Comparison of the ratings by size showed that the sizing system fit women in sizes 8 and 10 the best, and that there were more unacceptable fits in sizes 14 and 16.

The judges found that the 3D scans were an effective tool for analysis and that ease, line, balance, and set, four of the five elements of fit, could be clearly seen in the screen visualization. Ease, the fifth element, could be deduced in extreme cases by the hang and silhouette of the garment but not directly observed. The advantages of this method of fit analysis included the ability to assess the scans at a convenient time and place instead of in a fit session with all judges present, the ability to rotate and enlarge the images at will to examine areas of the scan, the ability to view the clothed and unclothed body together to identify interactions, and the ability to compare scans of different subjects easily. This method of fit analysis should prove useful for both academic research and industry product development.

# **The Effects of Supply Chain Management Factors On the Performance of SCM Adoption in Textile/Apparel Firms**

Sangmoo Shin

Visiting Scholar, University of California, Berkeley  
Associate Professor, Dept. of Textile Engineering, Soongsil University

In a global market environment with information technology, the textile and apparel industry tries to survive by having competitive power embedded in supply chain management to improve the interrelation among different stages of industries such as fiber, textile, apparel manufacturing, and retailing. In industries with highly volatile demand like fashion apparel and textile, the costs of such “stock outs” and markdowns can actually exceed the total cost of manufacturing. Most companies do not even measure how many sales they have lost, let alone consider those costs when they commit to production. Apparel and textile companies under this uncertain environment are experiencing many managerial problems in production planning, forecasting, inventory management, production system, and timely distribution. So, Supply Chain Management (SCM) which is reflected in the strategy of quick response in the apparel industry can boost the textile and apparel industry from a labor-intense and petty to information and technology-intense business. Therefore, the purpose of this study was to investigate how component factors of SCM affect the performance of textile and apparel firms in a competitive market.

For the methodology of this study, the questionnaire was developed based upon the literature review. Through the literature review, three component factors of SCM such as information system (standardization of computerized intra/inter business, information sharing with intra/inter business, computerization of infrastructure on intra/inter business), business environment (CEOs’ concern about incorporating SCM, degree of assistance from government and textile/apparel federation, individual participation from organization), and partnership (alliance, openness of corporate culture and information sharing with intra/inter business, credibility of partners) were identified and measured by 7 point Likert type scale (7: very much do so, 1: very much not do so). Based upon previous review of literature, enhancing customer services, cost reduction, improving operational management, and increasing sales & profits were measured by 7 point Likert type scale (7: very much do so, 1: very much not do so) for SCM performances of the textile and apparel firms. 230 questionnaires were distributed to the CEOs, CMOs, and experts who operate SCM in textile and apparel firms. The returned usable 149 were analyzed by SPSS10.0 with multiple regression analysis and Cronbach's Alpha for internal consistency and reliability.

The results of this study were as follows:

The performance of the textile and apparel firms that adopted SCM was affected by information system, business environment, and partnership in a descending order. For information system, standardized computerization from intra to inter business, information sharing from intra to inter business, and computerization with infrastructure on intra/inter business impacted the performance of the firms in a descending order. Among business environment, CEOs’ concern

about incorporating SCM and the degree of assistance from government and textile/apparel federation impacted the performance of SCM in a descending order. For partnership, strategic alliance, openness about corporate culture and information sharing with intra/inter business, and credibility of partnership impacted the performance of the firms in a descending order. Therefore information system with standardization and information sharing among the industries was the most important factor affecting the performance of SCM. Computerization might be the prerequisite to adopting SCM incorporating firms. Also, CEOs' concern about SCM and strategic alliance among businesses were important factors impacting the performance of the textile and apparel firms that adopted SCM.




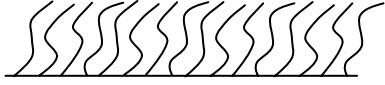
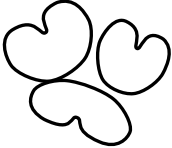
## THERMAL COMFORT PROPERTIES OF ARTIFICIAL FURS

Lubos Hes, Technical University of Liberec, Czech Republic, e-mail [lubos.hes@vslib.cz](mailto:lubos.hes@vslib.cz)

The advantages of artificial furs against animal ones are given by their lower price, lower square mass, very high resistance against biological damaging, easy dry clearing and easy confectioning, higher water vapour permeability, higher thermal insulation, warmer contact feeling by and saving of life of millions of animals.

In the study, thermal conductivity, thermal resistance, warm-cool feeling and water vapour permeability of 15 artificial PAN / PES furs manufactured by the Czech company BONEKA and differing mostly in the fabric structure were experimentally determined. All the measurements were carried out by means of the Czech commercial ALAMBETA and PERMETEST instruments, which serve for fast and non-destructive measurements [1]. Some results of measurement are presented below.

**Tab. 1 Examples of structure and composition of 2 Czech artificial furs used in the study**

<b>ARTIFICIAL FUR AFRODITA</b>	NOTE: ALL THE HAIRS MIXED IN SLIVER
HAIR STRUCTURE (SIMILAR TO: WOOL WITH 32 MM AND AMBRA 60 MM HAIR LEHGHT)	HAIR LENGHT : 60 mm
	HAIR FINENESS: 3,3 dtex / 38 mm modacryl 3,4 dtex / 28 mm polyacryl 4,4 dtex / 32 mm modacryl 17 dtex / 76 mm modacryl 22 dtex / 51 mm modacryl
HAIR TYPICAL CROSS SECTION:	AVERAGE EQUIVALENT HAIR PARAMETER: 35,2 $\mu\text{m}$
UNDERCOAT 	HAIR MATERIAL COMPOSITION: 2% polyacryl 98% modacryl
HAIRS (PILES) 	TOTAL DENSITY OF THE KNITTED FABRIC: 684520 loops/m <sup>2</sup>
	SQUARE MASS: 450g/m <sup>2</sup>
<b>ARTIFICIAL FUR NORSKO</b>	HAIRS MATERIAL COMPOSITION: 100% polyacryl
FUR STRUCTURE (SIMILAR TO BAKARA 8 MM, JAVOR 6 MM, BRIGITA 8 MM HAIR LENGHTS)	HAIR LENGHT: 10 mm
	Hair fineness 3,4 dtex / 28 mm polyacryl
TYPICAL HAIR SECTION	EQUIVALENT HAIR DIAMETER: 19,7 $\mu\text{m}$
	DENSITY OF KNITTED FABRIC: 767496 loops/m <sup>2</sup>
	SQUARE MASS: 370g/m <sup>2</sup>

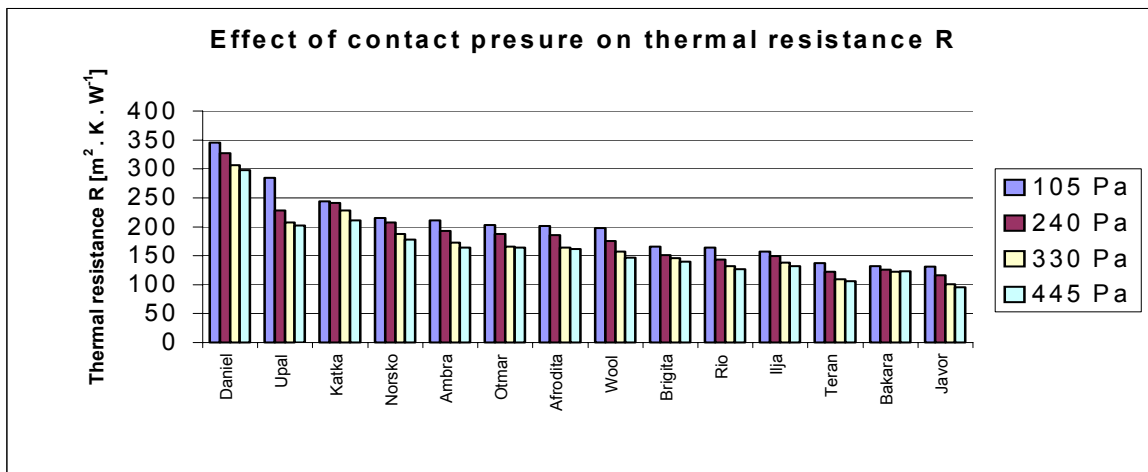


Fig. 1 Effect of contact pressure on thermal resistance of artificial furs

From the Fig. 1 follows, that artificial furs exhibit quite high resistance against compression. Other results revealed, that the artificial furs are warmer in thermal contact the animal ones.

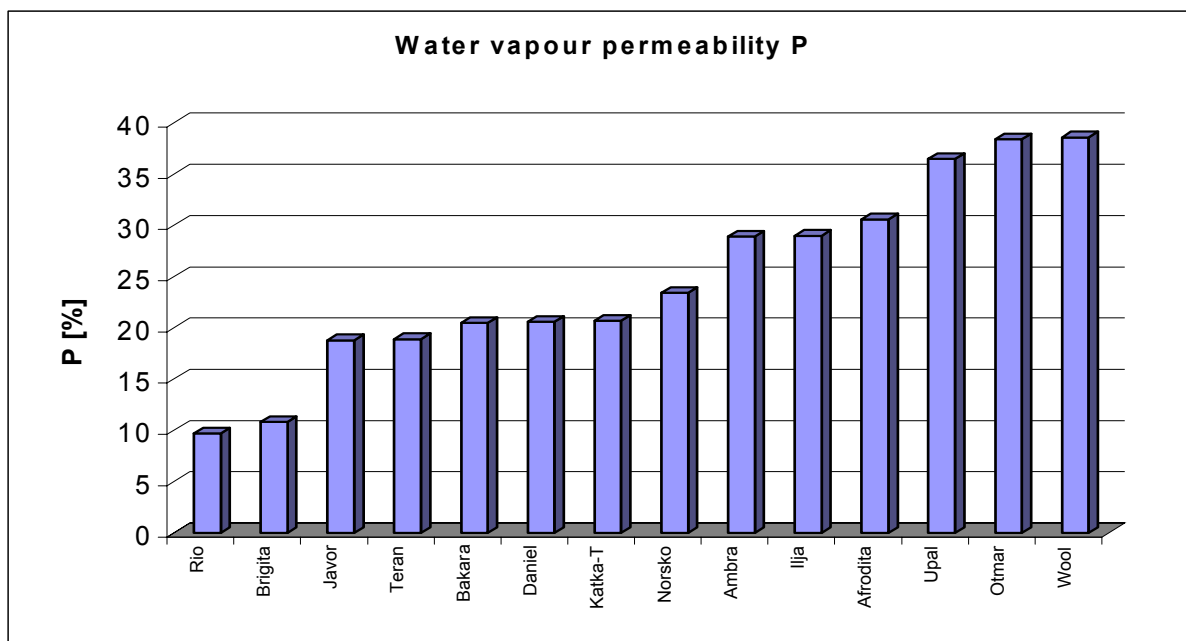


Fig. 2 Water vapour permeability of artificial furs

The Fig. 2 shows that the water vapour permeability of artificial furs is very high, if compared with the typical relative permeability of denims (about 10%). The lower is the basic knitted fabric density, the higher is the permeability. Surprisingly, the permeability of animal furs is mostly quite low – 5% [2], but this lack is compensated by very high moisture absorption capacity.

### Acknowledgement

Completing and presentation of this paper was partially supported by a grant No. LN00B090 offered by the Ministry of Education of Czech Republic.

### Literature cited

- [1] Hes L.: Thermal Properties of Nonwovens, in: Proc. INDEX 1987 Congress, Section B1, Geneva (1987)
- [2] Hes L.: A biomimetic study on thermal properties of animal furs. In: Fiber Society Fall Conference, Lake Tahoe 2001.



## **Automatic Identification of Armhole from 3D Data Cloud**

Zhaohui Wang<sup>1</sup>, Roger Ng<sup>1</sup>, Edward Newton<sup>1</sup>,  
Weiyuan Zhang<sup>2</sup>

<sup>1</sup>Institute of Textiles and Clothing, Hong Kong Polytechnic University

<sup>2</sup>Institute of Fashion Design, Donghua University

The form of armhole is an important element in constructing garment pattern. By definition, the armhole is defined as the seamline on torso joining the bodice and sleeve. However, this definition is insufficient in the transformation process from 3D body data into 2D pattern. In this paper, we established a mathematical model to represent the form of armhole. We find the shoulder point and armpit point from 3D body data, and describe the form of armhole by geodesic curve where the geodesic is the shortest distance between two points on a particular 3D surface. The identification of armhole from 3D data cloud is beneficial to the development of the automatic pattern generation process and the efficiency of flat pattern design can be greatly improved.

# Application of Nanofiber Technology to Nonwoven Thermal Insulation

Phil Gibson and Calvin Lee AMSRD-NSC-SS-MS U.S. Army Soldier Systems Center Natick, MA 01760-5020 508-233-4273 Phil.Gibson@natick.army.mil

Nanofiber technology (fiber diameter less than 1  $\mu\text{m}$ ) is currently being intensively pursued for the development of future Army lightweight protective clothing systems. Nanofiber applications for ballistic and chem-bio protection are being actively investigated, but the thermal properties of nanofibers and their potential protection against cold environments are relatively unknown. Previous studies [1,2] have shown that radiative heat transfer in fibrous battings is minimized at fiber diameters between 5 and 10  $\mu\text{m}$ . However, the radiative heat transfer mechanism of extremely small diameter fibers of less than 1  $\mu\text{m}$  diameter is not well known. Previous studies are limited to glass fibers, which have a unique set of thermal radiation properties governed by the thermal emissivity properties of glass. We will investigate the thermal transfer properties of high loft nanofiber battings composed of carbon fiber and various polymeric fibers such as polyacrylonitrile, nylon, and polyurethane. Preliminary studies on meltblown pitch carbon fibers show increased thermal efficiency over standard commercial insulation materials, as shown in Figure 1. Thermal insulation battings incorporating nanofibers could decrease the weight and bulk of current thermal protective clothing, and increase mobility for soldiers in the battlefield. Conductive, convective and radiative heat transfer properties/characteristics of nanofiber battings will be measured and compared with those of regular and microfiber battings, and other advanced novel commercial thermal insulation battings (such as flexible aerogel composites). If the extremely small diameter nanofiber battings provide more effective radiative and convective heat protection as described above, thinner and lighter thermal insulation battings can be made from these materials. This will decrease the weight and bulk of the current cold weather clothing systems for the soldiers and increase their mobility.

## References:

1. Lee, Calvin K., "Heat Transfer of Fibrous Insulation Battings", Natick Technical Report/TR-84/055, U.S. Army Natick RD&E Center, Natick, MA 01760, Jan 1984.
2. Larkin, Bert K. and Churchill Stuart W., "Heat Transfer by Radiation through Porous Insulations", *AICHE Journal*, Vol. 5, No. 4, Dec 1959.

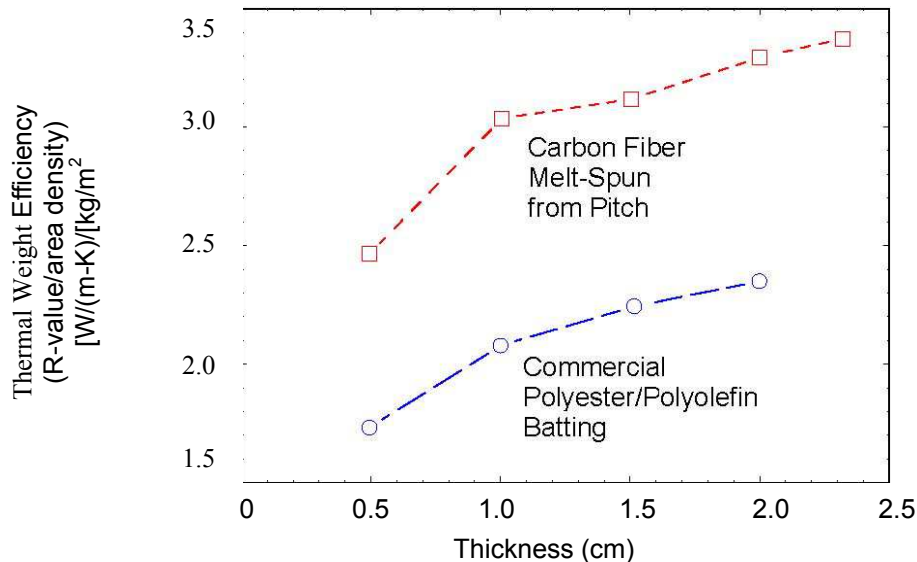


Figure 1. Thermal weight efficiency comparison between meltblown nanofiber batting and commercial thermal insulation.

Thermal Weight Efficiency (R-value/Areal Density)  $[W/(m-K)] / [kg/m^2]$

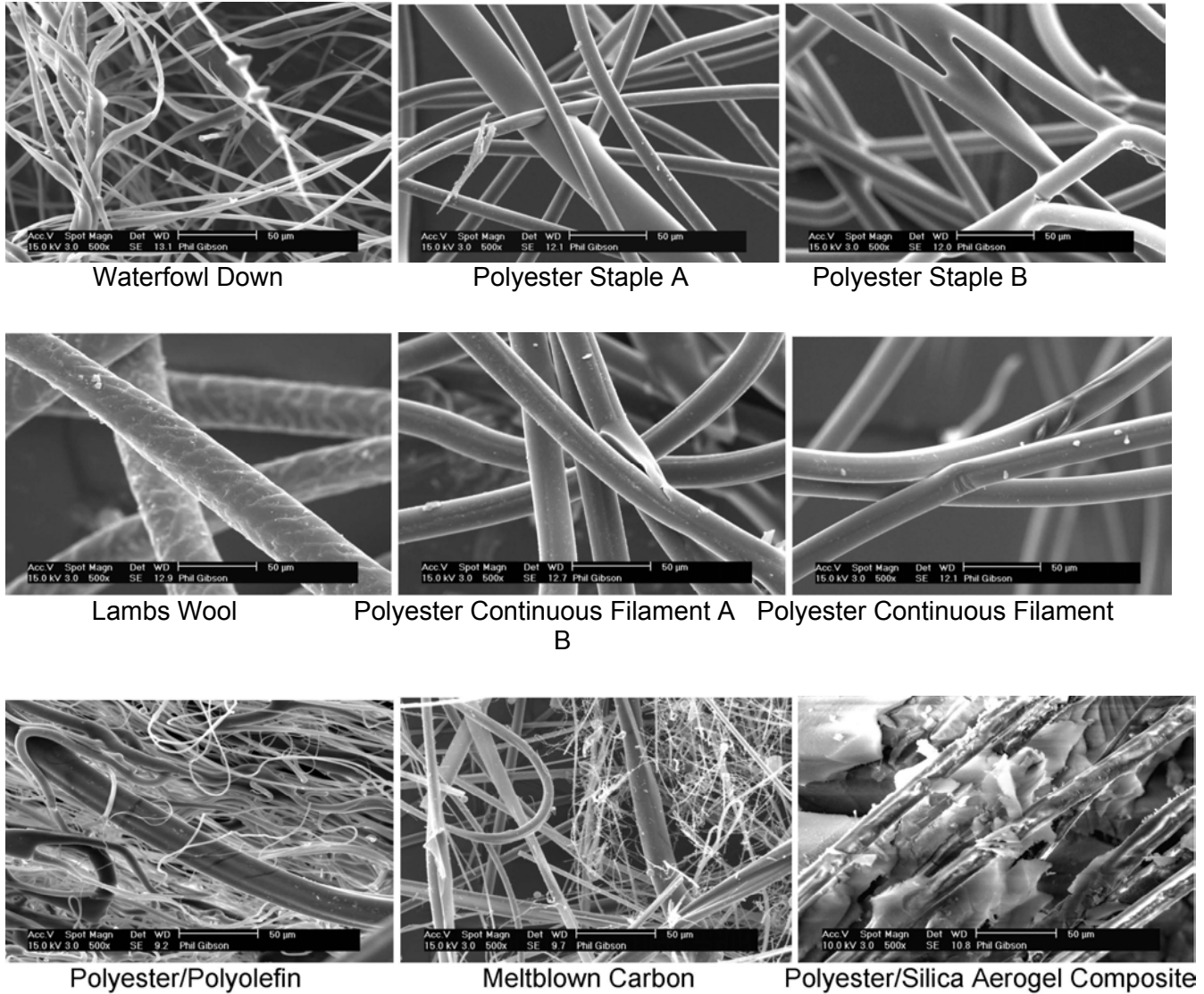
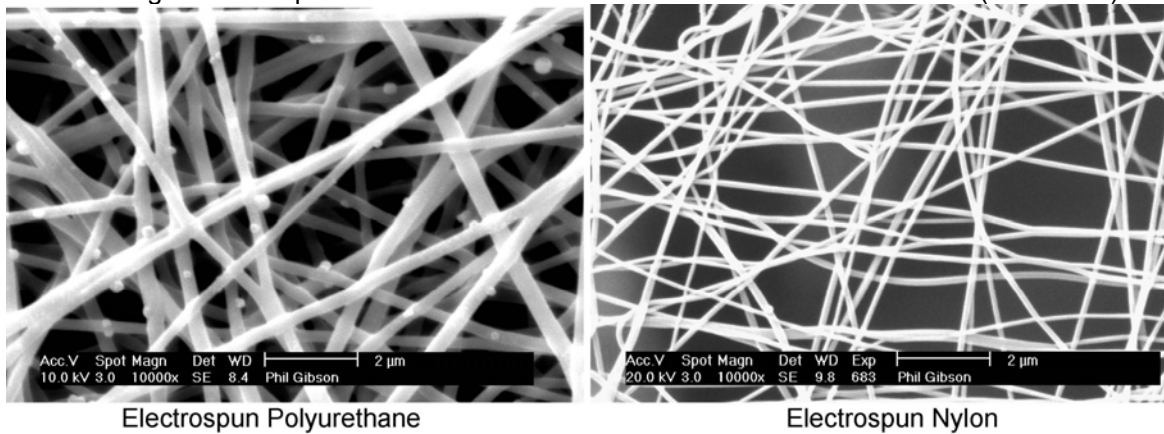


Figure 2. Comparative fiber sizes of various thermal insulation materials (all at 500x).



3. Micrographs of electrospun polyurethane and nylon at 10,000x. These fiber sizes can be as much as 100 times smaller than those present in commercial polyester thermal insulation battings.

## **Investigation into the properties of soybean fibres**

D. Vynias  
Department of Textiles  
UMIST

The Textiles industry is continually developing “new” fibres as the need to meet performance criteria for the apparel and Technical Textiles sectors increases. Associated with this innovation is the requirement to create, and establish fibres, which are both environmentally friendly and economically sustainable. Recently the potential for fibres derived from soybean has been reported and their performance profile characterised.

In this study the effect of bleaching on fibre properties, such as strength and handle (Kawabata Evaluation System) has been investigated, and the effect of fibre protective agents evaluated. The effect of processing on the surface topography and chemistry has also been studied using Scanning Electron Microscopy and X-ray Photoelectron Spectroscopy (XPS).

The thermal properties of soybean fibre have been investigated by Thermogravimetric Analysis (TGA) with a view to improving the flammability performance of the soybean fabric.

## **Synthetic HMPE Ropes Application in Hot Climates**

Eric McCorkle

Danielle Stenvers

James Byrne

Rafael Chou

Samson Rope Technologies

2090 Thornton St.

Ferndale WA, 98248

Edwin Grootendorst

DSM Dyneema

Eisterweg 3 Heerlen

The Netherlands

### **Abstract:**

Many areas of new oilfield and gas field development and production are occurring the Middle East, Northwest Shelf or in Northern Africa or in other regions that have extremely high climatic temperatures and utilize ocean going vessels to transport this cargo to their ultimate designation. With OCIMF recent acceptance of synthetic mooring lines, HMPE fiber based mooring lines are now being considered for use, but the fiber's relatively low melting point and critical temperature and the creep phenomena have raised concerns about the product viability in these climates..

The behaviors of HMPE rope in hot environment and contacting hot substance are studied to understand the short term effects of heat on HMPE lines. Long term creep behavior of HMPE fibers was also investigated and analyzed to address the concerns of application of HMPE lines under both thermal and mechanical fatigue in the field.

## Shaped fibers and their applications

Alex Lobovsky, PE  
Advanced Fiber Engineering, LLC  
8 Floral Ct  
Westfield, NJ07090  
Phone: 1-908-420-0092  
E-mail: alobovsky@afiber.com

Polymeric fibers have been made in various cross-sections in order to enhance their properties and performance. The desired properties may range from stiffness, luster, and dirt hiding capabilities in the case of carpets and textiles, to attraction and retention of dust in filtering applications, to increase in surface area and permeability for hollow fiber membranes.

Modern spinneret capillary manufacturing technology such as EDM (Electrical Discharge Machining) allows quick and inexpensive fabrication of elaborate capillaries shapes, thus giving us an ability to test hundreds capillary designs.

As a result testing of over 400 capillary designs and studying polymer flow effects in capillaries we have developed technology to produce practically any fiber shape.

In addition a number of various product prototypes were fabricated with the spun shaped fibers that verified fiber shape efficacies and improved product performance.

Combining fiber shape technology with multi-component fiber spinning offers even greater opportunities for new products with unique properties.

Lately new discoveries made in the field of nano-technology and bio-genesis pose a new challenge of handling and orienting substances on the scale of  $10^{-9}$  to  $10^{-6}$  m.

The shaped fibers with their micron sized geometric features and variety of materials present a flexible and inexpensive solution.

This presentation gives dozens of examples of fiber shapes and discusses their potential applications.

## Section IV

### Review of The Composites Pressure Resin Infusion System (ComPRIS) Process

*Professor Barry Goodell<sup>1</sup>, Dr. Roberto Lopez-Anido<sup>2</sup>, and Benjamin Herzog<sup>1</sup>  
<sup>1</sup>Wood Science and Technology; <sup>2</sup>Civil and Environmental Engineering; and  
<sup>1,2</sup>The Advanced Engineered Wood Composites Center (AEWC),  
The University of Maine, Orono, Maine.*

#### Abstract

ComPRIS is a new process for both laminating porous substrates and fabrication of Fiber Reinforced Polymer (FRP) products. Both lamination and FRP fabrication can be combined in a one-step process when reinforcement of laminate materials is desired. The ComPRIS process uses pressure to infuse resin into a part, which can include porous substrates such as wood, wood composite components, and/or FRP fabrics. Current resin transfer molding (RTM) processes are used to produce Fiber Reinforced Polymer (FRP) composite materials by infusing resins into different types of fiber reinforcement. RTM methods are characterized by resin infusion of fiber reinforcement, fabrics or preforms within a closed mold or tool normally using vacuum, as in the Vacuum Assisted Resin Transfer Molding (VARTM) process.

The ComPRIS process uses pressure to infiltrate the interface between wood and FRP fabric layers to provide better penetration into these substrates. Advantages of using the ComPRIS process with porous laminates such as wood include the creation of an interphase adhesive or resin boundary between substrate materials. This has also been termed a 'functionally graded interface' and it eliminates abrupt transitions between wood/and FRP matrices. The use of pressure rather than vacuum also eliminates the production of microvoids in the substrate due to vacuum-induced solvent ablation. The ComPRIS process also offers advantages over conventional RTM processes in that a closed system is used, allowing volatile emissions to be better controlled.

*Features of the ComPRIS process include:*

- The ComPRIS process uses pressure to infuse resin between component parts of a laminate and also to infuse resin into fabrics and other porous matrices to form an FRP composite part.

- The use of pressure is new for FRP production and it can be used with porous matrices such as wood because air can be displaced from bond lines and from porous fabrics and compressed in the interior of the porous matrix. This allows resin to penetrate into bondline regions and also penetrate the interior of fabric layers.

- A void-free infusion of resin into fabrics or other porous matrixes can be achieved using the ComPRIS process. Microvoids and other vacuum-induced defects are not created as the ComPRIS process does not employ the use of vacuum systems.

-A Graded Resin Interface, or Resin Interphase, is created instead of a distinct bondline because, in porous substrates such as wood, the resin penetrates the area between laminates but also penetrates into the wood itself. This interphase region potentially creates a stronger, more durable bondline.

-Preliminary strength and durability assessment indicates that high quality wood-wood bondlines can be produced. When using the ComPRIS process with vinyl ester resin and a HMR primer, preliminary cyclic delamination tests showed acceptable delamination percentages, and shear block testing shows wood failure percentages to exceed the ASTM acceptable level of 75%.



# Enhanced interfacial adhesion of UHMWPE fiber composites by cold plasma treatment

Bo Young Chu<sup>1</sup>, Sung Wook Lee<sup>2</sup>, Mi Yeon Kwon<sup>3</sup>, Seung Goo Lee<sup>1,+</sup> Tae Sang Lee<sup>3</sup>,  
Hun Seung Ha<sup>3</sup>, and Jong Il Yuck<sup>3</sup>

<sup>1</sup> : Dept. Textile Engineering, College of Eng., Chungnam National Univ., Daejeon 305-764, Korea

<sup>2</sup> : Institute of Advanced Materials, Chungnam National Univ., Daejeon 305-764, Korea

<sup>3</sup> : Agency for Defense Development, Daejeon, 305-600, Korea

<sup>+</sup> : Corresponding author: E-mail [lsgoo@cnu.ac.kr](mailto:lsgoo@cnu.ac.kr)

## Introduction

The gas plasma treatment is known to be the most powerful method to improve the wettability and the interfacial adhesion of UHMWPE fibers, since it is efficient, easy and environmentally friendly[1-3]. Plasma treatments can modify the fiber surface chemistry by reacting with fibers through abstraction of hydrogens in polymer chains and by creating free radicals that later are oxidized into hydroxyl and carbonyl groups when exposed to oxygen. These resulted oxygen containing groups play a important role to improve the wettability of fibers to polar matrix resins. In this study, UHMWPE fibers were subjected to plasma treatment aided by proper additives such as a photosensitizing agent, in order to improve the interfacial adhesion. The plasma treated fibers were analyzed by contact angle analyzer, XPS, SEM, and FTIR. Also, the interfacial shear strength of UHMWPE fibers to vinyl ester resin was measured with the plasma treatment condition.

## Experimentals

UHMWPE fibers (Dyneema SK-76) were provided by DSM as a roving of 1,580 deniers. Vinyl ester resin, XSR-10, was provided by National Synthesis Co., Korea. Cleaned and dried UHMWPE fibers were subjected to the oxygen plasma treatment aided by the additive, solvent diluted photosensitizing agent, in a parallel electrode type plasma chamber from Vacuum Science Inc. As soon as the plasma treatment was finished, the fiber samples were subjected to surface characterization or adhesion study in order to minimize the exposure of treated fibers to atmosphere. The contact angle of oxygen plasma treated fibers was measured by dynamic contact angle analyzer (Cahn, DCA-322) at 22 $\mu$ m/min of a fiber movement. XPS was utilized to investigate the surface chemistry of plasma treated UHMWPE fibers. The morphological changes of fibers by plasma treatment were investigated by SEM and AFM. The micro-droplet tests were conducted on an Instron model 1122 at a cross-head speed of 1mm/min.

## Results and Discussion

The water contact angle of UHMWPE fibers was greatly increased after oxygen plasma treatment. The increased contact angle is seemed mainly due to the polar component and rather than the dispersive component despite some contribution from the surface roughness changes. The O<sub>1s</sub>/C<sub>1s</sub> ratio of UHMWPE fibers was sharply increased by plasma treatment and rather slowly increased with longer treatment time. Increased surface energy of UHMWPE fibers can be explained by the oxygen containing functional groups introduced to the fiber surface by plasma treatment. As expected from the increased surface area, surface energy, and O<sub>1s</sub>/C<sub>1s</sub> ratio

after plasma treatment, the interfacial shear strength of UHMWPE fibers, evaluated via micro-droplet tests, increased sharply with plasma treatment. It is not difficult to find some similarities among interfacial shear strength, the  $O_{1s}/C_{1s}$  ratios and the surface free energy. Therefore, it could be said that the enhanced interfacial adhesion from plasma treatment is attributed to the increased surface energy and oxygen moieties. We will discuss more details about the optimum plasma treatment condition including additive variables and its effect on the surface modification and on the interfacial adhesion of UHMWPE fiber composites.

### **Conclusions**

- (1) Water contact angle,  $O_{1s}/C_{1s}$  ratio and surface roughness of UHMWPE fibers were greatly increased by plasma treatment.
- (2) XPS investigation revealed that increased oxygen content could be attributed to the functional groups such as C-O, C=O, and O=C-O introduced by plasma treatment.
- (3) Interfacial shear strength exhibited a same trend as the surface treatment, but showing a maximum value at the high power treatment.

### **Acknowledgement**

This work was supported by the Research Grant of the Dual Use Application Program(No. 10011171) in 2003 of Ministry of Commerce, Industry and Energy(MOCIE) – Agency for Defense Development(ADD) Joint Research.

### **References**

1. P. E. Reed and L. Bevan, Polymer Composite, 14 (4), 286 (1993)
2. S. Holmes and P. Schwartz, Comp. Sci. and Tech., 38, 1 (1990)
3. Z. F. Li and A. N. Netravali, J. Appl. Polym. Sci., 44, 319 (1992)

## **‘Green’ Composites Made of Bamboo Fibers and Modified Starch Based Resin**

Y. Yamamoto and A. N. Netravali  
Fiber Science Program, Cornell University

The use of biodegradable environment-friendly ‘green’ plastics made from natural resources, especially plant-based materials, has been growing gradually against the backdrop of environmental problems; decrease in the number of landfills, depletion of petroleum, increase of the amount of CO<sub>2</sub>, litter and other pollutions. However, green plastics still don’t possess adequate mechanical and thermal properties for industrial products. In this study, an emulsion type corn starch-based biodegradable resin (CP-300) was modified by blending with polyvinyl alcohol (PVA) to improve its mechanical and thermal properties. Those properties as well as the moisture absorption of the modified CP-300 (MCP-300) resin were characterized. Also, effect of different molecular weights of PVA and CP-300/PVA blend % was studied. The modified resin showed improved mechanical and thermal properties. Interfacial shear strength (IFSS) between the MCP-300 resin and a bamboo fiber was characterized using microbead test.

Bamboo fibers are one of the strongest and the stiffest plant fibers and hence are a promising reinforcement for replacement of conventional fibers. In addition, Bamboo plants can be harvested 3-4 times a year making their supply almost inexhaustible. In the present study, two different types of composites were fabricated using the MCP-300 resin and bamboo short fibers; random and unidirectional composites. The composites were hot pressed at 120°C into laminates. Cross-ply composites were prepared by hot pressing two sheets of the unidirectional composite in 0/90 degrees. The MCP-300 resin with the best properties was selected to fabricate these green composites. The fiber weight content was maintained at 50%. Tensile properties as well as moisture absorption of the composites were characterized.

The properties of these composites indicate that they can be used in many applications including packaging, consumer goods and automotive and housing interior. These green composites can be easily disposed of or composted at the end of their useful life keeping the environment safe.

## **Soy Protein Concentrate Based ‘Green’ Nano-Composites with Improved Mechanical and Thermal Properties**

X. Huang and A. N. Netravali  
Fiber Science Program, Cornell University, Ithaca, NY

Soy protein has been used as the resin to develop fully biodegradable and environment-friendly ‘green’ composites because of its low cost, environment-friendly manufacturing process and easy worldwide availability. Soy protein concentrate (SPC) is a commercially available product and contains 70% protein, 20% carbohydrates and the remaining is ash and other inorganic matter.

The objective of this research is to develop fully biodegradable nano-composite resin with improved mechanical properties, moisture resistance and thermal stability, which will be further used as the fabric composite matrix. A plasticizer, such as glycerol has been commonly employed to improve the processibility and toughness of SPC resin. In the present research, SPC resin was modified by nano sized Cloisite<sup>®</sup> Na<sup>+</sup> clay particles. Cloisite<sup>®</sup> Na<sup>+</sup> clay particles were exfoliated using magnetic stirring and ultrasonication. Exfoliated lamellar nanoparticles can provide superior mechanical properties. Effect of nano-particle loading, pH of the resin, glycerol and cross-linking by glutaraldehyde (GA) on the mechanical and thermal properties and moisture resistance was characterized. The results show that the modulus and stress of the clay-reinforced SPC increased significantly, while the fracture strain decreased with increased loading. Crosslinking by GA increased the tensile properties further while the fracture strain remained almost constant.

These nano-composites may be used for various applications or reinforced by biodegradable fibers to form environment-friendly ‘green’ composites.

# Fiber structure development in high-speed melt spinning of *atactic*-PS/*syndiotactic*-PS bicomponent fibers with various cross-sectional configurations

Yoshiaki Hada, Yuta Hoshino, Hiroshi Ito, and Takeshi Kikutani  
Department of Organic and Polymeric Materials,  
Graduate School of Science and Engineering, Tokyo Institute of Technology  
2-12-1, O-okayama, Meguro-ku, Tokyo 152-8552, Japan  
Phone +81-3-5734-2468, Fax +81-3-5734-2876, e-mail: [tkikutan@o.cc.titech.ac.jp](mailto:tkikutan@o.cc.titech.ac.jp)

## Introduction

In comparison with the widely used amorphous polymer, *atactic*-polystyrene (*a*-PS), syndiotactic polystyrene (*s*-PS) is a crystalline polymer and exhibits interesting properties such as high melting temperature, low density and good resistance to chemicals. In applying *s*-PS for the production of fibers, significant development of fiber structure is necessary for the enhancement of mechanical and thermal properties.

On the other hand, it has been reported that bicomponent spinning is a useful method for the control of fiber structure development in the high-speed melt spinning process. In this study, high-speed melt spinning of the bicomponent fibers of *a*-PS and *s*-PS with various cross-sectional configurations were carried out, and structure and properties of the as-spun fibers were investigated. Use of two polymers consisting of the same monomer unit but having different degree of tacticity was with the expectation of gaining high interfacial shear strength between the two polymers.

## Experimental

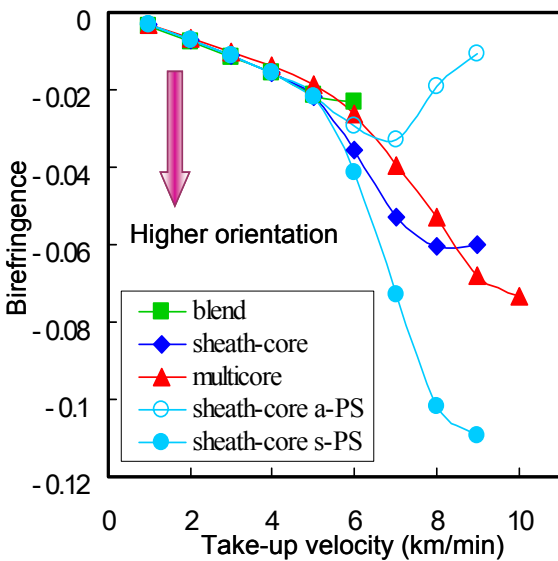
Three different cross-sectional configurations of the bicomponent fiber adopted in this study were blend, sheath-core, and islands-in-the-sea (multi-core) types. The blend type bicomponent fiber was extruded by feeding the mixture of *a*-PS and *s*-PS pellets to a single screw extruder equipped with a metering pump. On the other hand, the sheath-core type and the multi-core type bicomponent fibers were prepared by extruding the melts of *a*-PS and *s*-PS using two different extrusion systems, each of which is consisting of an extruder and a metering pump. Extrusion temperature was set to 290°C. Total throughput rate was 6 g/min, and *a*-PS:*s*-PS composition was 1:1. In the sheath-core type and multi-core type bicomponent fibers, *a*-PS was used as the sheath and the sea component, whereas *s*-PS was used as the core and multi-core component. For comparison, single component melt spinnings of *a*-PS and *s*-PS were also carried at the same extrusion temperature and total throughput rate. For the analysis of the structure and properties of as-spun fibers, birefringence and wide-angle X-ray diffraction (WAXD) pattern measurements, differential scanning calorimetry (DSC) and tensile test were conducted for as-spun fibers. For the better understanding of the mechanism of fiber structure development, measurement of the diameter profile along the spinning line was also carried out using a diameter monitor.

## Results and Discussion

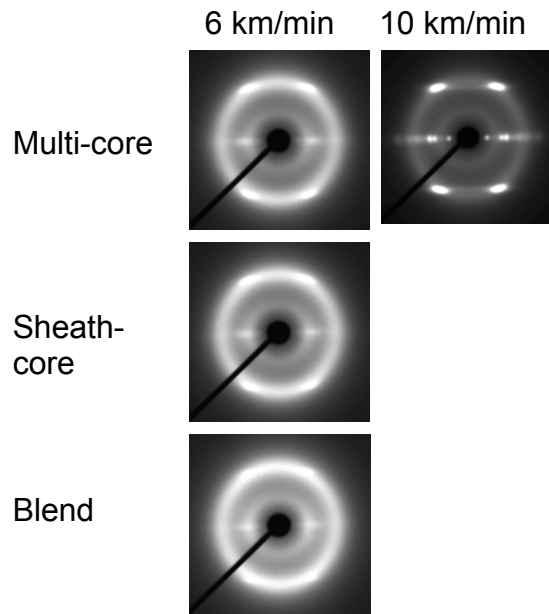
In comparison with the single component spinning of respective polymers, in which attainable highest take-up velocities were 4 and 5 km/min for *a*-PS and *s*-PS respectively, spinnability was significantly improved in bicomponent spinnings. Maximum take-up velocities of 6, 9 and 10

km/min were attained in the bicomponent spinnings of blend type, sheath-core type and multi-core type bicomponent spinnings, respectively.

Dependences of the birefringence of the three types of bicomponent fibers on take-up velocity are shown in Fig. 1. In the sheath-core type bicomponent fibers, it was possible to measure the birefringences of the *a*-PS and *s*-PS components separately. Up to the take-up velocity of 5 km/min, it was difficult to distinguish the two components in the bicomponent fibers under an optical microscope indicating that the two components have similar degree of molecular orientation and also that the *s*-PS component is amorphous. From 6 km/min, absolute value of birefringence started to increase steeply in the sheath-core and multi-core type fibers. Results for the sheath-core type fibers suggested that the molecular orientation of the *s*-PS component increased steeply, whereas that of the *a*-PS component was suppressed significantly in this velocity region. This phenomenon was speculated to be caused by the starting of the orientation-induced crystallization of the *s*-PS component, which was confirmed from the WAXD measurement of the as-spun fibers, in that the bicomponent fibers started to show crystalline reflections from 6 km/min. WAXD patterns of the three types of bicomponent fibers obtained at 6 km/min are compared in Fig.2. WAXD pattern of multi-core type fiber prepared at 10 km/min is also shown in the figure. If structure and mechanical properties of the fibers obtained at the attainable highest take-up velocities were compared, bicomponent high-speed melt spinning could yield fibers with enhanced structure and mechanical properties than the single component spinning of *s*-PS. Among the three types of bicomponent fibers, the multi-core type fiber showed the highest degree of fiber structure development of *s*-PS component, which was represented by the highest values of molecular orientation, melting point and tensile modulus.



**Fig.1** Birefringence vs. take-up velocity for various bicomponent fibers.



**Fig.2** WAXD patterns of high-speed spun bicomponent fibers with various cross-sectional configurations.

## Excimer Laser Treatment of Vectran<sup>®</sup> Fibers

J. Zeng and A. N. Netravali  
Fiber Science Program,  
Cornell University

Vectran<sup>®</sup> fibers, obtained from Hoechst Celanese, were treated with pulsed XeCl excimer laser (308 nm) to improve their adhesion to epoxy resin. The treatments were carried out in air at different laser fluences and varying numbers of pulses. The effects of laser treatment on the fiber surface topography, chemistry and wettability have been investigated. The fiber/epoxy resin interfacial shear strength (IFSS) was measured using the microbead test.

The surface roughness was characterized qualitatively and quantitatively by using scanning electron microscopy (SEM) and atomic force microscopy (AFM), respectively. The threshold for the formation of surface structure is less than 36 mJ/(pulse\*cm<sup>2</sup>). The laser treatments at fluences higher than the threshold introduced roll structures on the fiber surface perpendicular to the fiber axis, and increased the fiber surface roughness up to 3.5 times the root mean square (RMS) value. The microbead technique showed that the interfacial shear strength (IFSS) of Vectran<sup>®</sup>/epoxy increased up to 200% after the laser treatment. This improvement is mainly attributed to higher surface roughness of the fiber.

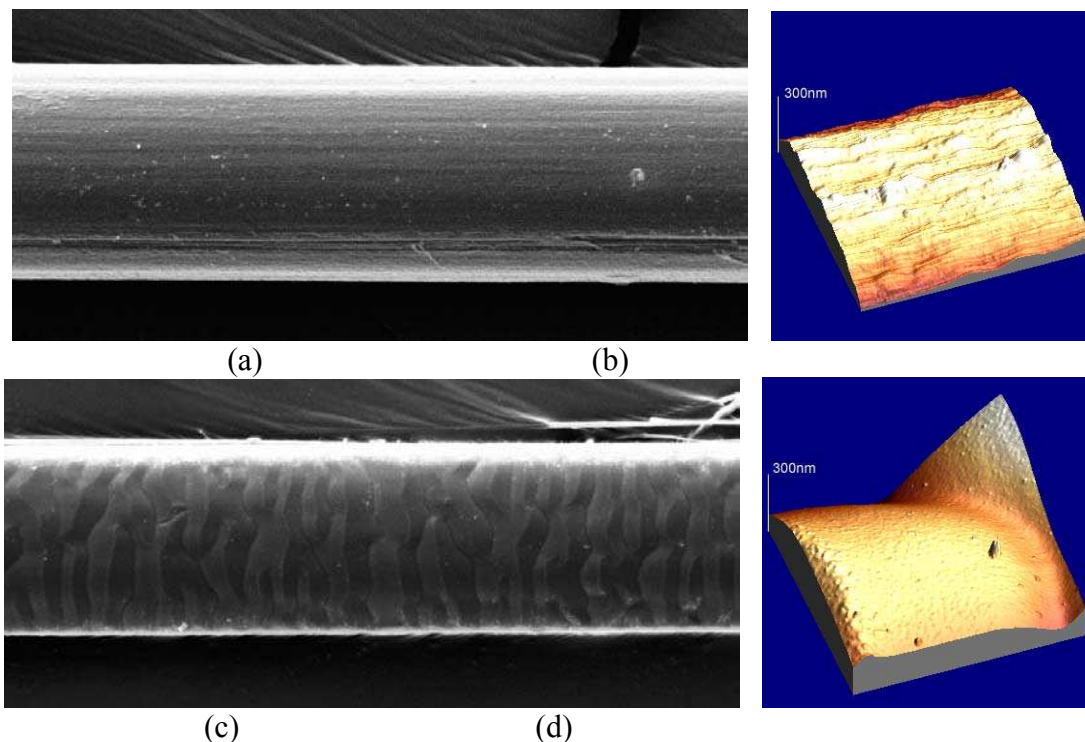


Figure 4. SEM photomicrographs of the Vectran<sup>®</sup> fiber surfaces and corresponding AFM images. (a) and (b): fiber treated with fluence of 24 mJ/(pulse\*cm<sup>2</sup>) and 30 pulses on each side, Ra = 26.0 nm; (c) and (d): fiber treated with fluence of 60 mJ/(pulse\*cm<sup>2</sup>) 75 pulses on each side, Ra = 60.8 nm.



# A THEORETICAL MODEL AND EXPERIMENTAL METHOD FOR EVALUATION OF YARN HAIRINESS

*Bohuslav Neckář and Jana Voborová*

Department of Textile Structures, Technical University of Liberec, Halková 6, Liberec 1  
Czech Republic-46117, E-mail: [bohuslav.neckar@vslib.cz](mailto:bohuslav.neckar@vslib.cz)

Hairiness is one of the very important properties of staple yarns. It gives pleasant hand to the textile materials as well as creates processing problems during the further technological operations. At present, the existing experimental methods (for example, Zweigle, Uster, etc.) can characterize yarn hairiness partly. Our method, which is based on our original theoretical model and utilization of image analysis techniques, is able to analyze this complex phenomenon more deeply.

Theoretical model: There exists different shapes of fibers in the sphere of hairiness between two radii  $r_1$  and  $r_2$ , such as fiber end (1), loop (2), protruding fiber (3), reversal end (4), and reversal loop (5) (fig. 1). The occurrence of the reversal shapes (4) and (5) is so small in yarn that these can be neglected. Imaginatively, the loop (2) can be cut so as to obtain a couple of fiber ends (2a, 2b). Based on this idea, the fiber segments (we call these shortly as “fibers”) protruding from the yarn body create the sphere of hairiness. It is evident from

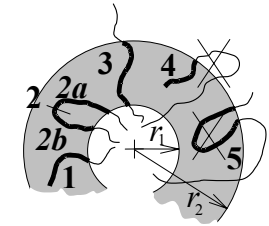


Fig. 1 Fiber types

fig.2 that the number of fibers protruding from the cylindrical shape of yarn compact body (diameter  $D$ , radius  $r_D = D/2$ ) is maximum and the number of fibers protruding from the radius  $r > r_D$  is smaller, because the free end of some of the fibers are terminated between these two radii.

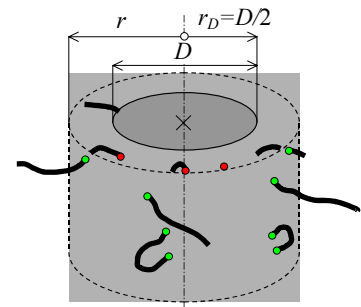


Fig. 2 Protruding fibers

The differential probability  $\varphi(r)dr$ , that a randomly chosen fiber surely protruding from the radius  $r$  having its free end lying in the differential layer following immediately after the radius  $r$  (fig. 3) is generally a function of the radius. But we assume that this probability is independent of the radius ( $\varphi(r) = \text{const.}$ ). Further we assume the character of fiber orientation is independent of the radius too. Based on these assumptions, we derived the following relation of packing density  $\mu$  at any radius of the hairiness sphere

$$\mu = (\mu_D r_D / r) 2^{-(r-r_D)/h}$$

Here  $\mu_D$  is the initial packing density corresponding to yarn radius  $r_D$  and  $h$  is the “half-decrease interval” of the number of protruding fibers. (It means always one half of the fibers that are protruding from the cylindrical area of radius  $r$  will also protrude from the same of radius  $r + h$ .) Some of the parallel light beams can pass beside the yarn at a distance  $x$ , but others are “hindered” by hairs (fig. 4). It is

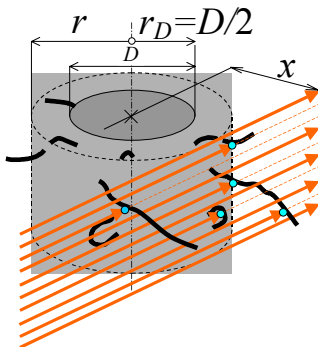


Fig. 4 Light beams

evident from fig.5 that the light beam can pass through the gray strip of width  $d^*$  if none of the fiber centers is lying exactly at the middle of the strip. (Here we idealize each

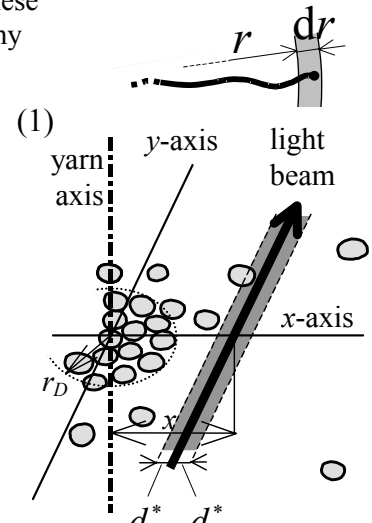


Fig. 5 “Hindering” of the light beam by yarn cross-sections



fiber cross section by a ring of diameter  $d^*$ .) Based on this idea, the probability  $P$  that the light beam passes beside the yarn at the distance  $x$  without any obstruction is

$$-\ln P = \left[ 8\mu_D r_D h 2^{r_D/h} / (\pi d^{*2} \ln 2) \right] \left[ \int_0^{\pi/2} 2^{-(x-d^*/2)/(h \cos \alpha)} d\alpha - \int_0^{\pi/2} 2^{-(x+d^*/2)/(h \cos \alpha)} d\alpha \right]. \quad (2)$$

We call the model according to equations (1) and (2) as an “exponential” model of hairiness. But, the experimental results showed that this model is not enough precise. It is necessary to think about 2 types (subscript 1 or 2) of fibers in the sphere of hairiness. Each of them follows the exponential model mentioned before, but with highly different values of parameters  $h_1, h_2$  and  $\mu_{D1}, \mu_{D2}$ . Then the packing density in this “double-exponential” model is

$$\mu = (r_D/r) \left[ \mu_{D1} 2^{-(r-r_D)/h_1} + \mu_{D2} 2^{-(r-r_D)/h_2} \right], \quad (3)$$

and the probability  $P$  that the light beam passes beside the yarn at the distance  $x$  is

$$-\ln P = \left[ 8r_D / (\pi d^{*2} \ln 2) \right] \sum_{i=1}^2 \left[ \mu_{Di} h_i 2^{r_D/h_i} \left( \int_0^{\pi/2} 2^{-(x-d^*/2)/(h_i \cos \alpha)} d\alpha - \int_0^{\pi/2} 2^{-(x+d^*/2)/(h_i \cos \alpha)} d\alpha \right) \right]. \quad (4)$$

Therefore, the probability  $Z(x)$  that the light beam cannot pass beside the yarn at the distance  $x$  is

$$Z(x) = 1 - P, \quad (5)$$

where  $P$  is given by equation (4). The so-called “blackening function”  $Z(x)$  can be obtained from the experimental investigation of images by using image analysis techniques.

**Experimental results:** The frequency of the black pixels (*i. e.*, fiber) at the distance  $x$  from the yarn axis (center of the widest black interval) determines the experimental “blackening function”  $Z(x)$  as shown in fig. 6. The parameters  $\mu_{D1}, h_1, \mu_{D2}, h_2$  can be calculated using (4), (5) by statistical regression technique. At the same time, we also evaluate yarn diameter (based on the defined value of blackening function -  $D_{cover}$ , or the defined value of packing

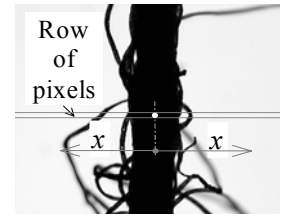


Fig. 6 Yarn image

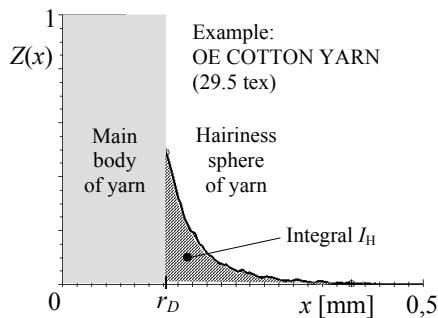


Fig. 7 Blackening function: theoretical and experimental

Technology	$T$ [tex]	$H$ Uster	Components of hairiness:				Yarn diameter $D_{cover}$ [mm]	Integral char. $I_H$ [mm]
			dense		loose			
			$\mu_{D,1}$	$h_1$ [mm]	$\mu_{D,2}$	$h_2$ [mm]		
R (○)	10	3.70	0.0893	0.00619	0.0062	0.0967	0.115	0.0151
N (□)		4.16	0.0775	0.00608	0.0098	0.0825	0.120	0.0182
R (○)	20	5.47	0.0527	0.01035	0.0074	0.0934	0.174	0.0229
N (□)		7.01	0.0409	0.01554	0.0069	0.1205	0.186	0.0312
OE (□)		4.12	0.0459	0.01675	0.0032	0.0734	0.210	0.0176
R (○)	29.5	7.00	0.0361	0.01460	0.0063	0.0987	0.246	0.0282
N (□)		9.07	0.0304	0.02001	0.0048	0.1691	0.264	0.0423
OE (□)		4.91	0.0307	0.01646	0.0084	0.0526	0.287	0.0215

R...ring yarns, OE...open end yarns, N...Novaspin yarns (new type)

density -  $D_{dens}$ ) and integral

characteristic  $I_H$ , which can be compared with the hairiness index  $H$  of Uster Tester 4. An example of the resulting curves is illustrated in fig. 7 and the evaluated parameters of some yarns are on the table. The correlation between  $I_H$  and  $H$  is usually very high ( $R^2 \cong 0.98$ ). The two types of hairs are significantly different to each other in terms of their characteristics: the dense type is very much concentrated on the yarn surface (high  $\mu_{D,1}$ ), but quickly decreasing (small  $h_1$ ). It creates some “moos” on the yarn surface. The loose type is not concentrated on the yarn surface, but decreasing slowly. It is created by long “drifty fibers”. **Acknowledgement: This work was sponsored by Research Center “Textile”, No. LN00B090.**

## **Element Labeling of Fiber Adhesives**

Dr. Jim Gullick

Goodyear Tire & Rubber Company

Tire and industrial cords are typically coated with one or more latex based adhesives to provide bonding between the fiber and the rubber matrix. Conventional optical and electron microscopy techniques cannot consistently distinguish the layers where multiple coatings are used. Methods were developed to introduce unique element labels into the adhesives so that electron dispersive spectroscopy (EDS) could be used to image the adhesive layers. Approaches evaluated included changes in the latex polymer, the resin bonding agent, and the base used to accelerate the resin crosslinking reaction. Several combinations were developed which permit easy discrimination of the adhesive distribution without adversely affecting the bonding of the cord to the matrix.

## **Biodegradation of lignocellulose fiber and the iron reducing activity of white and brown rot fungi**

Marieke Schmutzer<sup>1</sup>, Jody Jellison<sup>2</sup>, Barry Goodell<sup>3</sup>

<sup>1</sup> Technical University of Vienna, Getreidemarkt 9, 1060 Vienna, Austria

<sup>2</sup> Biological Sciences Department, University of Maine, Orono, ME 04469

<sup>3</sup> Wood Science and Technology, University of Maine, Orono ME 04469

Fungi play an important role in biomass recycling in nature through degradation of lignocellulosic materials, but they also cause enormous annual financial losses through destruction of lignocellulose based materials. Wood decay fungi can be divided in two main categories, brown rot and white rot, based on the process of decay. Brown rot fungi preferentially remove cellulose, leaving behind a brown, crumbly residue of modified lignin. White rot fungi are divided into two groups: the selective white rot fungi, which degrade both lignin and cellulose, but lignin at a higher rate, and the simultaneous white rot fungi, which degrade lignin and cellulose at about the same rate. To improve lignocellulose protection methods, and to explore fungal as a potential agents for selective fiber modification, basic information about the mechanisms of fungal wood decay is needed. While white rot fungi have a sophisticated enzymatic system causing degradation, brown rot fungi produce fewer enzymes. Brown rot decay is proposed to be caused by hydroxyl radicals that are produced in an iron-dependent, biochelator-mediated Fenton reaction. Ferrous iron and hydrogen peroxide participate in the Fenton reaction and produce an OH-radical, which is believed to attack the cellulose to initiate the breakdown. The production of the Fenton reagents has been investigated for a few brown rot fungi, but a general mechanism is not known. Several enzymes are capable of producing H<sub>2</sub>O<sub>2</sub>. The source of Fe<sup>2+</sup>, however is not clear. Metabolites produced by fungi have been found to be capable of reducing ferric iron to its active ferrous form. This work compares the iron reducing ability of white and brown rot fungi growing in liquid cultures supplemented with different carbon sources. Two white rot fungi, *Phanerochaete chrysosporium* and *Trametes versicolor*, and four brown rot fungi, *Coniophora puteana*, *Postia placenta*, *Gloeophyllum trabeum*, and *Meruliporia incrassata*, were tested for their ability to reduce ferric iron to ferrous iron, using the ferrozine assay